Structural characterization of lignin and some side-products from steam-exploded woody biomass

Strukturkarakterisering av lignin og noen biprodukter fra dampeksplodert biomasse fra trær

Ida Aarum

Structural characterization of lignin and some side-products from steam-exploded woody biomass
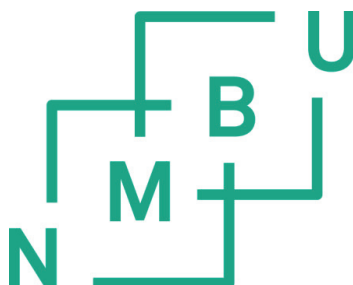
Strukturkarakterisering av lignin og noen biprodukter fra dampeksplodert biomasse fra trær

Philosophiae Doctor (PhD) Thesis

Ida Synnøve Aarum

Norwegian University of Life Sciences
Faculty of Chemistry, Biotechnology and Food Science

Ås (2018)

Acknowledgments

The work described in this thesis was carried out at the Faculty of Chemistry, Biotechnology and Food Science (KBM) at the Norwegian University of Life Sciences (NMBU), during the period 2014-2018.

First, I would like to thank my supervisor, Professor Yngve Stenstrøm, for his support and guidance. You gave me the chance to do this PhD, to be a part of your research group and believed in me from the start, thank you.

Second, I would like to thank Professor Dag Ekeberg and Dr. Hanne Devle for their superior involvement and support as co-supervisors. I have asked a lot of stupid questions and received only good answers. I would also thank my third co-supervisor Svein Horn, for the interesting project I was a part of, and all my co-authors for their contributions.

A special thank you to all of my colleagues, past and present that I have meet every day for the last four years. I really enjoyed working with you all, you have made my days better with all the ludicrous coffee discussions. Also a thank you to the students I have had the pleasure of supervising, Hördur, Anders, Ida and Morten, you're all great people and I have enjoyed my time with you.

At last, I would like to thank my family and friends for eternal support and comfort, especially Madelaine, you are my rock, my deepest thank you.

Ås, October 2018   Ida S. Aarum

Table of Contents

Abstract

The main objective of this thesis was to make a platform of libraries for characterization of lignin and other side-products after steam-explosion. The complete and effective utilization of renewable biomass will be important in the future as oil is slowly running out. Oil is already pretreated by nature, which eases the biorefining processes. In a similar way, biomass also needs to be pretreated for effective utilization.

Steam-explosion is an environmental and cost-efficient pretreatment of biomass, which degrades the hemicellulose into water soluble carbohydrates. The resulting residue is composed of lignin and cellulose which can be further refined. However, side-products formed under steam-explosion have been shown to be an obstacle for future enzyme refining of the biomass and is a challenge that needs to be overcome.

In this thesis, sample both from hardwood and softwood were steam-exploded at several different severity degrees (ranging from untreated to R_0 3.1 — 5.0). Common for both sources were the increase of Klason lignin content after steam-explosion. This is indicative of a common side-product termed pseudo-lignin. These samples were then analyzed by pyrolysis-GC-MS and NMR either with or without lignin extraction.

First, a library of untreated lignin monomeric units after pyrolysis at several isothermal pyrolysis temperatures (400 – 900 °C) was established. This revealed that lignin monomeric composition in the pyrolyzate has an evolving trend based upon increasing pyrolysis temperature. In addition, an estimated optimal pyrolysis temperature for lignin was noted. Later, these results were utilized in the subsequently studies where the side-product, pseudo-lignin, was the intended target.

Fractionated pyrolysis at two temperatures (350 and 600 °C, respectively) of both steam-exploded and non-extracted birch and Norway spruce, revealed that the composition of the lignin units had no significant change with increasing severity of pretreatment. Thus, the increase of Klason lignin, the pseudo-lignin, cannot be accredited to a benzene-like structure. Concurrently, the amount of furan-like units increased significantly in correlation to the Klason lignin increase, and it is therefore likely that pseudo-lignin consists of a furan polymer similar to humin.

Sammendrag

Hovedmålet med oppgaven var å opprette en ligninplattform med bibliotek for karakterisering av lignin og biprodukter etter dampeksplosjon. Komplett og effektiv utnyttelse av fornybare kilder er viktig for framtiden, siden oljen sakte blir brukt opp. Olje er naturlig forbehandlet, noe som forenkler bioraffineringsprosessene. På samme måte trenger biomasse også å bli forbehandlet for effektiv utnyttelse.

Dampeksplosjon er en miljøvennlig og kostnadseffektiv forbehandling av biomasse, som degraderer hemicellulose til vannløselig karbohydrater. Den gjenværende resten består av lignin og cellulose, som deretter kan bli videreforedlet. Imidlertid blir det samtidig dannet et biprodukt under dampeksplosjon som hindrer videre enzymatisk behandling av biomassen. Dette fører til en utfordring som må løses.

I denne oppgaven er trevirke fra både løvtrær og bartrær dampeksplodert ved flere forskjellige betingelser (fra ubehandlet til R_0 3.1 – 5.0). Felles for begge kildene er at det er en økning av Klason-ligninninnholdet etter dampeksplosjon. Dette er en indikasjonen på biproduktet; pseudolignin. Disse prøvene ble deretter analysert med pyrolyse-GC-MS og NMR, enten med eller uten ligninekstraksjon.

I første omgang ble det etablert et bibliotek over ubehandlede ligninmonomere som er i pyrolysatet ved flere isotermiske pyrolysetemperaturer (400 – 900 °C). I dette fremgikk det at sammensetningen til pyrolysatet hadde en utvikling som endret seg etter pyrolysetemperaturen. I tillegg ble det estimert en optimal pyrolysetemperatur for lignin. Senere ble disse resultatene benyttet i etterfølgende studier hvor biproduktet, pseudolignin, var målet.

Fraksjonert pyrolyse ved to temperaturer (hhv. 350 og 600 °C) av dampeksplodert og ikke ekstrahert bjørk og gran viste at ligninkomposisjonen endret seg lite med økende grad av hydrolysebetingelser (severity factor, log R_0) under dampeksplosjon. Dermed vil ikke økningen av Klason-lignin, pseudolignin, kunne beskrives som benzen-lignende strukturer. Derimot øker innholdet av furan-lignende forbindelser merkbart med økningen av Klason-lignin innholdet. Det er derfor rimelig å anta at pseudolignin består av en furanpolymer, tilsvarende humin.

List of papers

I. **The effect of flash pyrolysis temperature on compositional variability of pyrolyzates from birch lignin**
Ida Aarum[*], Hanne Devle, Dag Ekeberg, Svein J. Horn and Yngve Stenstrøm. *Journal of analytical and applied pyrolysis*, **2017**, 127, 211-222. DOI: 10.1016/j.jaap.2017.08.003

II. **Characterization of pseudo-lignin from steam exploded birch**
Ida Aarum[*], Hanne Devle, Dag Ekeberg, Svein J. Horn and Yngve Stenstrøm. *ACS Omega*, **2018**, 3 (5), 4924-4931. DOI: 10.1021/acsomega.8b00381

III. **Impact of milled wood lignin purifications on spruce lignocellulose**
Ida Aarum[*], Ander Solli, Hördur Gunnarsson, Hanne Devle, Dag Ekeberg, Dayanand Kalyani and Yngve Stenstrøm. *Wood science and technology*, **2018**, submitted.

IV. **Effects of pH adjustment on steam explosion extraction of acetylated galactoglucomannan from Norway spruce.**
Leszek Michalak, Svein Halvor Knutsen, Ida Aarum and Bjørge Westereng*. *Biotechnology for biofuels*, **2018**, submitted.

Author contributions

I. This author planned and performed the experimental work, and wrote the manuscript taking into account the comments of the coauthors.

II. This author planned and performed the experimental work, and wrote the manuscript taking into account the comments of the coauthors.

III. This author planned the experimental work and wrote the manuscript taking into account the comments of the coauthors.

IV. This author performed the experimental work for the NMR analyses and wrote the corresponding part of the paper considering the comments of the coauthors.

Abbreviations

^{13}C NMR	Carbon-13 nuclear magnetic resonance
^{1}H NMR	Proton nuclear magnetic resonance
4-O-MeGlucA	4-O-Methylglucoronic acid
ASL	Acid soluble lignin
CEL	Cellulolytic enzyme lignin
D-Gal	D-Galactose
D-Glu	D-Glucose
D-Man/D-Man[a]	D-Mannose or D-mannose acetylated in C5 position
D-Xyl/D-Xyl[a]	D-Xylose or D-xylose acetylated in C2 position
FT-IR	Fourier-transform infrared spectroscopy
G	4-(3-Hydroxy-1-propenyl)-2-methoxyphenol (guaiacyl unit)
H	4-(3-Hydroxy-1-propenyl)phenol (*p*-hydroxyphenyl unit)
HSQC	Heteronuclear singular quantum coherence
L-Arab	L-Arabinose
LCC	Lignin-carbohydrate complex
M_W	Molecular weight
MWL	Milled wood lignin
NMR	Nuclear magnetic resonance
Py-GC-MS	Pyrolysis-gas chromatography-mass spectrometry
S	4-(3-Hydroxy-1-propenyl)-2,6-dimethoxyphenol (syringyl unit)
S/G	Syringyl-/guaiacyl-unit lignin ratio

1 Introduction

1.1 Project background and aims

Traditionally the conversion of wood in pulp and paper industry has had its main focus on cellulose. The remaining wood mass has been regarded as waste and has mainly been burned to generate energy and heat for power. The total utilization of wood will be important in future economic and environmental developments.[1,2] Cellulose has already claimed its important role in wood refining, but in recent years the interest in lignin has also surged. Lignin is the most abundant aromatic polymer on earth, naturally occurring, and has the potential to replace crude oil refining.[3] It has a complex and diverse structure, which lacks analytical methods for detailed characterization after various wood treatments.[4,5] This makes scrutiny often challenging.

A research group at NMBU (Norwegian University of Life Sciences) has implemented steam explosion, fermentation and extraction of cellulose for processing wood and timber, leaving behind lignin as a side-product. The aim of this project was to make a platform of library for characterization of lignin and other side-products after steam-explosion. Both hardwoods and softwoods were to be analyzed mainly with pyrolysis-GC-MS (py-GC-MS) and NMR.

Figure 1. An illustration showing several different possible wood products.

1.2 Wood worth in the world

Today most chemicals and fuels are synthesized from fossil sources, this is a non-sustainable way of living. In recent years an effort has been put into research of alternative and sustainable ways of fulfilling this ever-increasing demand of energy and chemicals. The most promising alternative so far has been lignin, and the effort into effectively utilizing it has recently increased.[6,7]

Lignin today is mainly used in its low to mid-grade form of refining as concrete-substituent, animal-feed, in mining industries, in oil-quarrying, as low-grade chemicals etc.[8,9] Now, efforts of refining lignin are more towards e.g. bio-fuel, high-value chemicals, polymers.[1,6,7] Despite the opportunities the heterogeneity of lignin after depolymerization poses a severe challenge in refining to high value chemicals.[7,10,11]

1.3 Wood cell composition, structure and biosynthesis

Wood is divided into two subgroups, softwood and hardwood, the classification comes from biology and retains to propagation of the plant. Hardwoods are angiosperms and have their seeds enclosed in the ovary of the flower, commonly known hardwoods are; birch, ash and oaks. Softwood are gymnosperms, commonly called conifers, their seeds are not enclosed, common softwoods are; spruce, pine and fir.[12]

All organic plant material is composed of mainly three different constituents; cellulose, hemicellulose and lignin. The ratio of the three constituents differ between species (and even between individuals), but typically there is about 40 – 50% cellulose, 25 – 35% hemicellulose and 20 – 35% lignin in the stem wood.[13,14] In addition there are some extractives (lipids and proteins) and ash (inorganic residue), but these all amounts to less than 5 – 10%.[15]

The wood cells in the stem has an ultrastructure that can be divided into several layers. The two main walls, the primary and secondary wall and in addition to the warty layer, the intercellular space is called the middle lamella, Figure 2. The secondary wall is further divided into outer layer (S1), middle layer (S2) and inner layer (S3).[16]
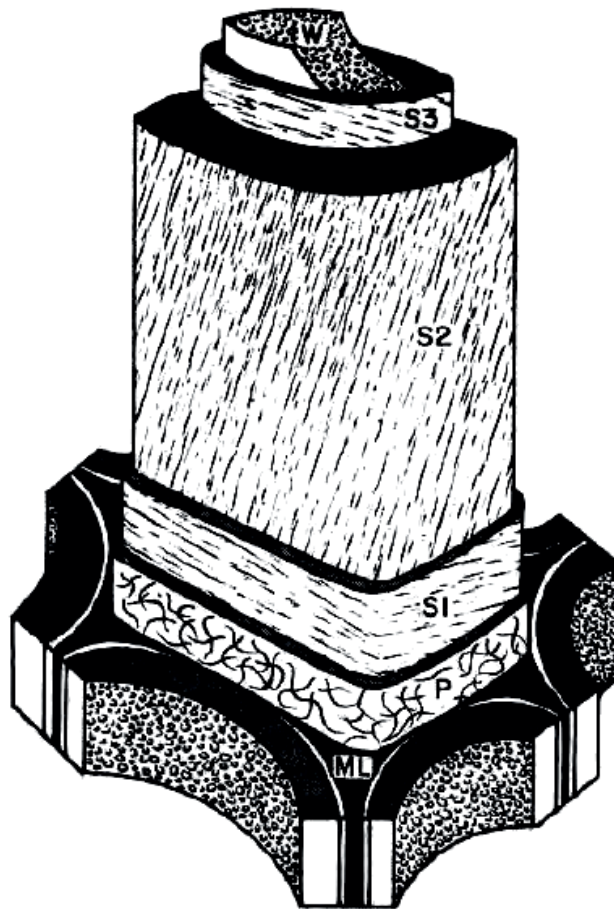
Figure 2. Anatomical overview of the ultrastructure layers in a mature wood cell. The wall layers consist of the primary wall (P), the secondary wall (S) and the warty layer (W). The secondary wall is divided into; outer layer (S1), middle layer (S2) and inner layer (S3). The middle lamella (ML) is the intercellular region.[16]

The primary wall is mostly composed of cellulose, hemicellulose, proteins and pectin, while the secondary wall contains cellulose, hemicellulose and lignin.[17-19] All plant cells have a primary wall to keep the protoplasm within, it is deposited while the cell is still expanding. The secondary cell walls are specialized cells mainly to facilitate support or water transport in the plant, but it is common in wood cells as it provides a more rigid structure.[20,21]

Even today there are discussions about the intermolecular linkage between the constituents of the cell wall (*i.e.* cellulose, hemicellulose and lignin), and the overall

structure. A very influential model from Keegstra *et al.* (with modification by Albersheim)[22] has been leading the field since the 70's, but recent advances in technology have provoked a new hypothesis; the hotspot hypothesis. The established theory depicts that a bundle of multiple cellulose strands (microfibrils) are "evenly" and "neatly" spaced apart by matrix polymers (hemicellulose, lignin and pectin).[23] The hotspot hypothesis depicts more interactive microfibrils where they are directly linked to each other at "load-bearing" junctions, by the means of hemicelluloses.[24] A comparison of the reigning theory and the new hypothesis is shown in Figure 3
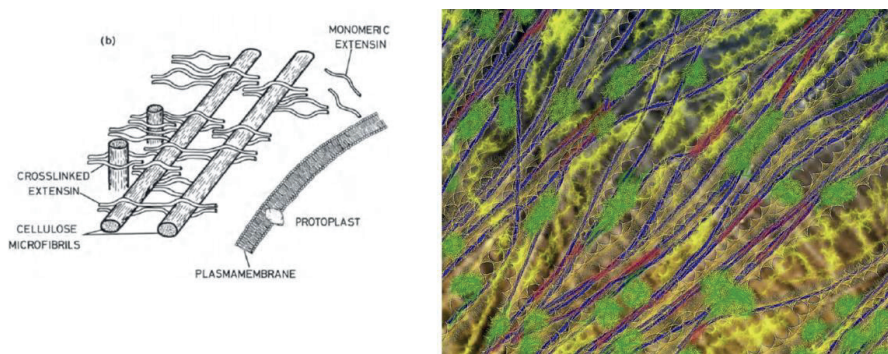

Figure 3. The two different models that show the morphology of cellulose, hemicellulose and lignin interaction. Left is the reigning model, where the cellulose strands are clearly separate. Right is the hotspot model, where the cellulose strands (blue) bend and touch each other.[22-24]

Either way there is an intermolecular linkage between carbohydrates and lignin, commonly called lignin-carbohydrate complexes (LCC). This is a structure which has lignin covalently bonded to carbohydrates, Figure 4 shows a schematic view.[25-29] These are complex molecules and it is theorized that LCC in its native state only binds with hemicellulose.[30]
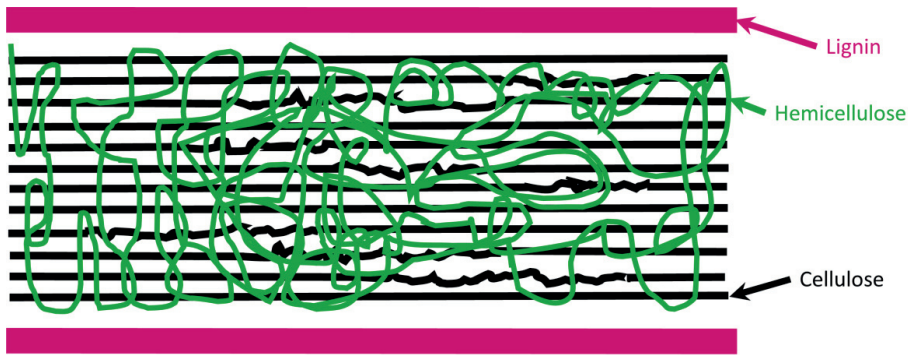
Figure 4. A schematic view of the interlinkage between cellulose, hemicellulose and lignin. Inspired by Mosier et al [28]

1.3.1 Cellulose

Cellulose is the most abundant organic polymer on the planet; it is a homopolymer composed of cellobiose. Cellobiose is a dimer of β-D-glucose, where every glucose unit is rotated 180 ° with respect to its neighbor.[3,31,32] The dimers are linked together in (1 → 4)-glucoside bonds (acetal linkage) and the number of monomers in a strand can amount to about 15 000 units, Figure 5.[3] It was first isolated and named by the French chemist Payen in 1838.[33,34]
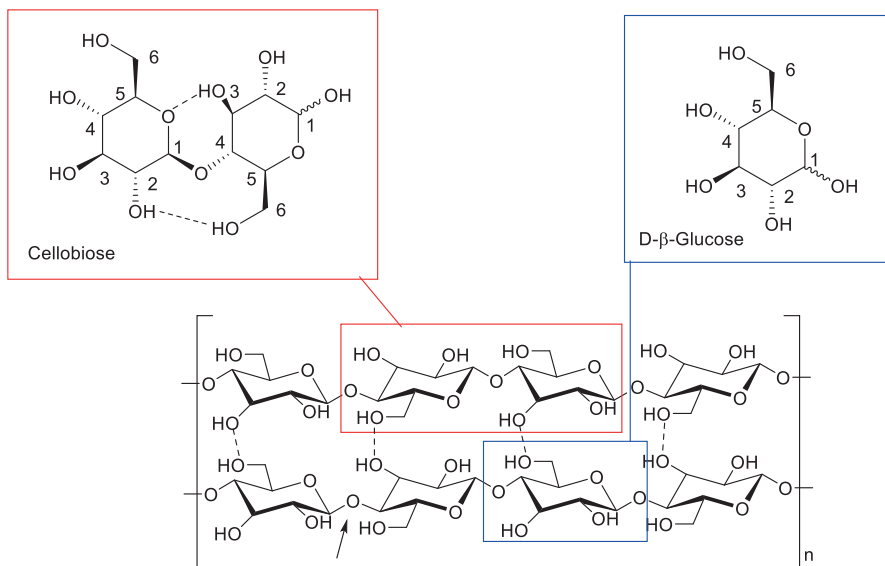
Figure 5. An overview of the chemical structure of cellulose, cellobiose is marked in red, a glucose unit is marked in blue and a glucoside bond is designated by the arrow. The dashed line indicates the hydrogen-bonding in intra and inter linkage in the strands of cellulose. The number of units (n) can amount to about 15 000.

The multiple hydroxyl groups in cellulose gives rise to intramolecular hydrogen bonds (C2 – C6 and C3 – C5) and intermolecular hydrogen bonds (C3 – C6). The intramolecular hydrogen bonds stabilize the individual glucopyranose rings in a coplanar orientation. This results in a ribbon-shape polymer, where the equatorial hydroxyl groups forms the edge.[32] The intermolecular hydrogen bonds will interact with neighboring stands and pack them together into a dense crystalline structure, microfibrils, that have a high tensile strength.[3] The crystallinity in the microfibrils will intermittently be exchanged with amorphous areas, where the intermolecular linkage happens, Figure 6.[35]
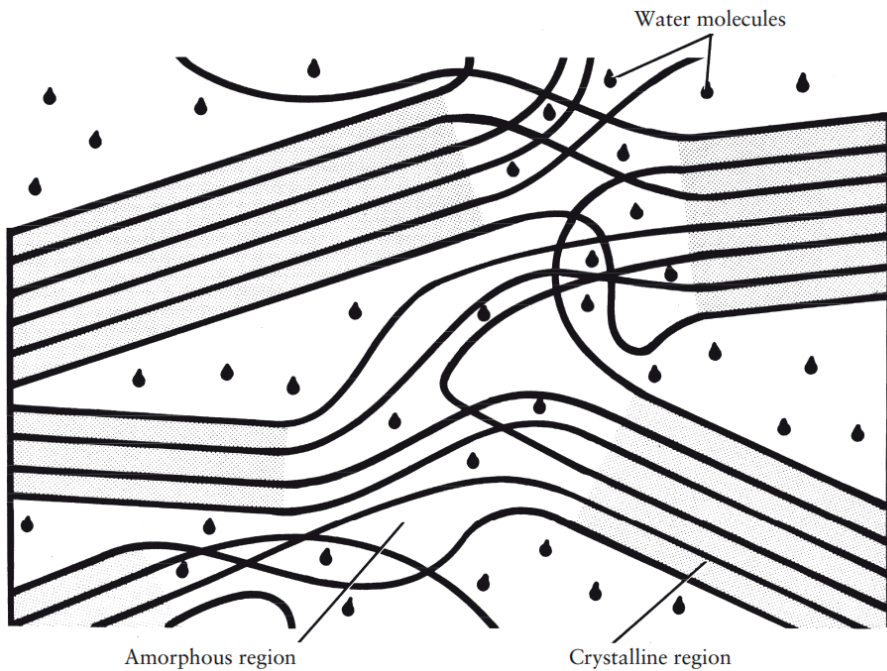
Figure 6. Schematic view of the ordered crystalline and the amorphous areas of microfibrils.[35]

1.3.2 Hemicellulose

The second constituent in wood cells is hemicellulose; it is a heteropolymer structure, which is chemically related to cellulose as it has a carbohydrate backbone. Despite this similarity to cellulose the structure is decidedly more complex and amorphous with shorter chain lengths (up to approximately 3 000). It is branched and composed of several different carbohydrates, Figure 7.[3] The main chemical composition also changes depending on wood-type (hardwood, softwood) in addition to the location in the cell wall. Two of the most important hemicelluloses are xylan and glucomannan.[23]
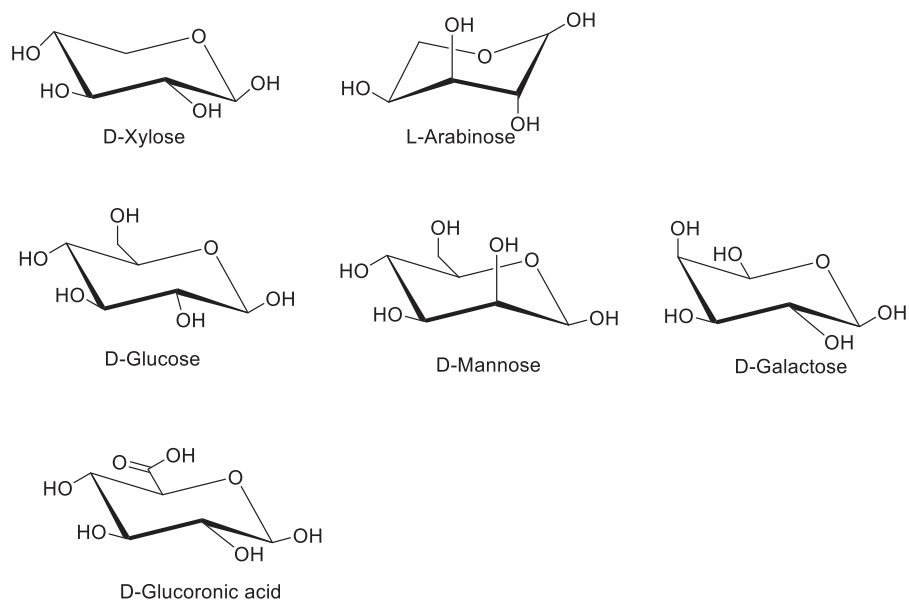
Figure 7. Hemicellulose monomeric units.

Xylan has a backbone of β-1,4-linked xylose, which is substituted by i) α-4-O-methylglucuronic acid in C2 position on xylose, ii) α-arabinose in C2 or C3 position on xylose (most common in softwoods) and iii) acetyl esters in C2 or C3 position on xylose (most common in hardwoods), Figure 8.[23]

Glucomannans have a backbone of β-1,4-glucose and mannose, in a ratio of 1:3, and it is the major hemicellulose in the secondary wall of softwood. They are often substituted with a single galactose in C6 position on mannose and are commonly called galactoglucomannans, Norway spruce is rich in this variety of hemicellulose, Figure 8.[23,36]

Xylan - hardwood

$\vdash$—4D-Xyl^a$_1$ —β— 4D-Xyl$_1$ —β— [4D-Xyl$_1$]$_9$ —β— 4D-Xyl^a$_1$ —β— 4D-Xyl$_1$ ——$\}$

|2
|1
4-O-MeGlucA

|3
|1
4-O-MeGlucA

Xylan - softwood

$\vdash$—4D-Xyl$_1$ —β— [4D-Xyl$_1$]$_5$ —β— 4D-Xyl$_1$ —β— [4D-Xyl$_1$]$_5$ —β— 4D-Xyl$_1$ —β— 4D-Xyl$_1$ —$\}$

α|2
|1
4-O-MeGlucA

α|2
|1
4-O-MeGlucA

α|3
|1
L-Arab

Glucomannan - hardwood

$\vdash$— 4D-M$_1$ —β— 4D-M$_1$ —β— 4D-M$_1$ —β— 4D-M$_1$ —β— 4D-Glu$_1$ —β— 4D-M$_1$ ——$\}$

Glucomannan - softwood

$\vdash$—4D-M^a$_1$ —β— 4D-Glu$_1$ —β— 4D-M$_1$ —β— 4D-Glu$_1$ —β— 4D-M$_1$ —β— 4D-M^a$_1$ —$\}$

α|3
|1
D-Gal

α|6
|1
D-Gal

Figure 8. Xylan structures in hardwood and softwood. D-Xyl/D-Xyl^a = D-xylose or D-xylose acetylated in C2 position, 4-O-MeGlucA = 4-O-methylglucoronic acid. Glucomannan structures in hardwood and softwood. D-M/D-M^a = D-mannose or D-mannose acetylated in C5 position. L-Arab = L-arabinose, D-Glu = D-glucose. [37]

1.3.3 Lignin

Lignin is the largest reservoir of renewable aromatic molecules on earth.[38,39] It is the third main constituent in all biomass and it is an amorphous polymer made up of three different building blocks called monolignols, Figure 9. The monolignols are 4-(3-hydroxy-1-propenyl)phenol (H), 4-(3-hydroxy-1-propenyl)-2-methoxyphenol (G) and 4-(3-hydroxy-1-propenyl)-2,6-dimethoxyphenol (S).[40,41]
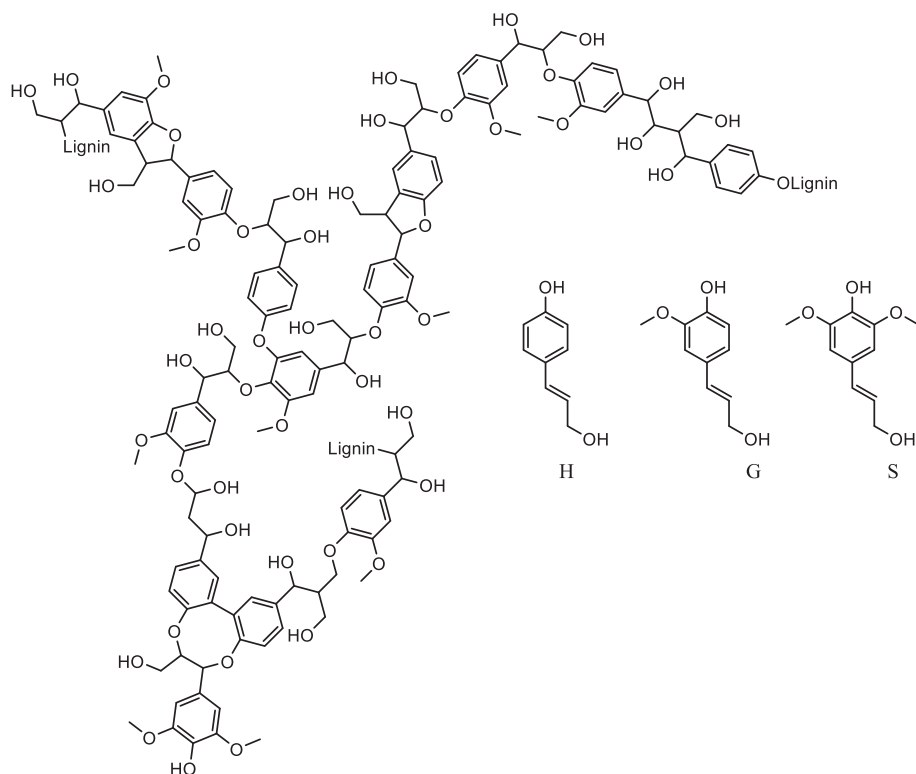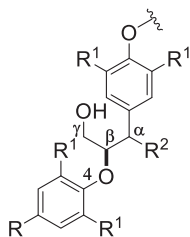

Figure 9. Lignin macrostructure and the monolignols; 4-(3-hydroxy-1-propenyl)phenol (H), 4-(3-hydroxy-1-propenyl)-2-methoxyphenol (G) and 4-(3-hydroxy-1-propenyl)-2,6-dimethoxyphenol (S).[30]

Lignin is a complex molecule with branching and an amorphous structure that fills area of the cell wall in between the hemicellulose and cellulose.[3] The average molecular weight (M_W) for lignin ranges from 7-8 000 to over 20 000 Da, but the extraction method has a great impact on exctracted size.[42-44] One property that increases lignin complexity is the diversity of the monolignols bonding pattern. Figure 10 shows the most abundant bonding patterns, but there are additional bonding patterns (a total of 20 different bonding
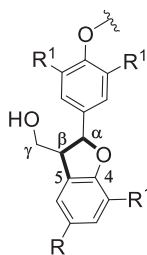
patterns[44,45]).[46-48] Despite of this, lignin is still mostly bound together by the β-O-4 bonding pattern (60 – 70%[49]) that makes the lignin inherently linear.[44]
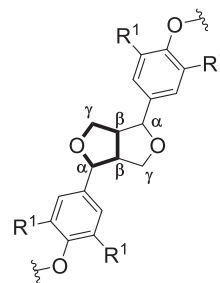
R = alkyl
R^1 = H, MeO

β–O–4 and β–O–4'
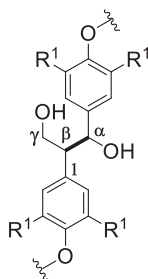BDE (R^2= OH): 290.79 kJ/mol
BDE (R^2= =O): 239.07 kJ/mol

β–5 and α–O–4
BDE (α–O): 175.73 kJ/mol
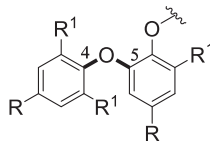BDE (α–β): 246.69 kJ/mol
BDE (β–5): 685.97 kJ/mol

β–β
BDE (α–β): 273.50 kJ/mol
BDE (α–O): 285.60 kJ/mol
BDE (γ–O): 333.00 kJ/mol
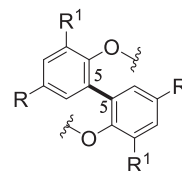BDE (β–γ): 330.49 kJ/mol
BDE (β–β): 339.30 kJ/mol

β–1
BDE (α–β): 345.14 kJ/mol

4–O–5
BDE (C–O): 345.35 kJ/mol

5–5
BDE (5–5): 480.95 kJ/mol

Figure 10. The most common lignin bonding patterns.[50-54] The BDE energy listed corresponds to the bold marked bonds and their respective annotation.

The ratio of S/G varies based on the origin of the biomass and even eventual strain from living conditions. Softwood has mostly a G-type lignin with 90 – 95% G and 5 – 10% S-monolignols.[6] In softwood the growth conditions can lead to formation of reaction wood which has a larger content of lignin, it is called compression wood (35 – 40% lignin).[16,55] Hardwoods have larger diversity in the S/G ratio, but on average it is 50% G and S-monolignols.[6,56] In comparison, the reaction wood in hardwoods have an increase of cellulose content.[16]

12
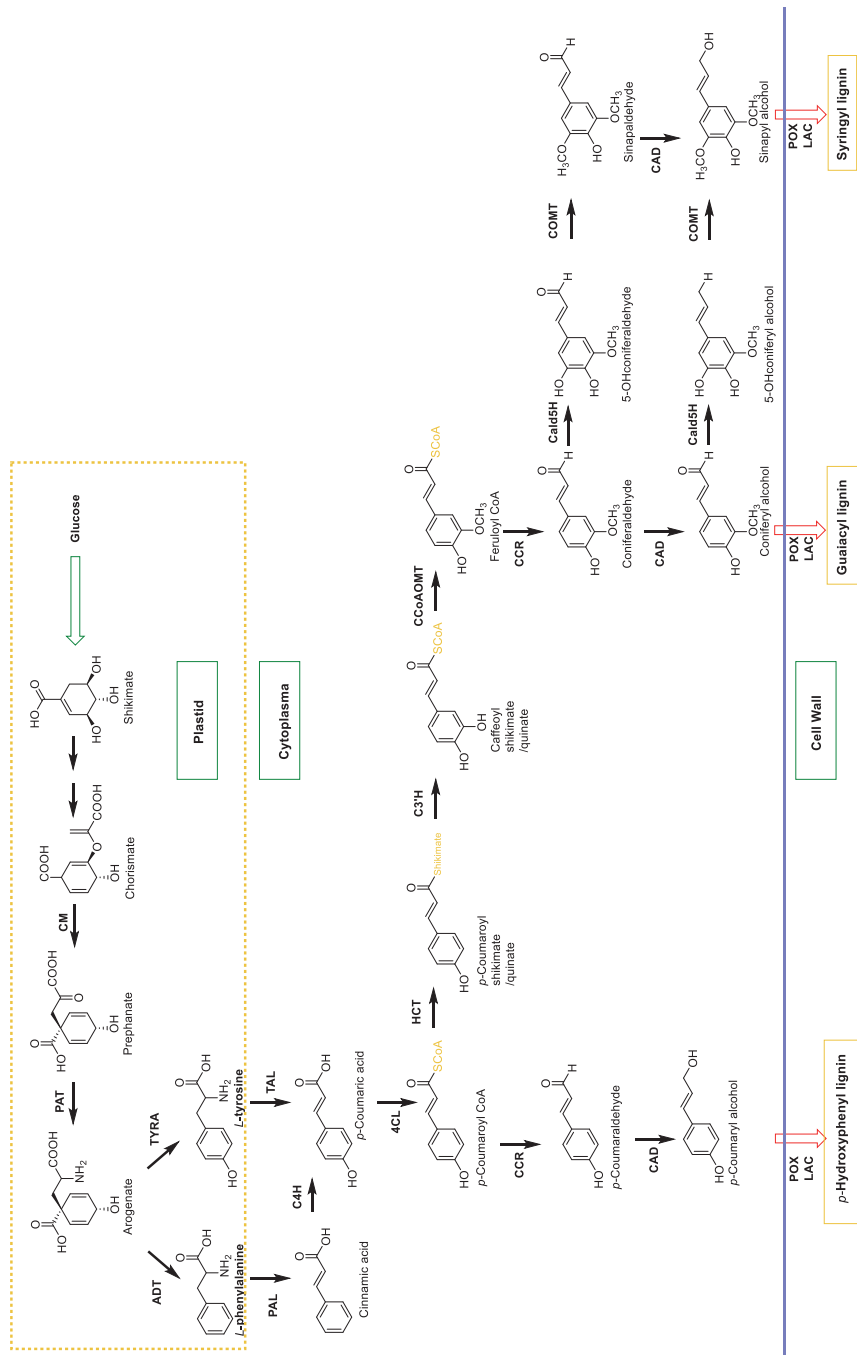
Scheme 1. The Scheme of the Simplified Shikimate–Phenylpropanoid–Lignin Biosynthetic Pathway, Illustrating Different Compartmentalization.[57]

The biosynthesis of lignin starts by converting glucose into shikimate and then *p*-coumaric acid, Scheme 1. The second and third phase include the transport of the monolignols to the cell wall, Scheme 1.[57] The current hypothesis on how the lignin polymer is formed, uses a radical coupling reaction of the monolignols adding to the end of a polymer.[58,59] The monolignol are oxidative radicalized by hydrogen peroxide (H_2O_2), before coupling with another monolignols radical to form one of several bonding patterns.[44,58,59] The radicalization is favored on the β-position, and this results in all the β-bonds in lignin. In the next step the dimer is dehydrogenated into a new radical which then continues the endwise coupling of the polymer, Scheme 2.[44]

G: R^1 = OCH_3, R^2 = H
S: R^1 = OCH_3, R^2 = OCH_3

β-O-4   β–5   β–β
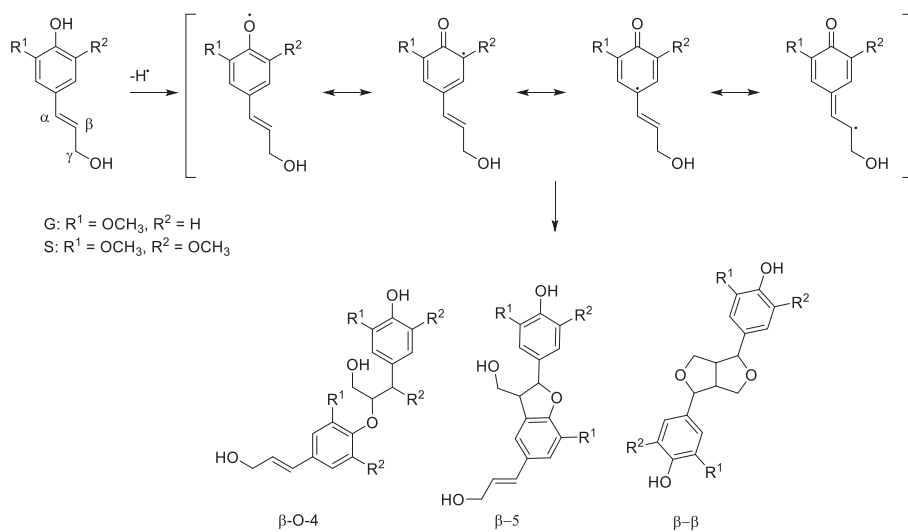
Scheme 2. Radicalization of the monolignols favored in the β-position and endwise coupling.[44]

1.4 Pretreatment

Wood has a matrix that is closely tied together and there are challenges in utilizing all parts of the raw material if not pretreated in some way. Pretreatment is an umbrella term for all treatment done before extraction or product refining, and the main objective is separation of the three main constituents, Scheme 3. Pretreatment can be easily classified into three major categories, 1) physical, 2) biological and 3) chemical.
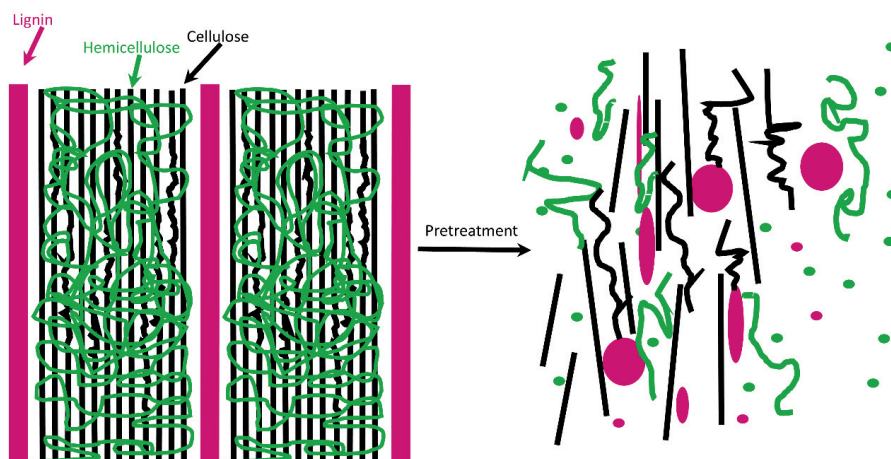
Scheme 3. Schematic representation of pretreatment effect on biomass.

Physical pretreatment is almost always applied as it encompasses all mechanical treatments such as; cutting, grinding and ultrasonic treatment of the wood. Chemical pretreatment utilizes chemicals in a range of different ways. A few different methods include; acid hydrolysis, lignosulfonates, Kraft lignin and organosolv lignin.[6,60,61]

Chemical treatment will often alter the structure of the constituents and depending on the intended products this is either a wanted or a negative side-effect. Lignosulfonates is a type of chemically altered lignin (addition of a sulfonic acid) after sulfite pulping. This lignin is water soluble to some extent, and has certain properties that are in demand in for example construction.[8] Biological pretreatment utilizes nature's own degradation system, either with microorganisms or enzymes by themselves.[62]

As pretreatment separates the three constituents of wood from each other, this is often at the expense of one of them. Choosing a pretreatment type is therefore an important with regard to the later product goals. Which constituents that are preserved under chemical

pretreatment is for instance dependent on the pH under pretreatment, Figure 11, or the choice of microorganism in biological pretreatment, cf. 1.4.2.[62]
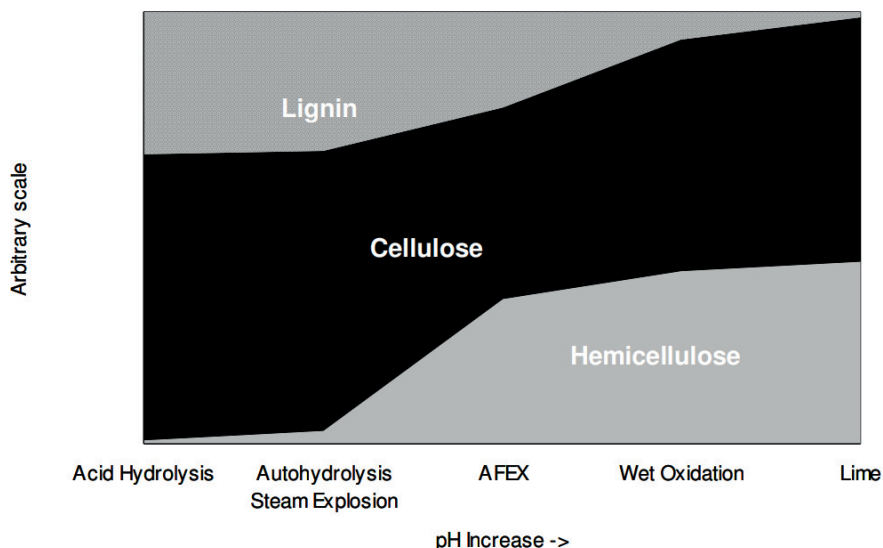

Figure 11. Typical polymeric solids composition after biomass pretreatment as a function of reaction pH characteristic of each pretreatment.[63]

1.4.1 Kraft

Today the most extensively used pretreatment in production is "Krafting" (with 95% of biorefineries/paper and pulp utilizes this method). This is a chemical pulping method that produces what is termed "black-liquid", from wood and $NaOH/Na_2S$. The black-liquid contains liberated lignin, either as lignin phenolate or ligno-sulphate together with degraded carbohydrates and some extractives. It is only about 40 – 50% lignin in black liquid and the rest are various amounts of partially degraded polymer carbohydrates and small amounts of extractives. Since this usually is a side-product from paper milling it will in most factories just be dried and then burned as a low value energy source, while the inorganic chemicals are recovered. This type of treatment is detrimental to potentially very valuable products. One of the biggest problems with this pretreatment, if high value chemicals are the goal, is the huge product diversity which makes separation and upgrading difficult.[30,64]

1.4.2 Biological pretreatment

With biological pretreatment there is an addition of microorganisms directly on to the wood without any other pretreatments. This causes a vast difference in results depending on mode of action and choice of microorganism, Table 1.[62]

Table 1. A few microorganisms used in biological pretreatment, and their major effect on biomass.

Microorganism	Biomass	Major effects	References
Punctualaria sp. UFC20056	Bamboo culms	50% of lignin removal	[65]
Irpex lacteus	Corn stalks	82% of hydrolysis yield	[66]
P.ostreatus/P.pulmonarius	*Eucalyptus grandis*saw dust	Twenty fold increase in hydrolysis	[67]
Fungal consortium	Corn stover	43.8% lignin removal/seven fold increase in hydrolysis	[68]
Ceriporiopsis subvermispora	Wheat straw	Minimal cellulose loss	[69]
Fungal consortium	Plant biomass	Complete elimination of use of hazardous chemicals	[70]

1.4.3 Steam-explosion

Steam-explosion (SE) is a pretreatment that is a combination of physical and chemical means, since it utilizes high temperature and pressure in combination with steam or low concentration of acids.[61,71,72]

The biomass is exposed to saturated steam typically from $160 - 260\ °C$, under high pressure $0.69 - 4.83$ MPa for a short time $(1 - 15$ min).[61,72-74] When the steam hits the "cold" wood fibers, it condenses inside the pores of the wood. Thereafter the pressure is rapidly removed inducing an "explosion" when condensed water turns into vapors. This in turn pulls the fibers apart and hydrolyses the hemicellulose into monomeric units Figure 12.[61,71,72]

SE is considered a green and environmentally friendly method as the need for chemicals is minimal if any, and when used it is usually diluted acids (0.1%wt.). This also affects the price and SE is considered to be a relatively cheap method for degradation of the wood.[21,73] Structurally the constituents in wood should be unaltered, but some

degradation of lignin, and in some cases cellulose, has been reported with diluted acids.[60,63,75,76]

Sometimes there is not even a need for addition of diluted acids under SE. This is usually the case with hardwoods as they will release acetic acid from hemicellulose that will act as the diluted acid. This is called autohydrolysis since the hemicellulose hydrolyze itself.[77] The amounts of released acid under similar conditions have been measured to result in pH as low as $3 - 4$.[78,79]

Since the main parameters for SE is time and temperature and both have direct and independent impact on the degradation of biomass, the need for an independent comparison factor arises. Overent and Chornet[80] did develop this factor based on the amounts of water soluble saccharides after SE, called severity factor (log R_0, equation beneath). T is temperature of the steam under pressure, and retention time (rt) is the time the biomass is under pressure with the temperature, T.

$$\log R_0 = \log(rt \times e^{\frac{T-100}{14.75}})$$

With SE there is also the option of presoaking the biomass in solvent before SE in the reactor. SE can be a sensitive method depending on biomass type, for instance hardwoods are generally easier to steam explode as they hydrolyze by themselves (autohydrolysis). Softwoods often needs additional help, such as presoaking with diluted acids.[64] The diluted acid will penetrate the biomass fully and the degradation will be more complete.
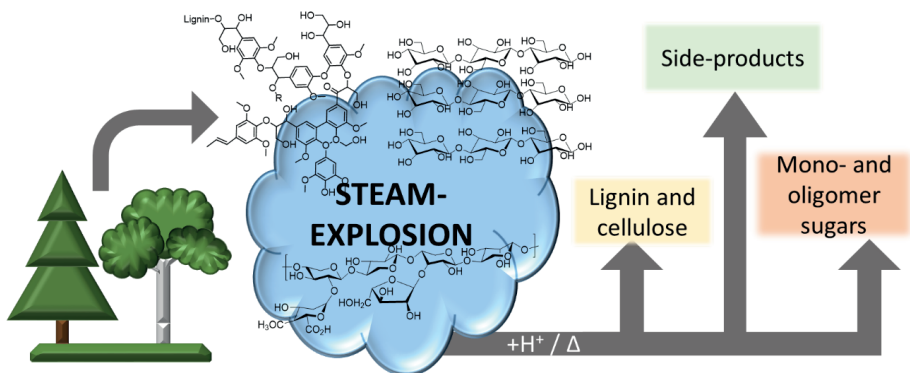

Figure 12. Overview of a typical steam-explosion with start material and products.

1.5 Extraction of lignocellulose

In characterization, the extraction of an analyte is an important step, as the influence of impurities can make the identification difficult, time consuming, impossible or, in the worst case, lead to misidentification. With heterogeneous polymeric molecules this will be even more important as identification is increasingly difficult with increasing heterogeneous of polymers.

In biomass there is an intricate matrix of cellulose, hemicellulose and lignin. The extraction of these for analytical purposes is a challenge, but there are several solutions of which some have both benefits and drawbacks.
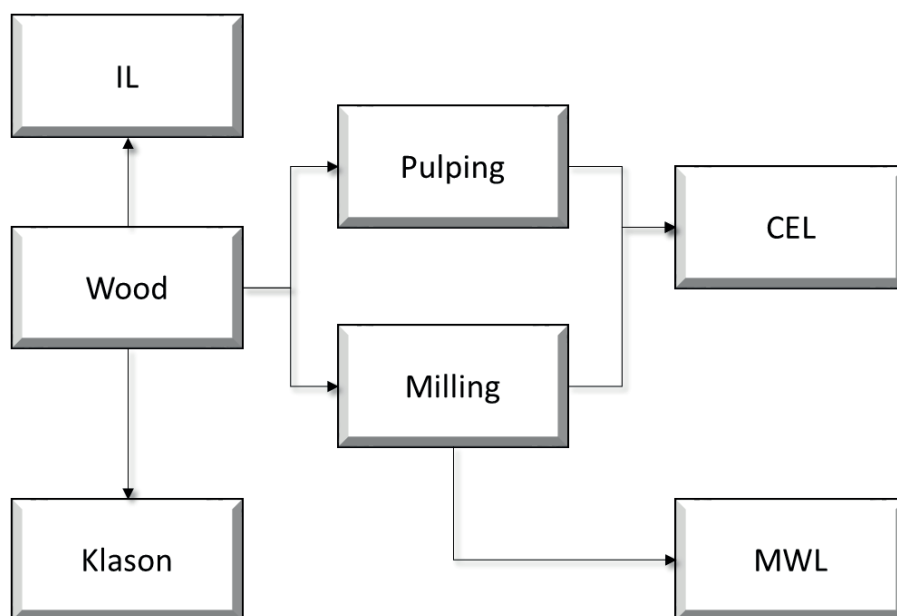
Scheme 4. Schematic overview of several different extraction methods. IL=Ionic liquid, Klason=Klason lignin, CEL=Cellulolytic enzyme lignin, MWL=Milled wood lignin.

1.5.1 Milled wood lignin

The extraction method that is considered to be one of the least invasive and structurally altering of lignin is milled wood lignin (MWL) method. It was first reported by Björkman in 1956.[81] Later it has been modified slightly by other researchers[82,83] but this method has been considered to be the most representative of protolignin[84] in wood, and is often called

"native"-lignin. The largest drawback of the MWL method is the low extracted yield (crude extraction yields only 20 – 30% wt. of total lignin).[83]

Initially the wood is divided into fine powder and washed with organic solvents to remove extractives found in the wood, such as steroids, terpenes and waxes. The extraction of lignin is then done with aqueous *p*-1,4-dioxane (96:4 v/v), which yields crude MWL.[83]

The grinding of the wood is performed by a planetary or vibrating ball mill, and certain precautions have to be taken in order not to alter the lignin. During the grinding procedure the friction will cause a rise in temperature. To avoid this, the grinding should be done either with intervals that keep the temperature below 35 °C, or with a cooling air flow.[81,85]

Recent studies of MWL have shown that the lignin is slightly more condensed than other methods. It is suggested that the MWL contains more lignin from the middle lamella than the cell walls.[86,87]

1.5.2 Cellulolytic enzyme lignin

In the cellulolytic enzyme lignin (CEL) method the wood is first treated with cellulolytic enzymes to remove most of the carbohydrates prior to the aqueous *p*-1,4-dioxane extraction of grinded wood meal.[59,87,88]

This type of lignin is structurally similar to MWL and even more representative of the protolignin, with a part of the LCC being retained in the extraction. Additionally, it has a yield that corresponds to a high percentage of total lignin in the wood.[85-87] An advantage the CEL method has over the MWL method, with regards to industry, is that chemical pulp is digestible by cellulolytic enzymes without the need for grinding of the pulp. This means that there is no additional alteration of the lignin after pulping.[89] The drawback is that the procedure for preparing the CEL method is tedious and the gain in structural knowledge is not sufficient compared to the relatively ease of the MWL method.[85]

1.5.3 Klason lignin

This extraction method includes the complete acid hydrolysis of all carbohydrates into water soluble monosaccharides. Complete hydrolysis is achieved with strong concentrated acids such as sulfuric acid (72% H_2SO_4), the residue remaining after drying is termed the Klason lignin. This was first discovered by Payen in 1838, when he treated

wood with concentrated H_2SO_4 and was left with a brown residue.[34] Klason lignin has later become an analytical standard for quantification of total lignin in wood and other biomasses, either by the TAPPI[90] or the NREL[91] protocols. Unfortunately, while refluxing with concentrated acid, the Klason lignin will also degrade to some extent. For this reason, the protocol is not considered to be a good extraction method for characterization purposes.

There is some lignin which dissolves under extraction, called acid soluble lignin (ASL). For softwoods this constitute only about 0.2 – 0.5% and for hardwoods it is 3 – 5%.[90] It is then possible to quantify the ASL by ultraviolet spectroscopy after total hydrolysis.[90]

1.6 Main analysis techniques

Choice of analysis techniques is an important first step after determining the goals of a project. Often the analysis techniques do not give the whole picture and only fractionated information of the components in question. By performing several different analytical techniques on the same component, the picture becomes more complete and a structural characterization more confident.

1.6.1 Pyrolysis-GC-MS

Normally GC-MS is not an analytical technique that is optimal for intact macromolecules and polymer compounds, as the compounds needs to be volatile and thermally stabile. However, coupled with a pyrolysis the polymer of interest will decompose into smaller, volatile compounds before separation and detection on the GC-MS.

Pyrolysis is a thermodynamic bond-cleavage without the use of oxygen, and is more generally termed thermolysis. It can be divided into two main groups, slow pyrolysis and fast pyrolysis (flash pyrolysis). Flash pyrolysis is defined by IUPAC to; "*A pyrolysis that is carried out with a fast rate of temperature increase, of the order of 10 000 K/s*."[92] It is important to have a fast heating rate in structural analysis to keep the secondary unwanted reactions and formation of char to a minimum.

Pyrolysis reactions are divided into primary and secondary mechanism, the primary include; i) char formation, ii) depolymerization and iii) fragmentation, Figure 13. Char formation is an unwanted reaction as it degrades the biomass into low-grade products, such as charcoal (biochar). It is the result of intra- and intermolecular rearrangement

reactions that can be favored under low temperature and heating rates.[10,93-101] Under depolymerization the polymer is degraded into the monomeric units that make up the polymer. This will yield a bio-oil of valuable components that can later be refined into high-valuable components.[102-105] A fragmentation mechanism is the pathway of degrading the polymer directly into incondensable gasses.[10,93-101]
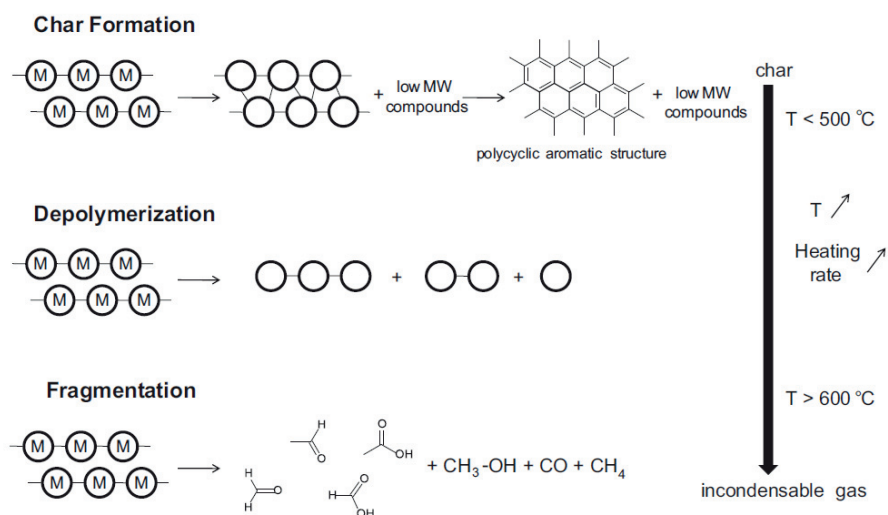

Figure 13. Pathways of primary mechanism of biomass conversion in pyrolysis.[93]

The secondary mechanism includes crackling or recombination. Both reactions are the consequence of pyrolysis products being unstable under the temperature conditions, and subsequently undergo further degradation. Crackling reactions encompasses pyrolysis products that decompose into low molecular weight (M_W) molecules. Recombination reaction encompasses pyrolysis products that recombine or rearrange into high M_W molecules. When recombination happens within a polymer pore it is called secondary char.[93,94,106-108]

As pyrolysis is a thermolysis-type degradation, the temperature and time of heating are important factors for pyrolyzate composition. In general the energy, in form of heat, will break the weakest bond first, and then subsequently increasingly stronger bonds. [6] This can be manipulated to yield different compositions in the bio-oil, which can be predicted to a certain degree by the bond dissociation energy in molecules, (BDE).[109-112] The

mechanisms of lignin degradation are still disputed, and many questions have so far remained unanswered regarding to what degree i) homolysis, ii) "retro-ene" and iii) Maccoll elimination is part of it, Scheme 5.[113-120]
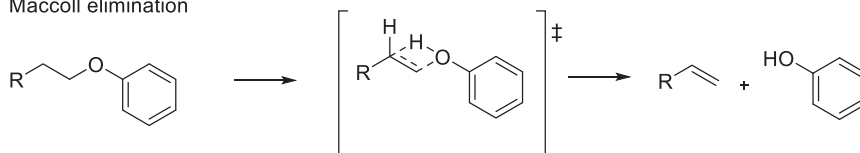
Homolysis
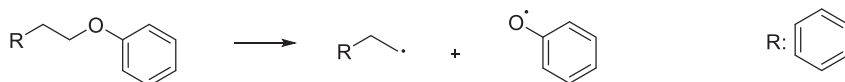
"retro-ene"
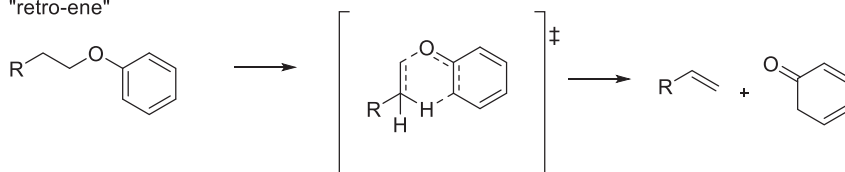
Maccoll elimination

Scheme 5. Simplified reaction mechanisms possible under pyrolysis of lignin.[116]

1.6.2 2D NMR

Nuclear magnetic resonance spectroscopy (NMR) is a strong analytical tool for characterization purposes. It can detect functional groups, neighboring atoms and even distinguish isomeric substances such as stereoisomers. With more complex compounds and/or mixtures the need for more sophisticated techniques are in demand. The most common is two-dimensional NMR (2D NMR), even though both three- and four-dimensional NMR techniques are possible.

2D NMR can either be plotted with the coupling constant orthogonally to the chemical shift or the chemical shift can be plotted on two orthogonal axes, creating a contour map of coupling and functionality of the compound. The two dimensions can either be two ^1H, two ^{13}C or ^1H-^{13}C.[121]

Heteronuclear single quantum coherence (HSQC) is a two-dimensional ^1H-^{13}C type NMR, which measures the coupling constant between proton and carbon, visualized as the cross-peaks. This method is particularly useful on samples with complex and versatile

structures, such as lignin and hemicellulose, as it utilizes proton-detection of the ^{13}C signals. This results in a higher resolution of the carbon-dimension, than other hetero-correlation experiments, for example heteronuclear multiple quantum coherence (HMQC).[121-124]
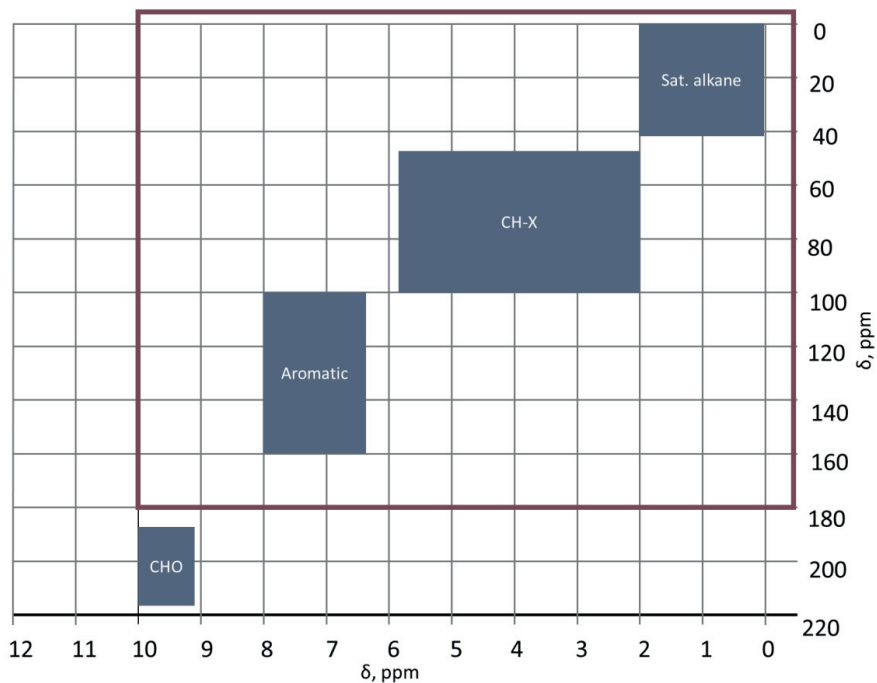

Figure 14. Schematic overview of typical areas of functionality and coupling visible in HSQC. The red area is usually the area of most interest.

A method of quantification has in recent years been developed for MWL in HSQC.[125,126] This yield a quantification of the different interunit bonding patterns in lignin, which gives valuable insight into structural differences in lignin between biomass types. It has also been applied after treatments on biomass, and as structural elucidator for LCC, Figure 14.[26,44,56,125-128]

Some considerations have to be evaluated before quantification; i) the sample has to be fully dissoluble in the solvent of choice, and stay dissolved during the time of the measurements; ii) standards have to be inert and stable over the time needed for the

measurements; iii) signal-to-noise ratios increases with only 0.25 times per scans taken, and available time is a limiting factor in NMR spectroscopy.[125]

1.7 Pseudo-lignin

There has been noted a rise in Klason lignin content after SE, which is not accounted for by the loss of carbohydrates under the treatment.[5,129] This rise has been denoted to a side-product that is formed with increasing severity factor and named pseudo-lignin. The definition is a broad and diffuse term, but the most accepted states; "*an aromatic material that yields a positive Klason lignin value that is not derived from native lignin.*"[130] This side-product has been shown to hamper further enzymatic hydrolysis of cellulose.[5,129-134] Klason lignin is on the other hand only a quantifying measurement of non-hydrolysable residue (usually aromatic) after complete hydrolysis of the carbohydrates in biomass, and identifies no specific structure.[130] There has been several reports around the structure of pseudo-lignin, but characterization of this has been challenging as Klason is a destructive method.

Characterizations of pseudo-lignin has shown that it has a higher degree of polymerization than "native"-lignin.[135] It is often visualized as a lignin-like polymer, because of its aromatic functionality visible in Fourier-transform infrared spectrum (FT-IR).[129,136] This has caused the hypothesis that pseudo-lignin is condensed lignin (lignin that has reacted with itself), this is reinforced to a certain degree by NMR and the reaction possibilities that lignin can undergo under SE, Scheme 6.[49,137-139] In addition, another hypothesis is that pseudo-lignin is a type of flavonoid-like structure, caused by rearrangement in the lignin structure, these have been detected after SE with LC-MS.[132]
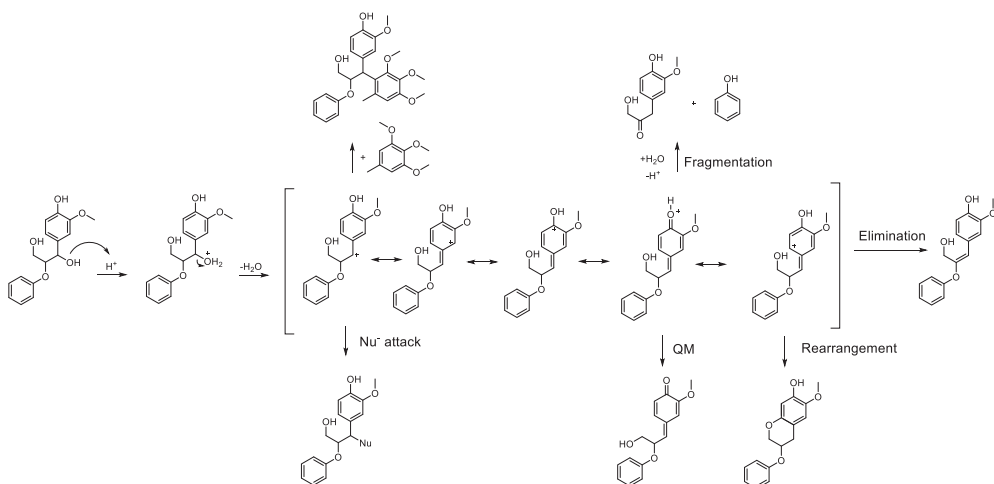
Scheme 6. Reaction pathways and resonance structures under steam explosion of lignin that might take place. The first resonance structure is open for a nucleophilic attack, Li et al.[135] and Shimada et al.[140] The fragmentation reaction in the fourth resonance form is calculated to be exothermic by Sturgeon et al.[141] QM is the formation of Quinone Methide-structure. The rearrangement in the fifth resonance would yield flavonoid-like structures as detected by Rasmussen et al.[132]

A third hypothesis has also been introduced, stating that pseudo-lignin is a degradation product of carbohydrates, either through reaction with lignin directly or through reaction of carbohydrates with themselves. This has emerged by doing SE with only xylan or other carbohydrate sources.[130,133,136] All three side-products are possible and detected after SE, but the definition of pseudo-lignin is an increase of weight in Klason residue after SE.[49,132,136,138,139] By this definition the first two hypotheses are excluded as both self-condensation and rearrangement will not increase the mass weight of the residue.

Under SE there are mildly acidic conditions either as a result of release of acetic acid from hemicellulose or addition of this into the reactor prior to treatment. This causes the acid catalyzed hydrolysis followed by conversion of hemicellulose into water soluble saccharides, as depicted for lignin in Scheme 6. However, the acid can also catalyze further reaction of monomeric carbohydrates into dehydrated furan molecules, Scheme 7.[133,142]
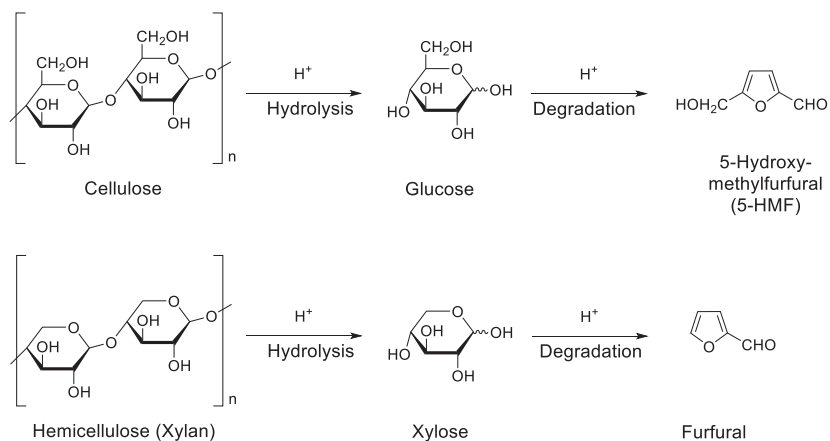
Scheme 7. Overview of reaction pathway of cellulose and hemicellulose into furan components.[142]

These furan compounds are aromatic and contains several oxygen based functional groups that will contribute to the polarity. This will make them more water soluble, resulting in a furan-free residue after Klason lignin. However, furans and carbohydrates can under acidic conditions, with heat, dehydrate and polymerize into a structure called humin. The definition of humin is; "*an organic compound class which are insoluble in water at all pH's*". The term is used in two related contexts, soil and carbohydrate chemistry.[143,144] It has been described as far back as 1910 by Nef[145] and later several times by other chemist as a side-product which forms under conditions with heat and acid.[143,146-154]

2 Relationship and key results within papers

All the papers in this thesis involve characterizing the effect of either extraction, steam-explosion or both, on biomass from birch and Norway spruce, using NMR and py-GC-MS. The complete flowchart of the process from biomass to treatment and analysis is shown in Scheme 8. In **paper I** the method for py-GC-MS and NMR was developed, which was later utilized for the subsequent papers, **paper II**, **paper III** and **paper IV**.
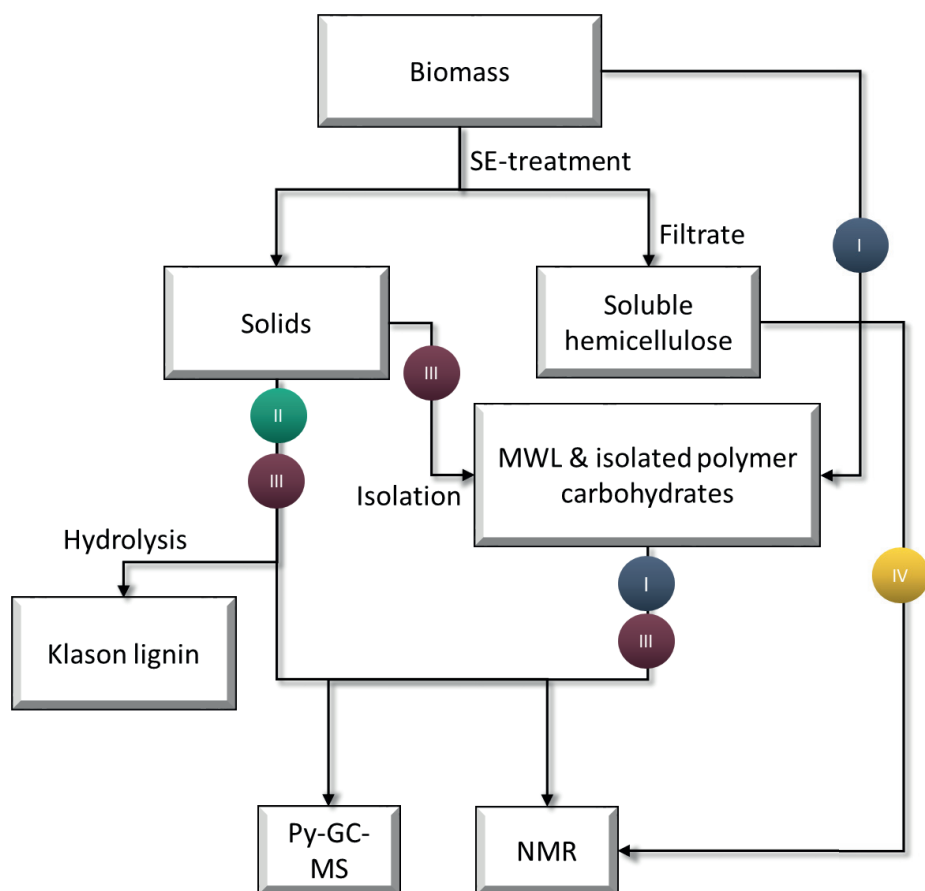
Scheme 8. Flowchart of the pretreatment, extraction and analysis done on biomass. The numbered circles indicate the papers' relationship to the flowchart.

In **paper I** extracted MWL without pretreatment was analyzed with py-GC-MS and 2D-NMR (HSQC). The NMR results confirmed that the birch MWL was comparable to previous studies on hardwoods and birch MWL published[25,56,137,155], with regards to bonding patterns and S:G- ratio.

The flash filament pyrolyzer utilized has a heating rate of 175 000 °C/s, with 8 ms temperature rise time and a total heating time of 2 s per sample. This means that the generation of char and secondary pyrolysis mechanism products are not a problem. The main products in the volatile pyrolyzate are directly depolymerized into mostly monomeric lignin units. The pyrolysis was done isothermally with several different pyrolysis temperatures (400, 450, 500, 600, 650, 700, 750, 800, 850 and 900 °C), and 38 of 46 pyrolyzate components were identified with retention times and standards.

The relative amounts of each component varied as a function of pyrolysis temperature. A correlation between the temperature and composition in the pyrolyzate revealed trends based on the bonding pattern and functionality of the alkyl sidechain, Figure 15. At low pyrolysis temperatures the composition was mainly aldehyde components such as; 4-hydroxy-3,5-dimethoxybenzaldehyde and (*E*)-3-(4-hydroxy-3,5-dimethoxyphenyl)prop-2-enal. When the pyrolysis temperature increased (400 – 500 °C) the aldehydes decreased from 42% until 21%. The aldehyde amounts are then constant with increasing pyrolysis temperature (at approximately 23%) and several other components emerged such as; 2,6-dimethoxy-4-prop-2-enylphenol, 4-ethenyl-2-methoxyphenol and 2-methoxyphenol.

The composition of the pyrolyzate is directly correlated to the bonding patterns in lignin and the energy demanded to break the bonding patterns under pyrolysis. The temperature profile for each sidechain functionality makes it possible to control, at least to an extent, the composition in the pyrolyzate. This resulted in an identification of several optimal pyrolysis temperatures depending on wanted results: i) low valorization, ii) high valorization and iii) carbonization of lignin.
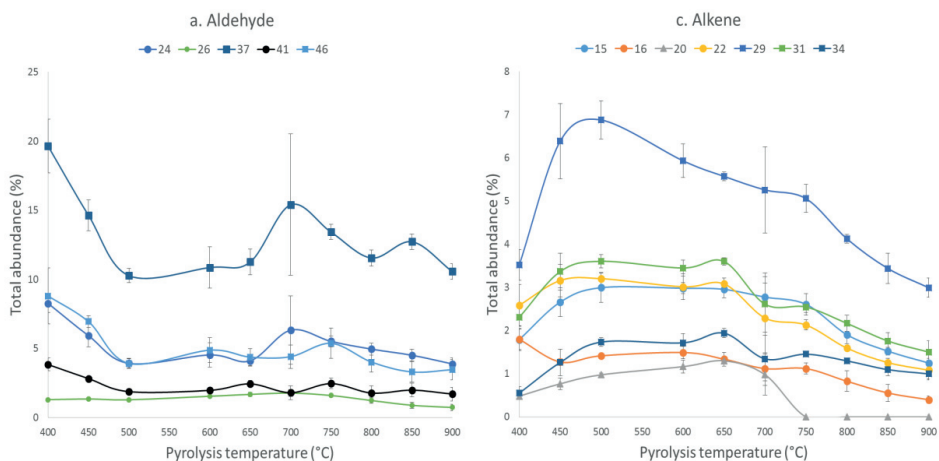
Figure 15. An excerpt of two figures from paper I, showing the correlation between components and pyrolysis temperature.

In **paper II** the effect of steam explosion on the biomass and lignin composition and side products were examined. The samples were not extracted after SE and contained polymeric carbohydrates and side-products, such as pseudo-lignin. The birch biomass was steam exploded at several temperatures and times (170, 180, 190 and 200 °C for 10 min, in addition to 210, 220 and 230 °C for 5, 10 and 15 min). The Klason lignin content increased from 22% in the untreated sample up to 40 – 42% at the highest severity, which means that the samples had about 20% pseudo-lignin content.

Since the samples were not extracted the pyrograms would be too complex to analyze with isothermal pyrolysis, so fractionated pyrolysis was utilized instead. Fractionated pyrolysis is a technique in which the same sample is pyrolyzed several times with increasing temperature. The first pyrolysis temperature was 350 °C as this would valorize most of the polymeric carbohydrates not hydrolyzed under SE, but is insufficient to valorize the lignin part, Figure 16.[156] This turned out to be a mostly correct assumption, as the 350 °C pyrogram contained only small amounts of lignin components. The second pyrolysis temperature was 600 °C as this was seemingly the most optimal temperature to pyrolyze lignin, based on previous results.[157]
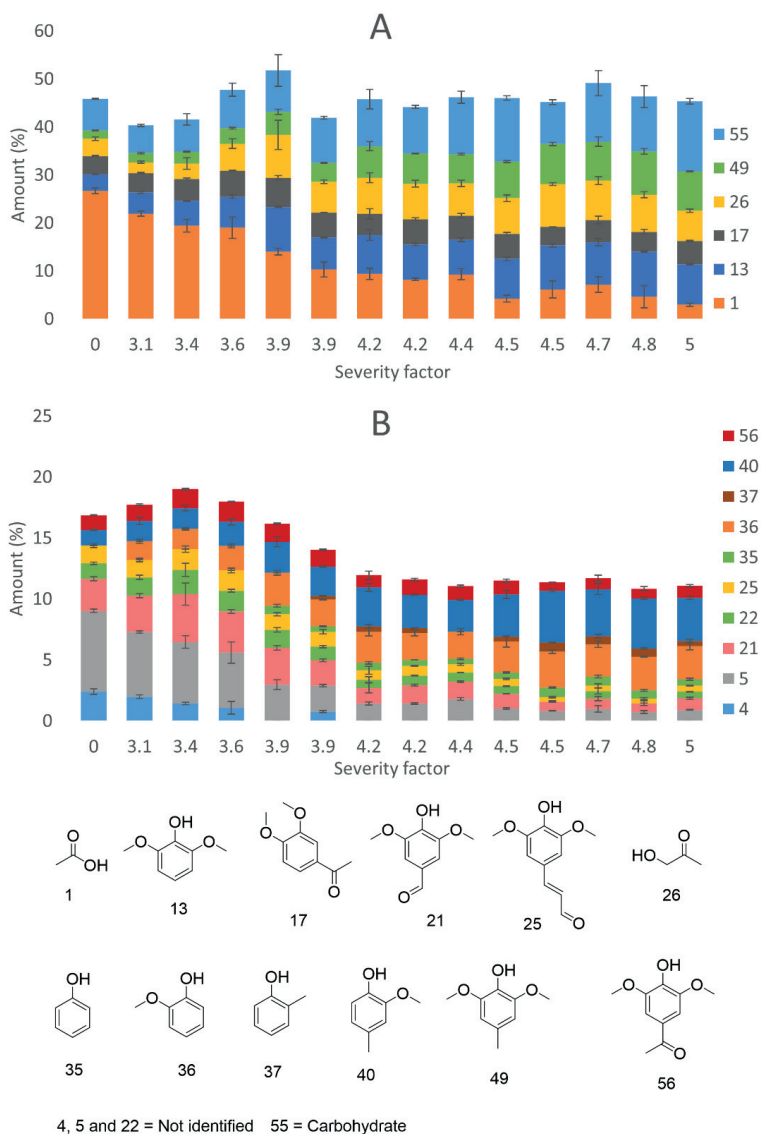
Figure 16. From paper II. Amount and structure of several components in the pyrolyzate at 350 °C. A=Components of major amounts, B=Components of minor amounts.

According to the HSQC-NMR results, going from untreated to pretreated birch an increase of soluble carbohydrates was observed, and with increasing treatment there was no significant change in the lignin spectrum. Some condensation in the aromatic area could be seen in addition to a degraded carbohydrate product, 5-HMF. Unfortunately, the

signal intensity of 5-HMF in the HSQC-NMR spectrum was not strong enough to validate the weight increase after Klason lignin (20%). A reasonable conclusion seemed to be that pseudo-lignin was not soluble in the NMR solvents.

From the pyrolyzate the results again revealed that there was no significant change in the monomeric lignin composition after pyrolysis with increasing steam-explosion severity. This means that the pseudo-lignin structure cannot be "lignin-like" components such as benzene or phenols. On the other hand, there was a steady increase of "furan-like" components from severity factor 3.9 (above 200 °C) in the pyrograms. This incidentally corresponded to when the acetic acid starts to be consumed under SE, Figure 17.
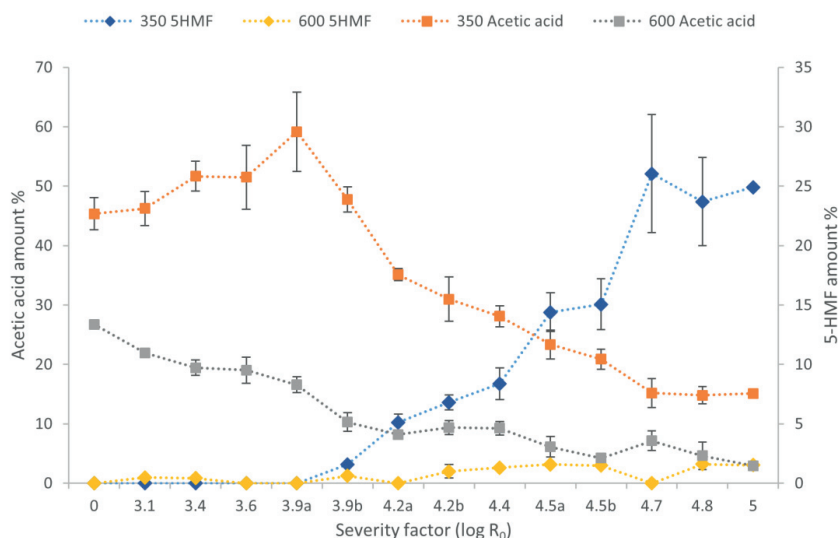

Figure 17. From paper II. The correlation between 5-HMF and acetic acid, in both 350 and 600 °C, as a function of log R_0.

From general knowledge in carbohydrate and soil chemistry, we know that the degraded carbohydrate product, 5-HMF, can polymerize into a macromolecule structure called humin, Figure 18.[133,143,149,150,152-154] Our results show that the temperature where this occurs is at 200 °C, which coincide with several published works as the same temperature acetic acid start release from the hemicellulose of hardwoods, Figure 17.[79,135,142,158]

The side-product called pseudo-lignin, apparent in the increase of Klason lignin content, is formed under SE-treatment with identical conditions to what is needed for formation of humins. The pseudo-lignin definition states that it has to be a mass increase in residue,

therefore lignin side-products from rearrangement and intramolecular nucleophilic attacks are excluded, as they will never increase the total mass. The only other source of the mass increase has to be the holocellulose, which is substantiated by the py-GC-MS results. The optimal SE temperature to preserve carbohydrates for enzymatic degradation and prevention of unwanted pseudo-lignin generation is then at 200 °C.
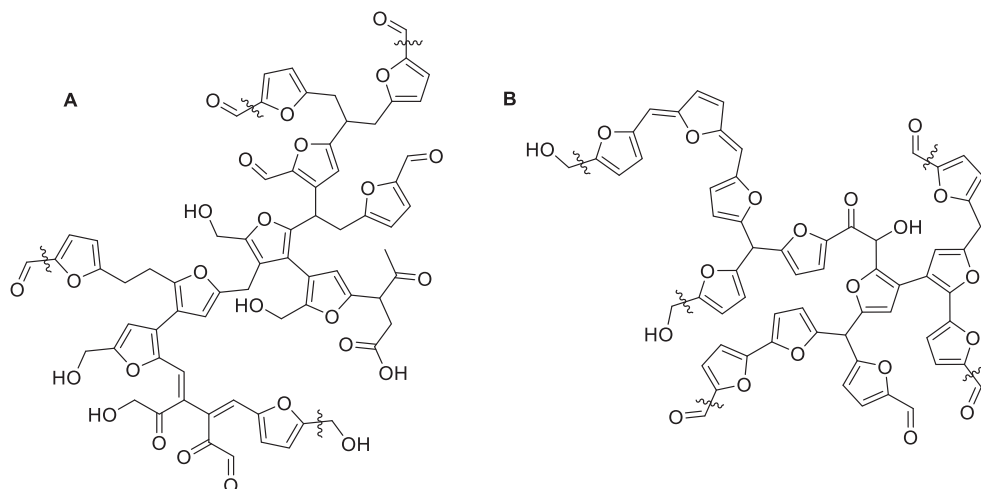

Figure 18. Humin structures derived from: A) glucose B) xylose (van Zandvoort et. al.*)[152]*

In **paper III** the effect MWL extraction has on the composition of the pyrolyzate of SE samples was investigated. Steam-exploded Norway spruce was extracted with MWL after SE, before being isothermally pyrolyzed. These pyrograms were then compared to the non-extracted fractionated pyrograms of the same samples. Klason lignin and carbohydrate analysis was also performed after SE for all samples.

Since Norway spruce is a softwood there was a need for diluted acid for optimal hydrolysis, and H_2SO_4 (0.5% w/w) was chosen for presoaking. The SE was performed at several temperatures (180, 190, 200 and 210 °C, respectively) using a 5 and 10 min residence time. Klason lignin and carbohydrate analyses showed that the pseudo-lignin content increased with an estimated 6.4%.

The extracted samples showed a decrease in polymeric degree with increasing SE severity, comparable to the results in **paper II**, from HSQC-NMR. The pyrolyzate after extraction showed again no significant change in lignin composition as a function of SE

severity, Figure 19. However, 4-hydroxy-3-methoxybenzaldehyde (vanillin) has a sudden increase from 10 to 16% from the untreated sample to pretreated sample before decreasing until 12%. In addition, there was a small increase of furan-like components from untreated sample to pretreated samples.
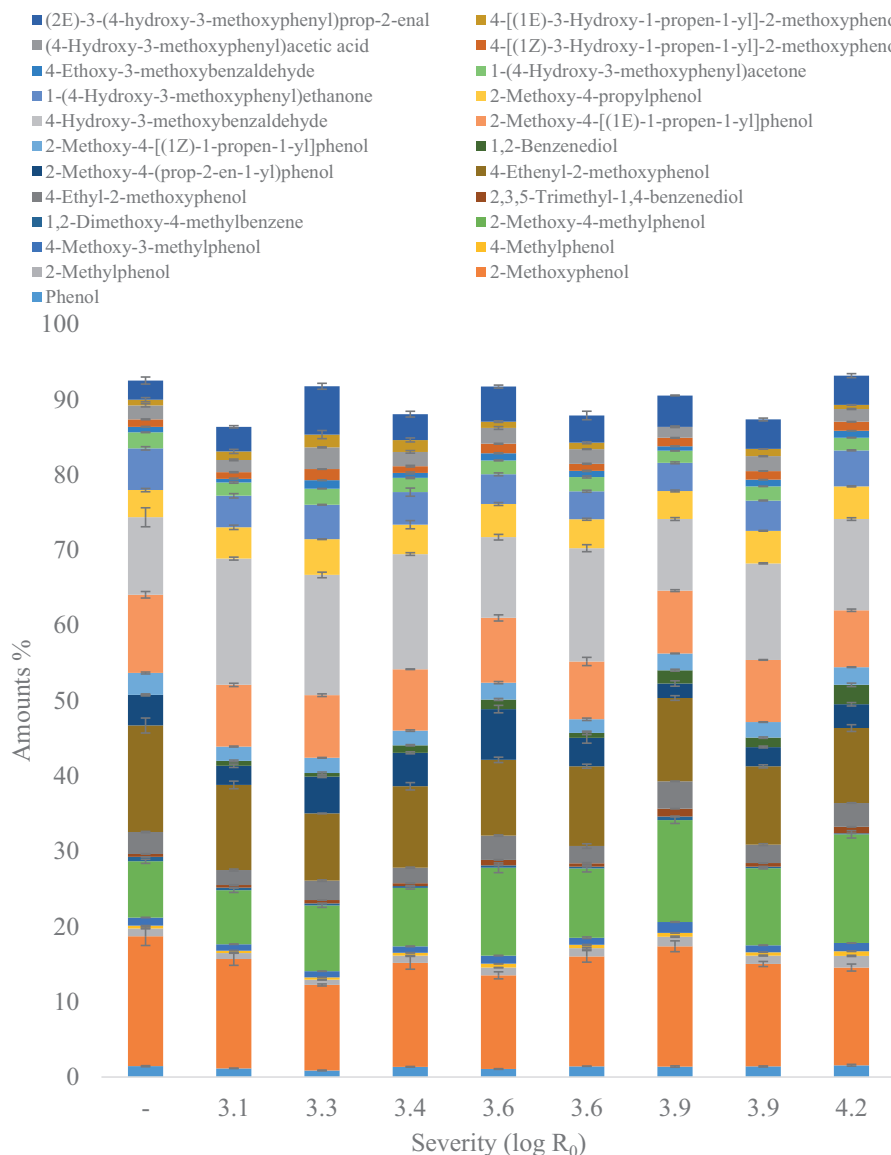

Figure 19. From paper III. Amount of all lignin components in MWL-extracted samples from py-GC-MS at 600 °C, non-lignin components are not shown and are less than 15 %. The SE-samples with identical log R_0 are placed with the low-high temperature from left to right.

The non-extracted samples, again, showed no significant change in benzene like components as a function of SE severity in the pyrograms, Figure 20. However, vanillin behaved differently in non-extracted than in extracted samples. In non-extracted samples the vanillin amount jumps from 11% in untreated sample to 31% in the first pretreated sample. Vanillin amounts are constant at around 31% for all SE severities. Since the yield of vanillin is lower with MWL extraction, it implies that vanillin is connected to the part which is removed under extraction, namely the carbohydrates. This is indicative that the LCC are connected to lignin through mostly vanillin monomers.
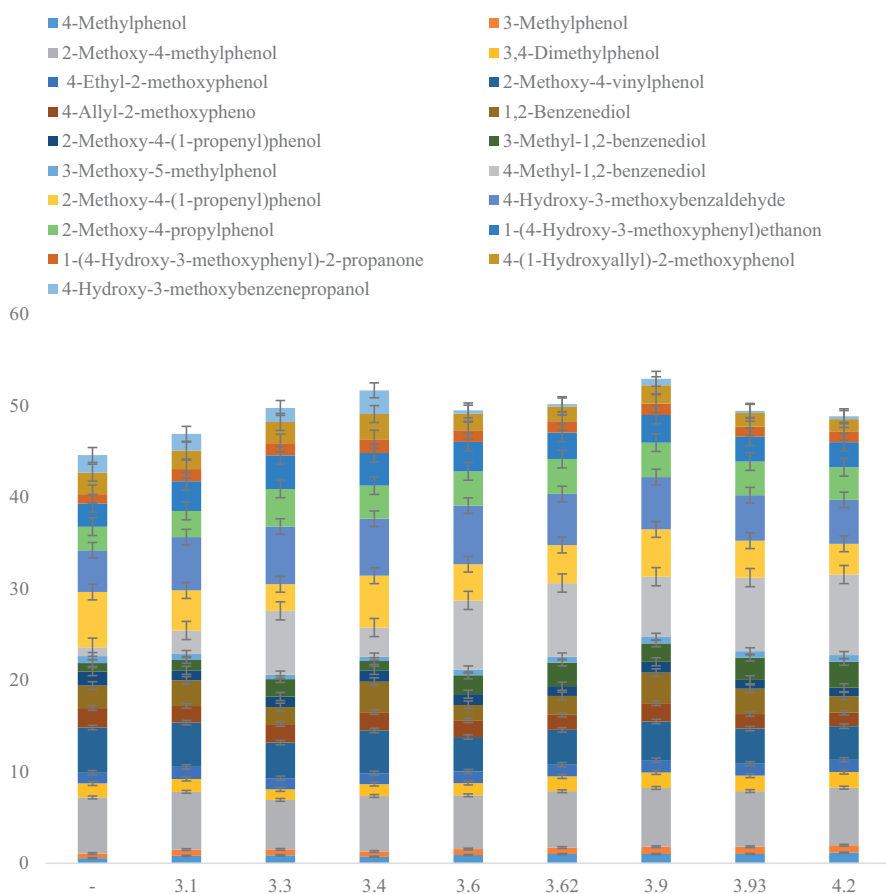

Figure 20. Benzene components from 600 °C fractionated pyrolysis of non-extracted lignin, from paper III. The SE-samples with identical log R_0 are placed with the low-high temperature from left to right.

The furan-like components did increase from a total of 18% in the untreated sample to 26% in the highest severity pretreated sample. The 5-HMF by itself increase from 9 to 20% in the pyrolyzate, Figure 21. This is a similar trend as observed in **paper II**, and there is no apparent evidence in the pyrolyzate indicating that pseudo-lignin is a lignin-like polymer (with 6-membered aromatic units). It is more likely that it is composed of a polymeric furan structure, similar to the humin structure.
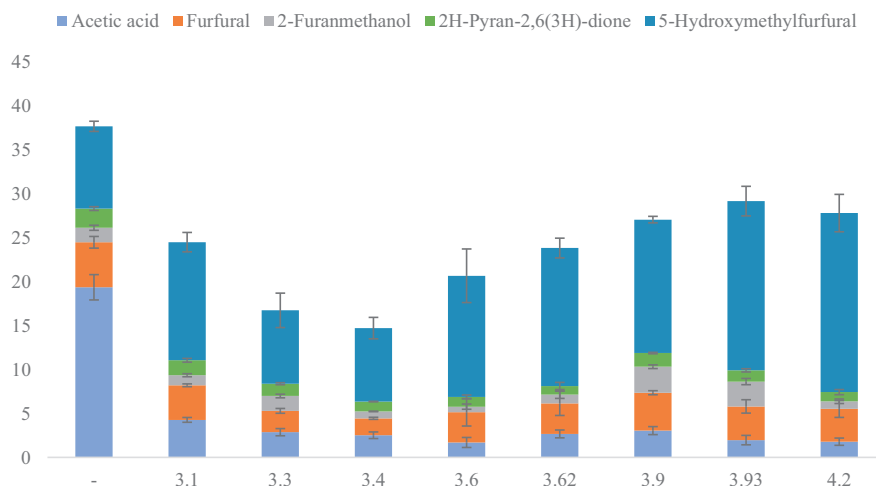

Figure 21. Non-benzene components from 350 °C fractionated pyrolysis of non-extracted samples, from paper III. The SE-samples with identical log R_0 are placed with the low-high temperature from left to right.

In **paper IV** the effect of pH control under SE, and subsequent extraction of acetylated galactoglucomannan from Norway spruce, was investigated. The HSQC-NMR spectra of the filtrate after SE revealed that the negative control sample (no buffer) and the sample buffered at pH 4 (sodium citrate) degrades lignin and carbohydrates, to a bigger extent than neutral pH (pH 6, sodium citrate and pH 7, potassium phosphate). The HSQC-NMR spectra showed 5-HMF in the control and acidic sample, and confirm that carbohydrates are degraded into 5-HMF under acidic conditions, Figure 22.
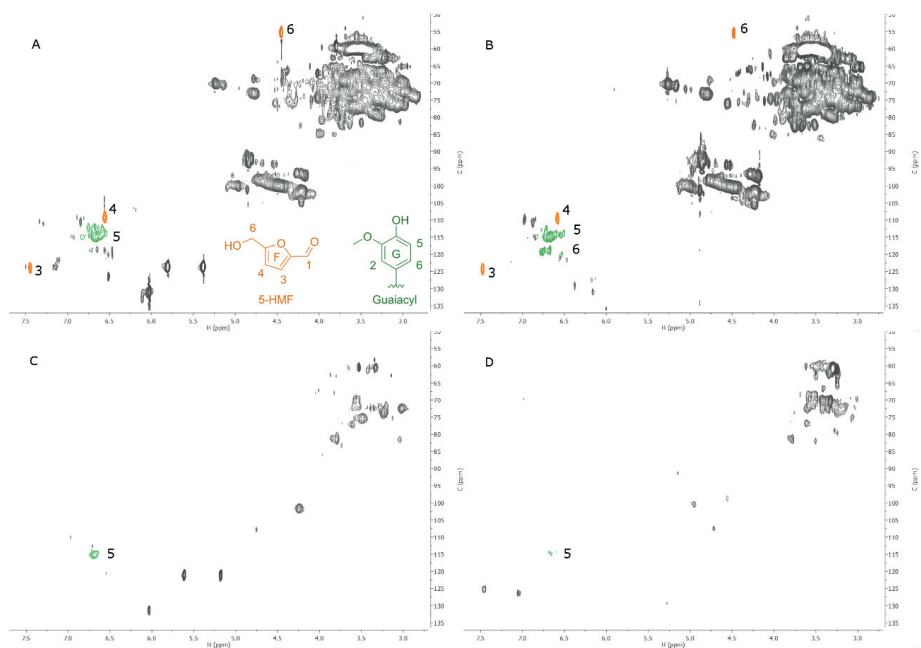
Figure 22.From paper IV. HSQC 2D NMR Spectra of lignin content in biomass residues: (A) sodium citrate pH 4.0 buffered sample, (B) no buffer control, (C) sodium citrate pH 6.0 and (D) potassium phosphate pH 7.0. 5-hydroxymethylfurfural (5-HMF) and Guaiacyl are depicted in the lower right of panel A, signals are colored and numbered according to the structures they relate to.

3 Concluding remarks and future work

As the aim states, there is a need for a better understanding of the changes happening with the lignin structure when different wood types are SE treated and the side-products formed. We established a library of several positively identified volatile pyrolyzate components from lignin, with reproducibility across severities and wood sources. The side-product, pseudo-lignin, was also identified to an extent, as furan-like components and seems to have a polymeric structure more similar to humin than native lignin. An important improvement to the studies in this thesis would be to develop a method for fully quantifying each component in the pyrograms. This will give a more detailed and correct picture of the evolution of lignin and side-products from SE.

A second possibility for the weight increases of Klason lignin is the addition reaction of degraded carbohydrates onto the lignin polymers. This was not investigated in our studies, but a project on this subject has been started within the group. These hypothesized structures will be synthesized and subsequently analyzed on py-GC-MS, for comparison towards genuine biomass samples.

An equally interesting possibility is to synthesize the pseudo-lignin hypothesized in this thesis, by steam-exploding both monomeric and polymeric carbohydrate sources under similar conditions as the biomass. Subsequent py-GC-MS analysis at several different isothermal pyrolysis temperatures and solid-state NMR should reveal an even better insight into the pseudo-lignin structure.

4 References

1. Leitner, W., Klankermayer, J., Pischinger, S., Pitsch, H. & Kohse-Höinghaus, K. (2017). Advanced Biofuels and Beyond: Chemistry Solutions for Propulsion and Production. *Angew. Chem. Int. Ed.*, 56 (20): 5412-5452. http://dx.doi.org/10.1002/anie.201607257.
2. Palkovits, R. (2018). Sustainable Carbon Sources and Renewable Energy: Challenges and Opportunities at the Interface of Catalysis and Reaction Engineering. *Chem. Ing. Tech.* http://dx.doi.org/10.1002/cite.201800042.
3. Moulijn, J. A., Makkee, M. & Diepen, A. v. (2013). Chemical process technology. In, pp. 7-40. Chichester, West Sussex, United Kingdom: John Wiley & Sons Inc.
4. Shinde, S. D., Meng, X., Kumar, R. & Ragauskas, A. J. (2018). Recent advances in understanding the pseudo-lignin formation in a lignocellulosic biorefinery. *Green Chem*, 20 (10): 2192-2205. http://dx.doi.org/10.1039/C8GC00353J.
5. Vivekanand, V., Olsen, E. F., Eijsink, V. G. H. & Horn, S. J. (2013). Effect of different steam explosion conditions on methane potential and enzymatic saccharification of birch. *Bioresour. Technol.*, 127 (0): 343-349. http://dx.doi.org/10.1016/j.biortech.2012.09.118.
6. Azadi, P., Inderwildi, O. R., Farnood, R. & King, D. A. (2013). Liquid fuels, hydrogen and chemicals from lignin: A critical review. *Renew. Sustainable Energy Rev.*, 21 (0): 506-523. http://dx.doi.org/10.1016/j.rser.2012.12.022.
7. Beckham, G. T., Johnson, C. W., Karp, E. M., Salvachua, D. & Vardon, D. R. (2016). Opportunities and challenges in biological lignin valorization. *Curr. Opin. Biotechnol.*, 42: 40-53. http://dx.doi.org/10.1016/j.copbio.2016.02.030.
8. Mullick, A. K. (1996). 7 - Use of lignin-based products in concrete. In Chandra, S. (ed.) *Waste Materials Used in Concrete Manufacturing*, pp. 352-429. Westwood, NJ: William Andrew Publishing.
9. McCoy, M. (2016). *Has lignin's time finally come?* Chemical & engineering news: ACS. Available at: https://cen.acs.org/articles/94/i39/lignins-time-finally-come.html (accessed: 02.10.2018).
10. Azeez, A. M., Meier, D. & Odermatt, J. (2011). Temperature dependence of fast pyrolysis volatile products from European and African biomasses. *J. Anal. Appl. Pyrolysis*, 90 (2): 81-92. http://dx.doi.org/10.1016/j.jaap.2010.11.005.
11. Bridgwater, A. V. (2012). Review of fast pyrolysis of biomass and product upgrading. *Biomass Bioenergy*, 38: 68-94. https://doi.org/10.1016/j.biombioe.2011.01.048.
12. Miller, R. B. (1999). Characteristics and Availability of Commercially Important Woods. In Laboratory, F. P. (ed.) *Wood handbook : wood as an engineering material*, pp. 1-2.
13. Fengel, D. & Grosser, D. (1975). Chemische Zusammensetzung von Nadel- und Laubhölzern. *Holz als Roh- und Werkstoff*, 33 (1): 32-34. http://dx.doi.org/10.1007/BF02612913.
14. Sjöström, E. (1993). Wood chemistry : fundamentals and applications. In, pp. 53-62. San Diego: Academic Press.
15. Pettersen, R. C. (1984). The Chemical Composition of Wood. In Advances in Chemistry, vol. 207 *The Chemistry of Solid Wood*, pp. 57-126: American Chemical Society.
16. Côté, W. A. (1977). Wood Ultrastructure in Relation to Chemical Composition. In Loewus, F. A. & Runeckles, V. C. (eds) *The Structure, Biosynthesis, and Degradation of Wood*, pp. 1-44. Boston, MA: Springer US.

17. Endler, A. & Persson, S. (2011). Cellulose Synthases and Synthesis in Arabidopsis. *Mol Plant*, 4 (2): 199-211. https://doi.org/10.1093/mp/ssq079.

18. Carpita, N. C. & Gibeaut, D. M. (1993). Structural models of primary cell walls in flowering plants: consistency of molecular structure with the physical properties of the walls during growth. *The Plant Journal*, 3 (1): 1-30. http://dx.doi.org/10.1111/j.1365-313X.1993.tb00007.x.

19. Turner, S. R. (2007). Cell Walls: Monitoring Integrity with THE Kinase. *Curr. Biol.*, 17 (14): R541-R542. https://doi.org/10.1016/j.cub.2007.05.033.

20. Cosgrove, D. J. (2005). Growth of the plant cell wall. *Nat Rev Mol Cell Biol*, 6 (11): 850-861. http://dx.doi.org/10.1038/nrm1746.

21. Kumar, M., Campbell, L. & Turner, S. (2016). Secondary cell walls: biosynthesis and manipulation. *J. Exp. Bot.*, 67 (2): 515-531. http://dx.doi.org/10.1093/jxb/erv533.

22. Keegstra, K., Talmadge, K. W., Bauer, W. D. & Albersheim, P. (1973). The Structure of Plant Cell Walls: III. A Model of the Walls of Suspension-cultured Sycamore Cells Based on the Interconnections of the Macromolecular Components. *Plant Physiol*, 51 (1): 188-197.

23. Brett, C. T. & Waldron, K. W. (1990). Physiology and biochemistry of plant cell walls. In, pp. 4-57: Unwin.

24. Cosgrove, D. J. (2014). Re-constructing our models of cellulose and primary cell wall assembly. *Current opinion in plant biology*, 22: 122-131. http://dx.doi.org/10.1016/j.pbi.2014.11.001.

25. del Rio, J. C., Prinsen, P., Cadena, E. M., Martinez, A. T., Gutierrez, A. & Rencoret, J. (2016). Lignin-carbohydrate complexes from sisal (*Agave sisalana*) and abaca (*Musa textilis*): chemical composition and structural modifications during the isolation process. *Planta*, 243 (5): 1143-1158. http://dx.doi.org/10.1007/s00425-016-2470-1.

26. Balakshin, M. Y., Capanema, E. A. & Chang, H.-m. (2007). MWL fraction with a high concentration of lignin-carbohydrate linkages: isolation and 2D NMR spectroscopic analysis. *Holzforschung*, 61 (1): 1-7. http://dx.doi.org/10.1515/HF.2007.001.

27. Du, X., Gellerstedt, G. & Li, J. (2013). Universal fractionation of lignin-carbohydrate complexes (LCCs) from lignocellulosic biomass: an example using spruce wood. *Plant J*, 74 (2): 328-338. http://dx.doi.org/10.1111/tpj.12124.

28. Mosier, N., Wyman, C., Dale, B., Elander, R., Lee, Y. Y., Holtzapple, M. & Ladisch, M. (2005). Features of promising technologies for pretreatment of lignocellulosic biomass. *Bioresour. Technol.*, 96 (6): 673-686. https://doi.org/10.1016/j.biortech.2004.06.025.

29. Sjöström, E. (1993). Wood chemistry : fundamentals and applications. In, pp. 73-86. San Diego: Academic Press.

30. Christopher, L. P. (2013). Integrated forest biorefineries: challenges and opportunities. In Christopher, L. P. (ed.) *Integrated Forest Biorefineries*, pp. 1-66. Cambridge: Royal Society of Chemistry.

31. McNamara, J. T., Morgan, J. L. W. & Zimmer, J. (2015). A Molecular Description of Cellulose Biosynthesis. *Annu. Rev. Biochem*, 84 (1): 895-921. http://dx.doi.org/10.1146/annurev-biochem-060614-033930.

32. Gardner, K. H. & Blackwell, J. (1974). The hydrogen bonding in native cellulose. *Biochimica et Biophysica Acta (BBA) - General Subjects*, 343 (1): 232-237. https://doi.org/10.1016/0304-4165(74)90256-6.

33. ACS. (2017). *The Anselme Payen Award*. ACS. Available at: https://cell.sites.acs.org/anselmepayenaward.htm (accessed: 18.09.2018).

34. McCarthy, J. L. & Islam, A. (1999). Lignin Chemistry, Technology, and Utilization: A Brief History. In ACS Symposium Series, vol. 742 *Lignin: Historical, Biological, and Materials Perspectives*, pp. 2-99: American Chemical Society.

35. Shmulsky, R. & Jones, P. D. (2011). Forest products and wood science : an introduction. In, pp. 141-174. Chichester, West Sussex, U.K. ; Ames, Iowa: Wiley-Blackwell.

36. Willför, S., Sundberg, K., Tenkanen, M. & Holmbom, B. (2008). Spruce-derived mannans – A potential raw material for hydrocolloids and novel advanced natural materials. *Carbohydr. Polym.*, 72 (2): 197-210. https://doi.org/10.1016/j.carbpol.2007.08.006.

37. Holtzapple, M. T. (2003). HEMICELLULOSES. In Caballero, B. (ed.) *Encyclopedia of Food Sciences and Nutrition (Second Edition)*, pp. 3060-3071. Oxford: Academic Press.

38. Lora, J. H. & Glasser, W. G. (2002). Recent Industrial Applications of Lignin: A Sustainable Alternative to Nonrenewable Materials. *J. Polym. Environ.*, 10 (1): 39-48. http://dx.doi.org/10.1023/A:1021070006895.

39. Gosselink, R. J. A., de Jong, E., Guran, B. & Abächerli, A. (2004). Co-ordination network for lignin—standardisation, production and applications adapted to market requirements (EUROLIGNIN). *Ind. Crops. Prod.*, 20 (2): 121-129. https://doi.org/10.1016/j.indcrop.2004.04.015.

40. Calvo-Flores, F. G. & Dobado, J. A. (2010). Lignin as Renewable Raw Material. *ChemSusChem*, 3 (11): 1227-1235. http://dx.doi.org/10.1002/cssc.201000157.

41. Li, J., Li, B. & Zhang, X. (2002). Comparative studies of thermal degradation between larch lignin and manchurian ash lignin. *Polym. Degrad. Stab.*, 78 (2): 279-285. https://doi.org/10.1016/S0141-3910(02)00172-6.

42. Tolbert, A., Akinosho, H., Khunsupat, R., Naskar, A. K. & Ragauskas, A. J. (2014). Characterization and analysis of the molecular weight of lignin for biorefining studies. *Biofuel Bioprod Biorefin*, 8 (6): 836-856. http://dx.doi.org/10.1002/bbb.1500.

43. El Hage, R., Brosse, N., Chrusciel, L., Sanchez, C., Sannigrahi, P. & Ragauskas, A. (2009). Characterization of milled wood lignin and ethanol organosolv lignin from miscanthus. *Polym. Degrad. Stab.*, 94 (10): 1632-1638. https://doi.org/10.1016/j.polymdegradstab.2009.07.007.

44. Crestini, C., Melone, F., Sette, M. & Saladino, R. (2011). Milled Wood Lignin: A Linear Oligomer. *Biomacromolecules*, 12 (11): 3928-3935. http://dx.doi.org/10.1021/bm200948r.

45. Hu, T. Q. (2008). Characterization of lignocellulosic materials. In, pp. 148-170. Oxford, UK ; Ames, Iowa, USA: Blackwell.

46. Parthasarathi, R., Romero, R. A., Redondo, A. & Gnanakaran, S. (2011). Theoretical Study of the Remarkably Diverse Linkages in Lignin. *J.Phys. Chem. Lett.*, 2 (20): 2660-2666. http://dx.doi.org/10.1021/jz201201q.

47. Munk, L., Sitarz, A. K., Kalyani, D. C., Mikkelsen, J. D. & Meyer, A. S. (2015). Can laccases catalyze bond cleavage in lignin? *Biotechnol. Adv.*, 33 (1): 13-24. http://dx.doi.org/10.1016/j.biotechadv.2014.12.008.

48. Hatfield, R. & Vermerris, W. (2001). Lignin Formation in Plants. The Dilemma of Linkage Specificity. *Plant Physiol*, 126 (4): 1351-1357. http://dx.doi.org/10.1104/pp.126.4.1351.

49. Jensen, A., Cabrera, Y., Hsieh, C.-W., Nielsen, J., Ralph, J. & Felby, C. (2017). 2D NMR characterization of wheat straw residual lignin after dilute acid

pretreatment with different severities. *Holzforschung*, 71 (6): 461-469. http://dx.doi.org/10.1515/hf-2016-0112.

50. Parthasarathi, R., Romero, R. A., Redondo, A. & Gnanakaran, S. (2011). Theoretical study of the remarkably diverse linkages in lignin. *J. Phys. Chem. Lett.*, 2 (20): 2660-2666. http://dx.doi.org/10.1021/jz201201q.

51. Younker, J. M., Beste, A. & Buchanan Iii, A. C. (2012). Computational study of bond dissociation enthalpies for lignin model compounds: β-5 arylcoumaran. *Chem. Phys. Lett.*, 545: 100-106. http://dx.doi.org/10.1016/j.cplett.2012.07.017.

52. Elder, T. (2014). Bond dissociation enthalpies of apinoresinol lignin model compound. *Energy Fuels*, 28 (2): 1175-1182. http://dx.doi.org/10.1021/ef402310h.

53. Kim, S., Chmely, S. C., Nimlos, M. R., Bomble, Y. J., Foust, T. D., Paton, R. S. & Beckham, G. T. (2011). Computational study of bond dissociation enthalpies for a large range of native and modified lignins. *J.Phys. Chem. Lett.*, 2 (22): 2846-2852. http://dx.doi.org/10.1021/jz201182w.

54. Aarum, I., Devle, H., Ekeberg, D., Horn, S. J. & Stenstroem, Y. (2017). The effect of flash pyrolysis temperature on compositional variability of pyrolyzates from birch lignin. *J. Anal. Appl. Pyrolysis*, 127: 211-222. http://dx.doi.org/10.1016/j.jaap.2017.08.003.

55. Lin, S. Y. & Dence, C. W. (1992). Methods in lignin chemistry. In *Springer series in wood science*, pp. 3-19. Berlin ; New York: Springer-Verlag.

56. Santos, R. B., Capanema, E. A., Balakshin, M. Y., Chang, H.-m. & Jameel, H. (2012). Lignin structural variation in hardwood species. *J. Agric. Food Chem.*, 60 (19): 4923-4930. http://dx.doi.org/10.1021/jf301276a.

57. Liu, C.-J. (2012). Deciphering the Enigma of Lignification: Precursor Transport, Oxidation, and the Topochemistry of Lignin Assembly. *Mol Plant*, 5 (2): 304-317. https://doi.org/10.1093/mp/ssr121.

58. Yaku, F., Tanaka, R. & Koshijima, T. (1981). Lignin Carbohydrate Complex. Pt. IV. Lignin as Side Chain of the Carbohydrate in Björkman LCC. *Holzforschung - International Journal of the Biology, Chemistry, Physics and Technology of Wood*, 35 (4): 177-181. http://dx.doi.org/10.1515/hfsg.1981.35.4.177.

59. Guerra, A., Filpponen, I., Lucia, L. A. & Argyropoulos, D. S. (2006). Comparative Evaluation of Three Lignin Isolation Protocols for Various Wood Species. *J. Agric. Food. Chem.*, 54 (26): 9696-9705. http://dx.doi.org/10.1021/jf062433c.

60. Lenihan, P., Orozco, A., O'Neill, E., Ahmad, M. N. M., Rooney, D. W. & Walker, G. M. (2010). Dilute acid hydrolysis of lignocellulosic biomass. *Chem. Eng. J.*, 156 (2): 395-403. https://doi.org/10.1016/j.cej.2009.10.061.

61. Kumar, P., Barrett, D. M., Delwiche, M. J. & Stroeve, P. (2009). Methods for Pretreatment of Lignocellulosic Biomass for Efficient Hydrolysis and Biofuel Production. *Ind. Eng. Chem. Res.*, 48 (8): 3713-3729. http://dx.doi.org/10.1021/ie801542g.

62. Sindhu, R., Binod, P. & Pandey, A. (2016). Biological pretreatment of lignocellulosic biomass – An overview. *Bioresour. Technol.*, 199: 76-82. https://doi.org/10.1016/j.biortech.2015.08.030.

63. Carvalheiro, F., Duarte, L. C. & Girio, F. M. (2008). Hemicellulose biorefineries: a review on biomass pretreatments. *J. Sci. Ind. Res.*, 67 (11): 849-864.

64. Gellerstedt, G., Tomani, P., Axegård, P. & Backlund, B. (2013). Integrated forest biorefineries: challenges and opportunities. In Christopher, L. P. (ed.) *Integrated Forest Biorefineries*, pp. 180-210. Cambridge: Royal Society of Chemistry.

65. Suhara, H., Kodama, S., Kamei, I., Maekawa, N. & Meguro, S. (2012). Screening of selective lignin-degrading basidiomycetes and biological pretreatment for enzymatic hydrolysis of bamboo culms. *Int Biodeterior Biodegradation*, 75: 176-180. https://doi.org/10.1016/j.ibiod.2012.05.042.

66. Du, W., Yu, H., Song, L., Zhang, J., Weng, C., Ma, F. & Zhang, X. (2011). The promoting effect of byproducts from Irpex lacteus on subsequent enzymatic hydrolysis of bio-pretreated cornstalks. *Biotechnol Biofuels*, 4 (1): 37. http://dx.doi.org/10.1186/1754-6834-4-37.

67. Castoldi, R., Bracht, A., de Morais, G. R., Baesso, M. L., Correa, R. C. G., Peralta, R. A., Moreira, R. d. F. P. M., Polizeli, M. d. L. T. d. M., de Souza, C. G. M. & Peralta, R. M. (2014). Biological pretreatment of Eucalyptus grandis sawdust with white-rot fungi: Study of degradation patterns and saccharification kinetics. *Chem. Eng. J.*, 258: 240-246. https://doi.org/10.1016/j.cej.2014.07.090.

68. Song, L., Yu, H., Ma, F. & Zhang, X. (2013). Biological pretreatment under non-sterile conditions for enzymatic hydrolysis of corn stover. *BioResources*, 8: 3802-3816.

69. Cianchetta, S., Di Maggio, B., Burzi, P. L. & Galletti, S. (2014). Evaluation of selected white-rot fungal isolates for improving the sugar yield from wheat straw. *Appl. Biochem. Biotechnol.*, 173 (2): 609-623. http://dx.doi.org/10.1007/s12010-014-0869-3.

70. Dhiman, S. S., Haw, J.-R., Kalyani, D., Kalia, V. C., Kang, Y. C. & Lee, J.-K. (2015). Simultaneous pretreatment and saccharification: Green technology for enhanced sugar yields from biomass using a fungal consortium. *Bioresour. Technol.*, 179: 50-57. https://doi.org/10.1016/j.biortech.2014.11.059.

71. McMillan, J. D. (1994). Pretreatment of Lignocellulosic Biomass. In ACS Symposium Series, vol. 566 *Enzymatic Conversion of Biomass for Fuels Production*, pp. 292-324: American Chemical Society.

72. Weil, J., Sarikaya, A., Rau, S.-L., Goetz, J., Ladisch, C. M., Brewer, M., Hendrickson, R. & Ladisch, M. R. (1997). Pretreatment of yellow poplar sawdust by pressure cooking in water. *Appl. Biochem. Biotechnol.*, 68 (1): 21-40. http://dx.doi.org/10.1007/BF02785978.

73. Sun, Y. & Cheng, J. (2002). Hydrolysis of lignocellulosic materials for ethanol production: a review. *Bioresour. Technol.*, 83 (1): 1-11. https://doi.org/10.1016/S0960-8524(01)00212-7.

74. Duff, S. J. B. & Murray, W. D. (1996). Bioconversion of forest products industry waste cellulosics to fuel ethanol: A review. *Bioresour. Technol.*, 55 (1): 1-33. https://doi.org/10.1016/0960-8524(95)00122-0.

75. Holtzapple, M. T., Humphrey, A. E. & Taylor, J. D. (1989). Energy requirements for the size reduction of poplar and aspen wood. *Biotechnol. Bioeng.*, 33 (2): 207-210. http://dx.doi.org/10.1002/bit.260330210.

76. Jacquet, N., Maniet, G., Vanderghem, C., Delvigne, F. & Richel, A. (2015). Application of Steam Explosion as Pretreatment on Lignocellulosic Material: A Review. *Ind. Eng. Chem. Res.*, 54 (10): 2593-2598. http://dx.doi.org/10.1021/ie503151g.

77. Carvalheiro, F., Duarte, L. C., Gírio, F. & Moniz, P. (2016). Chapter 14 - Hydrothermal/Liquid Hot Water Pretreatment (Autohydrolysis): A Multipurpose Process for Biomass Upgrading. In Mussatto, S. I. (ed.) *Biomass Fractionation Technologies for a Lignocellulosic Feedstock Based Biorefinery*, pp. 315-347. Amsterdam: Elsevier.

78. Li, J., Gellerstedt, G. & Toven, K. (2009). Steam explosion lignins; their extraction, structure and potential as feedstock for biodiesel and chemicals.

Bioresour.   Technol.,   100   (9):   2556-2561. http://dx.doi.org/10.1016/j.biortech.2008.12.004.

79. Sundqvist, B., Karlsson, O. & Westermark, U. (2006). Determination of formic-acid and acetic acid concentrations formed during hydrothermal treatment of birch wood and its relation to colour, strength and hardness. *Wood Sci Technol*, 40 (7): 549-561. http://dx.doi.org/10.1007/s00226-006-0071-z.

80. Overend, R. P., Chornet, E. & Gascoigne, J. A. (1987). Fractionation of Lignocellulosics by Steam-Aqueous Pretreatments [and Discussion]. *Philosophical Transactions of the Royal Society of London A: Mathematical, Physical and Engineering Sciences*, 321 (1561): 523-536.

81. Bjorkman, A. (1956). Finely divided wood. I. Extraction of lignin with neutral solvents. *Sven. Papperstidn.*, 59: 477-85.

82. Rencoret, J., Marques, G., Gutiérrez, A., Nieto, L., Jiménez-Barbero, J., Martínez, Á. T. & del Río, J. C. (2009). Isolation and structural characterization of the milled-wood lignin from Paulownia fortunei wood. *Ind. Crops. Prod.*, 30 (1): 137-143. http://dx.doi.org/10.1016/j.indcrop.2009.03.004.

83. Obst, J. R. & Kirk, T. K. (1988). Isolation of lignin. *Methods Enzymol.*, 161 (Biomass, Pt. B): 3-12.

84. Terashima, N., Nakashima, J. & Takabe, K. (1998). Proposed Structure for Protolignin in Plant Cell Walls. In ACS Symposium Series, vol. 697 *Lignin and Lignan Biosynthesis*, pp. 180-193: American Chemical Society.

85. Lin, S. Y. & Dence, C. W. (1992). Methods in lignin chemistry. In *Springer series in wood science*, pp. 65-70. Berlin ; New York: Springer-Verlag.

86. Holtman, K. M., Chang, H.-m. & Kadla, J. F. (2004). Solution-State Nuclear Magnetic Resonance Study of the Similarities between Milled Wood Lignin and Cellulolytic Enzyme Lignin. *J. Agric. Food. Chem.*, 52 (4): 720-726. http://dx.doi.org/10.1021/jf035084k.

87. Ikeda, T., Holtman, K., Kadla, J. F., Chang, H.-m. & Jameel, H. (2002). Studies on the Effect of Ball Milling on Lignin Structure Using a Modified DFRC Method. *J. Agric. Food. Chem.*, 50 (1): 129-135. http://dx.doi.org/10.1021/jf010870f.

88. Chang, H.-m., Cowling Ellis, B. & Brown, W. (1975). Comparative Studies on Cellulolytic Enzyme Lignin and Milled Wood Lignin of Sweetgum and Spruce. *Holzforschung - International Journal of the Biology, Chemistry, Physics and Technology   of   Wood*,   29   (5):   153-159. http://dx.doi.org/10.1515/hfsg.1975.29.5.153.

89. Lin, S. Y. & Dence, C. W. (1992). Methods in lignin chemistry. In *Springer series in wood science*, pp. 71-74. Berlin ; New York: Springer-Verlag.

90. TAPPI. (2006). *T 222 om-2 - Acid-insoluble lignin in wood and pulp*.

91. A. Sluiter, B. H., R. Ruiz, C. Scarlata, J. Sluiter, D. Templeton. (2004). Determination of Structural Carbohydrates and Lignin in Biomass [Electronic Resource]. *Laboratory Analytical Procedure (LAP)*.

92. Uden, P. C. (1993). Nomenclature and terminology for analytical pyrolysis (IUPAC Recommendations 1993). *Pure Appl. Chem.*, 65 (11): 2405-2409. http://dx.doi.org/10.1351/pac199365112405.

93. Collard, F.-X. & Blin, J. (2014). A review on pyrolysis of biomass constituents: Mechanisms and composition of the products obtained from the conversion of cellulose, hemicelluloses and lignin. *Renew. Sustainable Energy Rev.*, 38: 594-608. http://dx.doi.org/10.1016/j.rser.2014.06.013.

94.   Van de Velden, M., Baeyens, J., Brems, A., Janssens, B. & Dewil, R. (2010). Fundamentals, kinetics and endothermicity of the biomass pyrolysis reaction. *Renew. Energ.*, 35 (1): 232-242. http://dx.doi.org/10.1016/j.renene.2009.04.019.

95.   Mamleev, V., Bourbigot, S., Le Bras, M. & Yvon, J. (2009). The facts and hypotheses relating to the phenomenological model of cellulose pyrolysis. *J. Anal. Appl. Pyrolysis*, 84 (1): 1-17. http://dx.doi.org/10.1016/j.jaap.2008.10.014.

96.   Hosoya, T., Kawamoto, H. & Saka, S. (2009). Role of methoxyl group in char formation from lignin-related compounds. *J. Anal. Appl. Pyrolysis*, 84 (1): 79-83. http://dx.doi.org/10.1016/j.jaap.2008.10.024.

97.   Wooten, J. B., Seeman, J. I. & Hajaligol, M. R. (2004). Observation and Characterization of Cellulose Pyrolysis Intermediates by 13C CPMAS NMR. A New Mechanistic Model. *Energy Fuels*, 18 (1): 1-15. http://dx.doi.org/10.1021/ef0300601.

98.   Collard, F.-X., Blin, J., Bensakhria, A. & Valette, J. (2012). Influence of impregnated metal on the pyrolysis conversion of biomass constituents. *J. Anal. Appl. Pyrolysis*, 95: 213-226. http://dx.doi.org/10.1016/j.jaap.2012.02.009.

99.   Pastorova, I., Botto, R. E., Arisz, P. W. & Boon, J. J. (1994). Cellulose char structure: a combined analytical pyrolysis gas chromatography-mass spectrometry, FTIR, and NMR study. *Carbohydr. Res.*, 262 (1): 27-47. http://dx.doi.org/10.1016/0008-6215(94)84003-2.

100.   Lede, J., Blanchard, F. & Boutin, O. (2002). Radiant flash pyrolysis of cellulose pellets: Products and mechanisms involved in transient and steady state conditions. *Fuel*, 81 (10): 1269-1279. http://dx.doi.org/10.1016/S0016-2361(02)00039-X.

101.   Jakab, E., Faix, O. & Till, F. (1997). Thermal decomposition of milled wood lignins studied by thermogravimetry/mass spectrometry. *J. Anal. Appl. Pyrolysis*, 40,41: 171-186. http://dx.doi.org/10.1016/S0165-2370(97)00046-6.

102.   Sanghi, R. & Singh, V. (2012). Green Chemistry for Environmental Remediation. In *Green Chemistry for Environmental Remediation*, pp. 291-342. Hoboken: Wiley.

103.   Ragauskas, A. J., Beckham, G. T., Biddy, M. J., Chandra, R., Chen, F., Davis, M. F., Davison, B. H., Dixon, R. A., Gilna, P., Keller, M., et al. (2014). Lignin Valorization: Improving Lignin Processing in the Biorefinery. *Science (Washington, DC, U. S.)*, 344 (6185): 709. http://dx.doi.org/10.1126/science.1246843.

104.   FitzPatrick, M., Champagne, P., Cunningham, M. F. & Whitney, R. A. (2010). A biorefinery processing perspective: Treatment of lignocellulosic materials for the production of value-added products. *Bioresour. Technol.*, 101 (23): 8915-8922. http://dx.doi.org/10.1016/j.biortech.2010.06.125.

105.   Czernik, S. & Bridgwater, A. V. (2004). Overview of applications of biomass fast pyrolysis oil. *Energy Fuels*, 18 (2): 590-598. http://dx.doi.org/10.1021/ef034067u.

106.   Evans, R. J. & Milne, T. A. (1987). Molecular characterization of the pyrolysis of biomass. *Energy Fuels*, 1 (2): 123-137. http://dx.doi.org/10.1021/ef00002a001.

107.   Blanco Lopez, M. C., Blanco, C. G., Martinez-Alonso, A. & Tascon, J. M. D. (2002). Composition of gases released during olive stones pyrolysis. *J. Anal. Appl. Pyrolysis*, 65 (2): 313-322. http://dx.doi.org/10.1016/S0165-2370(02)00008-6.

108. Morf, P., Hasler, P. & Nussbaumer, T. (2002). Mechanisms and kinetics of homogeneous secondary reactions of tar from continuous pyrolysis of wood chips. *Fuel*, 81 (7): 843-853. http://dx.doi.org/10.1016/S0016-2361(01)00216-2.

109. Amen-Chen, C., Pakdel, H. & Roy, C. (2001). Production of monomeric phenols by thermochemical conversion of biomass: A review. *Bioresour. Technol.*, 79 (3): 277-299. http://dx.doi.org/10.1016/S0960-8524(00)00180-2.

110. Akazawa, M., Kojima, Y. & Kato, Y. (2016). Effect of pyrolysis temperature on the pyrolytic degradation mechanism of β-aryl ether linkages. *J. Anal. Appl. Pyrolysis*, 118: 164-174. http://dx.doi.org/10.1016/j.jaap.2016.02.001.

111. Akazawa, M., Kato, Y. & Kojima, Y. (2016). Application of two resinols as lignin dimer models to characterize reaction mechanisms during pyrolysis. *J. Anal. Appl. Pyrolysis*, 122: 355-364. http://dx.doi.org/10.1016/j.jaap.2016.09.006.

112. Wang, M. & Liu, C. (2016). Theoretic studies on decomposition mechanism of o-methoxy phenethyl phenyl ether: Primary and secondary reactions. *J. Anal. Appl. Pyrolysis*, 117: 325-333. http://dx.doi.org/10.1016/j.jaap.2015.10.016.

113. Beste, A. & Buchanan, A. C. (2011). Kinetic analysis of the phenyl-shift reaction in β-O-4 lignin model compounds: A computational study. *J. Org. Chem.*, 76 (7): 2195-2203. http://dx.doi.org/10.1021/jo2000385.

114. Kim, K. H., Bai, X. & Brown, R. C. (2014). Pyrolysis mechanisms of methoxy substituted α-O-4 lignin dimeric model compounds and detection of free radicals using electron paramagnetic resonance analysis. *J. Anal. Appl. Pyrolysis*, 110: 254-263. http://dx.doi.org/10.1016/j.jaap.2014.09.008.

115. Kawamoto, H., Horigoshi, S. & Saka, S. (2007). Effects of side-chain hydroxyl groups on pyrolytic β-ether cleavage of phenolic lignin model dimer. *J. Wood Sci.*, 53 (3): 268-271. http://dx.doi.org/10.1007/s10086-006-0839-7.

116. Wang, S., Dai, G., Yang, H. & Luo, Z. (2017). Lignocellulosic biomass pyrolysis mechanism: A state-of-the-art review. *Prog. Energy Combust. Sci.*, 62: 33-86. https://doi.org/10.1016/j.pecs.2017.05.004.

117. Kawamoto, H. (2017). Lignin pyrolysis reactions. *J Wood Sci*: 1-16. http://dx.doi.org/10.1007/s10086-016-1606-z.

118. Huang, J., Liu, C., Wu, D., Tong, H. & Ren, L. (2014). Density functional theory studies on pyrolysis mechanism of β-O-4 type lignin dimer model compound. *J. Anal. Appl. Pyrolysis*, 109: 98-108. https://doi.org/10.1016/j.jaap.2014.07.007.

119. Chen, L., Ye, X., Luo, F., Shao, J., Lu, Q., Fang, Y., Wang, X. & Chen, H. (2015). Pyrolysis mechanism of βO4 type lignin model dimer. *J. Anal. Appl. Pyrolysis*, 115: 103-111. https://doi.org/10.1016/j.jaap.2015.07.009.

120. Elder, T. & Beste, A. (2014). Density functional theory study of the concerted pyrolysis mechanism for lignin models. *Energy Fuels*, 28 (8): 5229-5235. http://dx.doi.org/10.1021/ef5013648.

121. Williams, D. H. & Fleming, I. (2008). Spectroscopic methods in organic chemistry. In, pp. 62-179. London: McGraw-Hill.

122. Bodenhausen, G. & Ruben, D. J. (1980). Natural abundance nitrogen-15 NMR by enhanced heteronuclear spectroscopy. *Chem. Phys. Lett.*, 69 (1): 185-189. https://doi.org/10.1016/0009-2614(80)80041-8.

123. Setälä, H., Pajunen, A., Rummakko, P., Sipilä, J. & Brunow, G. (1999). A novel type of spiro compound formed by oxidative cross coupling of methyl sinapate with a syringyl lignin model compound. A model system for the β-1 pathway in lignin biosynthesis. *J. Chem. Soc., Perkin Trans. 1* (4): 461-464. http://dx.doi.org/10.1039/A808884E.

124. Maunu, S. L. (2002). NMR studies of wood and wood products. *Prog. Nucl. Magn. Reson. Spectrosc.*, 40 (2): 151-174. https://doi.org/10.1016/S0079-6565(01)00041-3.

125. Sette, M., Lange, H. & Crestini, C. (2013). QUANTITATIVE HSQC ANALYSES OF LIGNIN: A PRACTICAL COMPARISON. *Comput Struct Biotechnol J*, 6 (7): e201303016. https://doi.org/10.5936/csbj.201303016.

126. Sette, M., Wechselberger, R. & Crestini, C. (2011). Elucidation of Lignin Structure by Quantitative 2D NMR. *Chem. Eur. J.*, 17 (34): 9529-9535. http://dx.doi.org/10.1002/chem.201003045.

127. Capanema, E. A., Balakshin, M. Y. & Kadla, J. F. (2004). A Comprehensive Approach for Quantitative Lignin Characterization by NMR Spectroscopy. *J. Agric. Food. Chem.*, 52 (7): 1850-1860. http://dx.doi.org/10.1021/jf035282b.

128. Balakshin, M., Capanema, E., Gracz, H., Chang, H.-m. & Jameel, H. (2011). Quantification of lignin-carbohydrate linkages with high-resolution NMR spectroscopy. *Planta*, 233 (6): 1097-1110. http://dx.doi.org/10.1007/s00425-011-1359-2.

129. Hu, F., Jung, S. & Ragauskas, A. (2013). Impact of Pseudolignin versus Dilute Acid-Pretreated Lignin on Enzymatic Hydrolysis of Cellulose. *ACS Sustainable Chem. Eng.*, 1 (1): 62-65. http://dx.doi.org/10.1021/sc300032j.

130. Hu, F., Jung, S. & Ragauskas, A. (2012). Pseudo-lignin formation and its impact on enzymatic hydrolysis. *Bioresour. Technol.*, 117 (0): 7-12. http://dx.doi.org/10.1016/j.biortech.2012.04.037.

131. Xianzhi, M. & Ragauskas, A. (2017). Pseudo-Lignin Formation during Dilute acid Pretreatment for Cellulosic Ethanol. *Recent Adv Petrochem Sci.*, 1 (1): 1-5. http://dx.doi.org/10.19080/RAPSCI.2017.01.555551.

132. Rasmussen, H., Tanner, D., Sorensen, H. R. & Meyer, A. S. (2017). New degradation compounds from lignocellulosic biomass pretreatment: routes for formation of potent oligophenolic enzyme inhibitors. *Green Chem*, 19 (2): 464-473. http://dx.doi.org/10.1039/C6GC01809B.

133. Sannigrahi, P., Kim, D. H., Jung, S. & Ragauskas, A. (2011). Pseudo-lignin and pretreatment chemistry. *Energy Environ. Sci.*, 4 (4): 1306-1310. http://dx.doi.org/10.1039/C0EE00378F.

134. Jönsson, L. J., Alriksson, B. & Nilvebrant, N.-O. (2013). Bioconversion of lignocellulose: inhibitors and detoxification. *Biotechnol Biofuels*, 6: 16. http://dx.doi.org/10.1186/1754-6834-6-16.

135. Li, J., Henriksson, G. & Gellerstedt, G. (2007). Lignin depolymerization/repolymerization and its critical role for delignification of aspen wood by steam explosion. *Bioresour. Technol.*, 98 (16): 3061-3068. http://dx.doi.org/10.1016/j.biortech.2006.10.018.

136. Kumar, R., Hu, F., Sannigrahi, P., Jung, S., Ragauskas, A. J. & Wyman, C. E. (2013). Carbohydrate derived-pseudo-lignin can retard cellulose biological conversion. *Biotechnol. Bioeng.*, 110 (3): 737-53. http://dx.doi.org/10.1002/bit.24744.

137. Shuai, L., Amiri, M. T., Questell-Santiago, Y. M., Heroguel, F., Li, Y., Kim, H., Meilan, R., Chapple, C., Ralph, J. & Luterbacher, J. S. (2016). Formaldehyde stabilization facilitates lignin monomer production during biomass depolymerization. *Science (Washington, DC, U. S.)*, 354 (6310): 329-333. http://dx.doi.org/10.1126/science.aaf7810.

138. Araya, F., Troncoso, E., Mendonça, R. T. & Freer, J. (2015). Condensed lignin structures and re-localization achieved at high severities in autohydrolysis of

Eucalyptus globulus wood and their relationship with cellulose accessibility. *Biotechnol. Bioeng.*, 112 (9): 1783-1791. http://dx.doi.org/10.1002/bit.25604.

139. Leschinsky, M., Zuckerstätter, G., Weber Hedda, K., Patt, R. & Sixta, H. (2008). Effect of autohydrolysis of Eucalyptus globulus wood on lignin structure. Part 1: Comparison of different lignin fractions formed during water prehydrolysis. *Holzforschung*, 62 (6): 645-652. http://dx.doi.org/10.1515/HF.2008.117.

140. Shimada, K., Hosoya, S. & Ikeda, T. (1997). Condensation Reactions of Softwood and Hardwood Lignin Model Compounds Under Organic Acid Cooking Conditions. *J. Wood Chem. Technol.*, 17 (1-2): 57-72. http://dx.doi.org/10.1080/02773819708003118.

141. Sturgeon, M. R., Kim, S., Lawrence, K., Paton, R. S., Chmely, S. C., Nimlos, M., Foust, T. D. & Beckham, G. T. (2014). A Mechanistic Investigation of Acid-Catalyzed Cleavage of Aryl-Ether Linkages: Implications for Lignin Depolymerization in Acidic Environments. *ACS Sustainable Chem Eng*, 2 (3): 472-485. http://dx.doi.org/10.1021/sc400384w.

142. Li, J., Henriksson, G. & Gellerstedt, G. (2005). Carbohydrate reactions during high-temperature steam treatment of aspen wood. *Appl. Biochem. Biotechnol.*, 125 (3): 175-188. http://dx.doi.org/10.1385/ABAB:125:3:175.

143. Rice, J. A. (2001). HUMIN. *Soil Science*, 166 (11): 848-857. http://doi.org/10.1097/00010694-200111000-00009.

144. Glasser, W. G. & Wright, R. S. (1998). Steam-assisted biomass fractionation. 2. Fractionation behavior of various biomass resources. *Biomass Bioenergy*, 14 (3): 219-235. http://dx.doi.org/10.1016/S0961-9534(97)10037-X.

145. Nef, J. U. (1910). Dissoziationsvorgänge in der Zuckergruppe. Über das Verhalten der Zuckerarten gegen Ätzalkalien. *Justus Liebigs Annalen der Chemie*, 376 (1): 1-119. http://dx.doi.org/10.1002/jlac.19103760102.

146. Moye, C. (1966). The formation of 5-hydroxymethylfurfural from hexoses. *Aust. J. Chem.*, 19 (12): 2317-2320. https://doi.org/10.1071/CH9662317.

147. Mednick, M. L. (1962). The Acid-Base-Catalyzed Conversion of Aldohexose into 5-(Hydroxymethyl)-2-furfural2. *J Org*, 27 (2): 398-403. http://dx.doi.org/10.1021/jo01049a013.

148. Newth, F. H. (1951). The Formation of Furan Compounds from Hexoses. In Hudso, C. S. & Canto, S. M. (eds) vol. 6 *Advances in Carbohydrate Chemistry*, pp. 83-106: Academic Press.

149. Patil, S. K. R., Heltzel, J. & Lund, C. R. F. (2012). Comparison of Structural Features of Humins Formed Catalytically from Glucose, Fructose, and 5-Hydroxymethylfurfuraldehyde. *Energy Fuels*, 26 (8): 5281-5293. http://dx.doi.org/10.1021/ef3007454.

150. Patil, S. K. R. & Lund, C. R. F. (2011). Formation and Growth of Humins via Aldol Addition and Condensation during Acid-Catalyzed Conversion of 5-Hydroxymethylfurfural. *Energy Fuels*, 25 (10): 4745-4755. http://dx.doi.org/10.1021/ef2010157.

151. van Zandvoort, I., Koers, E. J., Weingarth, M., Bruijnincx, P. C. A., Baldus, M. & Weckhuysen, B. M. (2015). Structural characterization of 13C-enriched humins and alkali-treated 13C humins by 2D solid-state NMR. *Green Chem*, 17 (8): 4383-4392. http://dx.doi.org/10.1039/C5GC00327J.

152. van Zandvoort, I., Wang, Y., Rasrendra, C. B., van Eck, E. R. H., Bruijnincx, P. C. A., Heeres, H. J. & Weckhuysen, B. M. (2013). Formation, Molecular Structure, and Morphology of Humins in Biomass Conversion: Influence of Feedstock and Processing Conditions. *ChemSusChem*, 6 (9): 1745-1758. http://dx.doi.org/10.1002/cssc.201300332.

153. van Putten, R.-J., van der Waal, J. C., de Jong, E., Rasrendra, C. B., Heeres, H. J. & de Vries, J. G. (2013). Hydroxymethylfurfural, A Versatile Platform Chemical Made from Renewable Resources. *Chem. Rev.*, 113 (3): 1499-1597. http://dx.doi.org/10.1021/cr300182k.
154. Tuercke, T., Panic, S. & Loebbecke, S. (2009). Microreactor Process for the Optimized Synthesis of 5-Hydroxymethylfurfural: A Promising Building Block Obtained by Catalytic Dehydration of Fructose. *Chem Eng Technol*, 32 (11): 1815-1822. http://dx.doi.org/10.1002/ceat.200900427.
155. Wen, J. L., Sun, S. L., Xue, B. L. & Sun, R. C. (2013). Quantitative structures and thermal properties of birch lignins after ionic liquid pretreatment. *J. Agric. Food. Chem.*, 61 (3): 635-45. http://dx.doi.org/10.1021/jf3051939.
156. Jurak, E. (2015). How mushrooms feed on compost: conversion of carbohydrates and linin in industrial wheat straw based compost enabling the growth of Agaricus bisporus. In, pp. 130-131. Wageningen: Wageningen University.
157. Aarum, I., Devle, H., Ekeberg, D., Horn, S. J. & Stenstrøm, Y. (2017). The effect of flash pyrolysis temperature on compositional variability of pyrolyzates from birch lignin. *J. Anal. Appl. Pyrolysis*, 127: 211-222. http://dx.doi.org/10.1016/j.jaap.2017.08.003.
158. Rissanen, J. V., Grenman, H., Willfor, S., Murzin, D. Y. & Salmi, T. (2014). Spruce Hemicellulose for Chemicals Using Aqueous Extraction: Kinetics, Mass Transfer, and Modeling. *Ind. Eng. Chem. Res.*, 53 (15): 6341-6350. http://dx.doi.org/10.1021/ie500234t.

Paper I

The effect of flash pyrolysis temperature on compositional variability of pyrolyzates from birch lignin

Ida Aarum[*], Hanne Devle, Dag Ekeberg, Svein J. Horn and Yngve Stenstrøm

The effect of flash pyrolysis temperature on compositional variability of pyrolyzates from birch lignin

Ida Aarum[*], Hanne Devle, Dag Ekeberg, Svein J. Horn, Yngve Stenstrøm

Faculty of Chemistry, Biotechnology and Food Science, Norwegian University of Life Sciences, P.O. Box 5003, N-1432 Ås, Norway

ABSTRACT

The influence of the temperature on product formation during flash pyrolysis of birch lignin was investigated by using Py-GC–MS. In this study, milled wood lignin was isolated from *Betula pubescens* and by using Heteronuclear Single Quantum Coherence (^{1}H-^{13}C–HSQC) spectroscopy the S:G ratio was found to be 4.3. The pyrolysis experiments were carried out at temperatures from 400 to 900 °C with a flash filament pyrolysis, Pyrola 2000. The GC–MS method used identified more than 30 different compounds, including aldehydes, aromatic compounds, alkenes, alkanes and ketones. The weakest lignin linkage was found to be the β–O–4, which was cleaved at the lowest temperature range applied (400–500 °C) and gave mainly rise to aldehydes and ketones in the pyrolyzate. At the highest temperature range (750–900 °C) the pyrolyzate contained mostly smaller aromatic compounds without the alkyl chain in C-1 position. Pyrolyzates with the same functional groups in C-1 position, were found to have similar degradation patterns over the temperature range. This was clearly seen for the aldehydes and ketones, but was also observable for alkanes and alkenes. Aldehydes decreased until 500 °C before leveling off, ketones peaked at 700 °C, alkene and C-1 with CH_3 or H peaked at 500 °C while phenylcoumaran increased after 700 °C. This study clearly shows that the HSQC-NMR and flash Py-GC–MS are techniques that provide valuable information of molecular structure of lignin and compositional variance in the products formed by flash pyrolysis. Finally, seven interesting high value compounds were identified which in total amounted to around 45% of the pyrolyzate at 500 °C. These components were 4-ethenyl-2-methoxyphenol, 2,6-dimethoxyphenol, 2,6-dimethoxy-4-methylphenol, 2-(4-hydroxy-3-methoxyphenyl)acetaldehyde, 1-(4-hydroxy-3-methoxyphenyl)ethanone, 4-ethenyl-2,6-dimethoxyphenol and 4-hydroxy-3,5-dimethoxybenzaldehyde.

1. Introduction

Lignin is a complex, hydrophobic biopolymer composed of phenylpropanoid units and is nature's dominant aromatic macromolecule. It is found in plant cell walls and thus in lignocellulosic biomass feedstock used in *e.g.* the pulp & paper industry and in the emerging cellulosic bioethanol industry. Traditionally the carbohydrate part of the biomass have been utilized and converted to other chemicals like ethanol, while the lignin has been burned to generate heat and electricity at the plant site. However, the bioethanol bio-refineries will generate much more lignin than needed to power the operation, and therefore efforts are under way to develop more high value-added products from lignin. There are many possible applications of lignin *e.g.* adhesives, plastics, high value chemicals and biofuels [1–6]. Thus, lignin valorization is an emerging field for research and development, and a better understanding of an optimal and efficient way of depolymerization is needed. Currently large efforts are being put into characterizing and understanding lignin [7–9]. However, previous work has

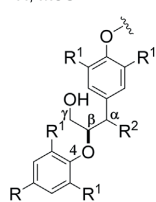often been focusing on simple pyrolysis and model systems.

The mechanisms of lignin degradation are still disputed and many questions have so far remained unanswered regarding to what degree homolysis, "retro-ene" and Maccoll elimination is part of it [10–22]. An improved understanding of these mechanisms can be crucial for a future exploitation of lignin into high value products. Previous studies have shown that the pyrolyzate composition is highly dependent on the utilized temperature [7,12,23–25]. In addition, chemical and physical pretreatments can affect the biomass severely, which also will have an impact on the product formation during the subsequent pyrolysis [6,7,26,27]. Birch is a hardwood species widespread and readily available throughout Northern Europe, and the potential use of this biomass for production of fuels and high value chemicals is of great interest.

Fig. 1 shows the main inter-unit linkages in lignin and their bond dissociation energies (BDE) [9,28–31]. There are several competing reactions in pyrolysis, divided into primary and secondary reactions. Of the primary mechanisms, there are three reaction pathways:

R = alkyl
R^1 = H, MeO

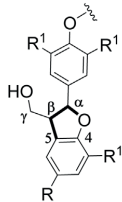

Fig. 1. Main bonding patterns in native lignin. The bond dissociation energy (BDE) is from [9,28–31] and corresponds to the bold marked bonds.
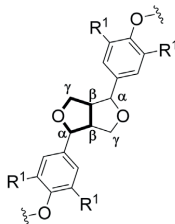
β–O–4 and β–O–4'
BDE (R^2= OH): 290.79 kJ/mol
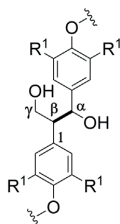BDE (R^2= =O): 239.07 kJ/mol
[31]

β–5 and α–O–4
BDE (α–O): 175.73 kJ/mol
BDE (α–β): 246.69 kJ/mol
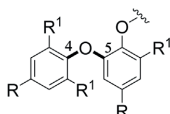BDE (β–5): 685.97 kJ/mol
[9, 30]

β–β
BDE (α–β): 273.50 kJ/mol
BDE (α–O): 285.60 kJ/mol
BDE (γ–O): 333.00 kJ/mol
BDE (β–γ): 330.49 kJ/mol
BDE (β–β): 339.30 kJ/mol
[29]

β–1
BDE (α–β): 345.14 kJ/mol
[9]

4–O–5
BDE (C–O): 345.35 kJ/mol
[9]

5–5
BDE (β–β): 480.95 kJ/mol
[31]

depolymerization, fragmentation, and char formation. Depolymerization and fragmentation are the most preferred reactions as they give rise to monomeric units and small organic products [32–37]. Formation of char is undesired as it gives rise to more condensed structures that are difficult to separate and utilize [1,38,39]. Secondary reactions including cracking, that destroy high value volatile products initially formed into low molecular weight (MW) molecules and recombination of these molecules. This causes enclosed char formation in the pores of the macromolecule, also called secondary char [37,38,40–45]. Both char and secondary reactions are expected to be minimal with a high heating rate during pyrolysis [46]. In this study, this was achieved by a fixed heating rate of 175 000 °C/s in 8 ms.

The objective of this study was to investigate the effect of pyrolysis temperature on the composition of the pyrolyzate obtained isothermal from birch milled wood lignin (MWL).

2. Materials and methods

2.1. Materials

Lignin samples were prepared from a birch tree (*Betula pubescens*) harvested in Tyristrand, Norway (60°07′00″N, 10°04′00″E) [47]. Stem wood without bark was shredded (20–30 mm chips), packed and shipped to the Norwegian University of Life Sciences, Ås, Norway. The material was dried at room temperature, then milled to pass a sieve of 10 mm (SM2000, Retsch, Haan, Germany), and stored at room temperature. The preparation of the lignin samples were done by the Bjorkman method [48,49] and stored in room temperature before being analyzed by Py-GC–MS.

For the Py-GC–MS analysis the following compounds were used as standards (all acquired from Sigma-Aldrich, Steinheim, Germany): 2-methoxyphenol, 3-methoxybenzene-1,2-diol, 1-(2-hydroxy-5-

methylphenyl)ethanone, 2,6-dimethoxyphenol, 1,2,4-trimethoxybenzene, 4-hydroxy-3-methoxybenzaldehyde, 2-methoxy-4-propylphenol, 1-(3-hydroxy-4-methoxyphenyl)ethanone, 1,2,3-trimethoxy-5-methylbenzene, 1(3,4-dimethoxyphenyl)ethanone, 2,6-dimethoxy-4-prop-2-enylphenol, 3,5-dimethoxy-4-hydroxybenzaldehyde, 1-(4-hydroxy-3,5-dimethoxyphenyl)ethanone, 2-t-butyl-6-[(3-t-butyl-5-ethyl-2-hydroxyphenyl)methyl]-4-ethylphenol, 2-methylphenol, 3-methylphenol, 4-methylphenol, 1,2-dihydroxybenzene, diphenylether, 4-methyl-2,6-dimethoxyphenol and 1-(4-hydroxy-3-methoxyphenyl)ethanone. Additional standards were acquired from VWR: 2-methoxy-5-methylphenol, 2-methoxy-4-propenylphenol, 2-methoxy-4-prop-2-enylphenol and 5-t-butylbenzene-1,2,3-triol. The standard 2-(4-hydroxy-3-methoxyphenyl)acetaldehyde was synthesized.

2.2. Synthesis of 2-(4-hydroxy-3-methoxyphenyl) acetaldehyde

The 2-(4-hydroxy-3-methoxyphenyl)acetaldehyde was synthesized from 2-methoxy-4-(prop-2-en-1-yl)phenol (500 mg, 3.045 mol) in 14 mL 1,4-dioxane:H$_2$O (3:1). To the solution 2,6-dimethylpyridine (653 mg, 6.09 mmol), OsO$_4$ (630 μL, in 2.5 wt.% *t*-butanol) and NaIO$_4$ (2.6 g, 12 mmol) were added. The reaction was stirred at ambient temperature for 1.5 h and monitored by thin-layer chromatography, until completion. The reaction was quenched by adding H$_2$O:CH$_2$Cl$_2$ (1:2, 30 mL), and the organic layer was separated. The water phase was extracted 3 times and the organic layers were combined, washed with saturated NaCl (aq) and dried (Na$_2$SO$_4$). The organic layer was filtered through a Hirsch-funnel with a layer of deactivated silica gel (10% v/v of triethylamine), before evaporation.

2.3. Sample preparation of birch milled wood lignin

The milling was done on 10 g of wood chips with a Retsch, Haan,

Germany, GmbH 100PM instrument at 350 rpm, for 12 h, with 30 min on/off increments, to make a fine wood powder. The milled wood was first extracted with acetone for 8 h to get rid of extractives. The milled wood was then dried in a desiccator with P_2O_5 for 72 h before extraction. Extraction was done on the entire sample altogether with a Soxhlet extractor, 1,4-dioxane and water (96:4, v/v) until the solvent was colorless. The solvents were evaporated in a rotary evaporator at 40 °C, and washed with 20 mL deionized water 3–6 times until the 1,4-dioxane was exchanged with water. Finally, the material was freeze-dried. This gave a yield of crude milled wood lignin (MWL) of 1.36 g, from 10 g of wood chips, these where then divided into three aliquots of 340 mg before purification. The crude lignin was dissolved in 90% acetic acid, filtered (Qualitative filter paper 303, 5–13 μm, VWR), and precipitated into deionized water. The precipitated lignin was evaporated and continuously washed 3–6 times until the acetic acid was exchanged with water, before freeze-drying. Thereafter it was dissolved in 1,2-dichloroethane and ethanol (2:1, v/v), filtered and precipitated into diethyl ether. The solvent was evaporated and washed 3–6 times with fresh ether to remove 1,2-dichloroethane; the precipitate was then freeze-dried to give about 200 mg of pure MWL in each aliquot.

2.4. Analysis

2.4.1. HSQC NMR

The NMR spectra were recorded on a Bruker Ascend 400 spectrometer (400 MHz) at 320 K using a 5 mm PABBO probe. The Heteronuclear Single Quantum Coherence (HSQC) spectroscopy was run with 15 mg sample dissolved in DMSO-d_6. The NMR spectra were recorded with a spectral width of 0–10 ppm and 0–165 ppm in ^{1}H and ^{13}C respectively. The number of scans for both were 128 at 27 °C. For the [1]H–[13]C parameters the relaxation time was 1.5 s and the free induction decay dimensions was 2048 and 256, while the number of scans were 120 at 27 °C. All three aliquots were recorded and integrated with respect to S:G ratio in MestReNova (version 9.1.0).

2.4.2. Py-GC–MS analysis of birch milled wood lignin

The flash filament Pyrola 2000 pyrolyzer (Pyrol AB, Lund, Sweden) was coupled to a GC–MS (7000C Triple Quadrupole GC–MS instrument from Agilent technologies) to identify the volatile pyrolyzate generated from fast pyrolysis of lignin over several isothermal temperatures. About 0.15 μg of dry lignin powder was weighted three times with a micropipette applicator on a Sartorius μweight, this was thereafter injected into the pyro-probe. The pyrolysis was set to the following isothermal temperatures at; 400, 450, 500, 600, 650, 700, 750, 800, 850 and 900 °C with a heating rate of 175 000 °C/s. The temperature rise time was 8 ms and the total heating time was 2 s. The volatile pyrolyzate were separated on a capillary column (TraceGOLD TG-1701MS, Thermo Fisher Scientific), with length 60 m, ID 0.25 mm and 0.25 μm film thickness. The injector temperature was 250 °C. The GC oven temperature was programmed from 50 °C (15 min) to 130 °C at a rate of 10 °C/min, then to 270 °C at a rate of 2 °C/min and held at 270 °C for 10 min. The He flow was 1.0 mL/min with a split ratio of 10:1. The mass spectra were obtained using an electron ionization source with 70 eV electrons. The quadrupole was scanned from m/z 40–700. The compounds were identified by the NIST 11 MS library and by comparing the retention times with the standards. The total abundances were obtained by summing the areas of the identified peaks in the pyrograms.

3. Results and discussion

3.1. HSQC 2D-NMR analysis

The HSQC spectra obtained shows that the most prominent linkages are β–O–4 and β–O–4′ (oxidized in α position on the alkyl chain), and several other linkages such as β–β, β–5 and α–O–4 were also identified

(Fig. 2 and Table 1). These results are in agreement with previously published works by del Rio et al. [50], Wen et al. [8] and Shuai et al. [51]. Based on the NMR spectra, (Fig. 2) the ratio of syringyl- and guaiacyl units (S:G) was found to be 4.27 ± 0.05 (n = 3), which is a bit higher reported by Santos et al. [52] who found this ratio to be 3.15 in birch. The comparisons between different hardwoods species shows that birch in general have a larger ratio of S:G [52]. The higher amount of S-units implies a more linear structure of the lignin in the birch used in our study.

3.2. Volatile pyrolyzate

The BDE of the three most abundant bonding patterns, Fig. 1 [9,29–31], in our samples are of similar values (239.07–339.30 kJ/mol), with the exception of C_α–O and C_β–C_{ar-5} in phenylcoumaran that is found to be 175.73 and 685.97 kJ/mol respectivly. The linkages may be cleaved by both primary and secondary mechanisms. Since the pyrolyzer used in this study has a rapid heating time, the secondary mechanisms are expected to be of minor importance. The prevalent pathways for bond cleavage will therefore result in depolymerization and fragmentation into volatile pyrolyzate. Table 2 shows all the integrated compounds in the pyrograms (see supplementary) across the pyrolytic temperature range. It was possible to clearly identify 38 out of 46 peak separated compounds. Fig. 3a–f shows the formation of some selected compounds in relative amounts as pyrolysis temperature was increased from 400 to 900 °C. The compounds are divided into functional groups based on the side chain, R at C-1. Depending on the type of functional group, there are distinct curve trajectories that represent the degradation of lignin at different pyrolysis temperatures.

Fig. 3a shows five different aromatic aldehyde compounds, **24**, **26**, **37**, **41** and **46** (Table 2), that all have similar curve trajectories, except for **26**. The relative amounts of the compounds decrease with increasing pyrolysis temperatures before leveling off at 500 °C. Compounds **24** and **37** have the same aldehyde group in the C-1 position on the aromatic ring, but **24** is a G-unit and **37** is an S-unit. This applies to several other components, such as **41** and **46**, which are G- and S-units of a different aldehyde. The relative amount of each aldehyde at a pyrolysis temperature of 400 °C, especially component **37** indicate that the bond energies releasing aldehydes are the weakest linkages in lignin. The β–O–4 (and β–O–4′) have been calculated to have one of the lowest BDE for the bonding patterns in lignin (290.79 and 239.07 kJ/mol respectively) [31]. These are also the two most abundant bonding patterns in lignin overall [9,28]. Both aldehyde **37** and **26** are actually interesting in regard to their properties within medicinal chemistry. Component **37** has been reported as a promising drug against colon cancer [53]. Additionally it has anti-inflammatory effects similar to the more disputed steroidal drugs [54]. This component is also the most abundant at all pyrolysis temperatures tested this study. Another interesting feature is component **26** that is closely related to a major component in the pheromone control of working honeybees, excreted from the queen bee [55–57].

There are different possible mechanisms for thermal cleavage of a β–O–4 and a β–O–4′ linkages as previously published by Akazawa et al. [16], Wang et al. [18], He et al. [15] and Wang et al. [22]. Component **26** does not seem to depend on pyrolysis temperature (Fig. 3a) and this would indicate that it has a different degradation mechanism than the other aldehydes. The mechanisms and pathways of degradation during pyrolysis, homolysis or concerted, is still disputed [10–22]. When the temperature increased to around 500 °C, the relative amount of aldehydes reaches a minimum. Aldehydes are known to be unstable and the increasing temperature can cause decarbonylation [58,59]. Other lignin linkages will also start degrading at the higher temperatures and the relative amount of aldehydes decreases. This trend is visible in Fig. 3c and d, where an increase of alkenes and alkanes parallel the decrease of aldehydes.

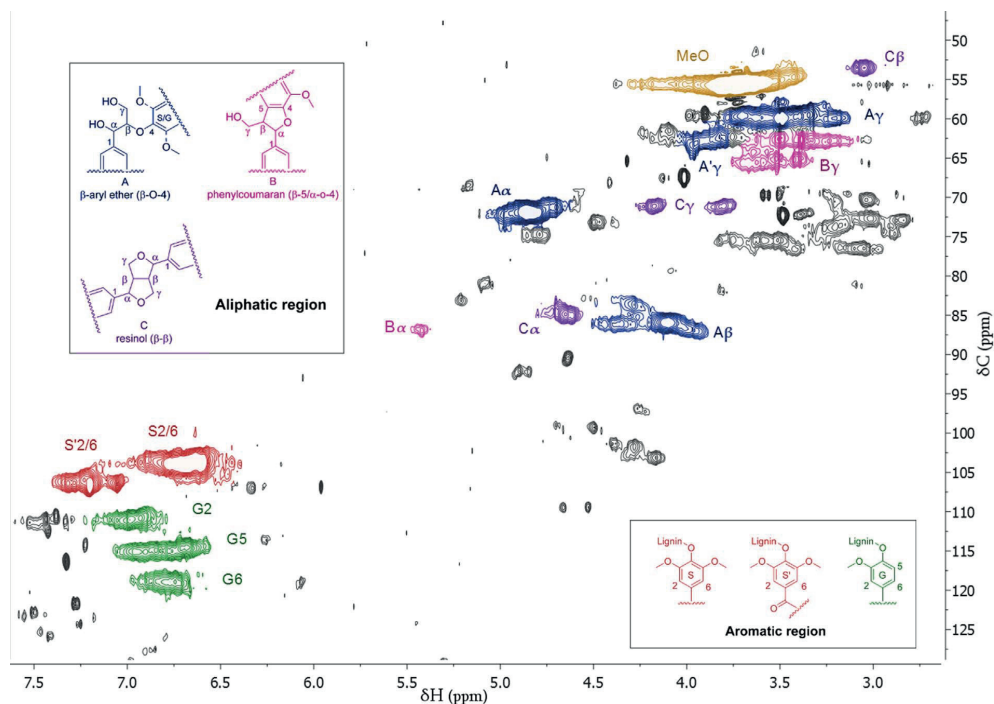The three components **28**, **30** and **40** have ketone functionality in

Fig. 2. HSQC-spectra of birch MWL in DMSO-d_6, assignment in Table 1.

Table 1
Determination of the $^{13}C/^1H$ correlation signals acquired in the 2D HSQC spectra of MWL birch [8,50,51]. The S- and G-units corresponds to the syringyl- and guaiacyl- lignin units.

Label	δ_C/δ_H (ppm)	Assignment
MeO	55.7/3.7	C/H in methoxy
Aα	71.9/4.8	C_α/H_α in β—O–4 substructure
Aβ	86.1/4.1	C_β/H_β in β–O–4 substructure
Aγ	59.7/3.5	C_γ/H_γ in β–O–4 substructure
A'γ	62.8/3.9	C_γ/H_γ in β–O–4' substructure (γ-OH is ester/ γ–C=COOR)
Bα	86.8/5.4	C_α/H_α in β–5/α–O–4 substructure
Bγ	65.3/3.5	C_γ/H_γ in β–5/α–O–4 substructure
Cα	84.6/4.7	C_α/H_α in β–β substructure
Cγ	71.0/3.8 and 71.1/ 4.2	C_γ/H_γ in β–β substructure
Cβ	53.5/3.1	C_β/H_β in β–β substructure
S2/6	104.0/6.7	C_2/H_2 and C_6/H_6 in a S-unit
S'2/6	106.3/7.2	C_2/H_2 and C_6/H_6 in a S'-unit (oxidized)
G2	111.0/7.0	C_2/H_2 in a G-unit
G5	114.9/6.8	C_5/H_5 in a G-unit
G6	118.9/6.8	C_6/H_6 in a G-unit

the α-position. The relative amounts of these compounds peak at 700–750 °C (Fig. 3b). One possible mechanism for ketone formation is hydrogen abstraction in the α-position and fragmentation into the corresponding enol which tautomer into a ketone. This has previously been demonstrated by Watanabe et al. [24] and Akazawa et al. [21,60] on model substances, either through α-hydrogen abstraction, after trimeric fragmentation into phenol radicals, homolysis or concerted mechanisms. Beste et al. [61] have previously published calculations on the H-abstraction in α- and β-position, where they concluded that α-H abstraction will be favored over β, but interestingly also found that if the propagating radical is an alkyl radical instead of phenol radical the
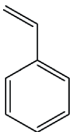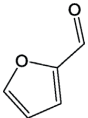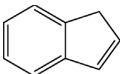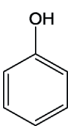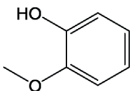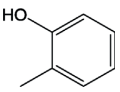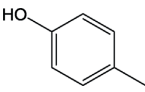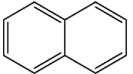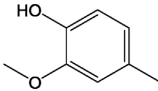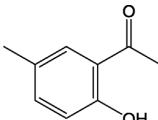
β-H abstraction would also be exothermic. Component **28** is of great interest in several medicinal aspects. It has been shown to decrease the oxidants related to heart deceases such as hypertension, atherosclerosis and heart failure [62–64]. It is also under investigation for treatment of drug addicts, as it shows potential for inhibiting enzymes responsible oxidative stress and mitochondrial dysfunction caused by a methamphetamine overdose [65].

Compound **30** have a different profile than the two other ketones and is not detectable above 700 °C. This was also observed for compound **20**, and both these compounds have adjacent dimethoxy groups (Fig. 4a). The weakest bond for fragmentation is either of the O—CH_3-bonds, but the amount of both dimethoxides are rather low (less than 2%). There is a slight increase of the corresponding fragmentation compounds **28** and **15,** respectively. Suryan et al. [66] have reported experimental data of the BDE of a singular methoxy bond to be 235.56 kJ/mol, which is similar to the other bonds in Fig. 1. Interestingly we do not observe much further fragmentation of methoxide on phenolic compounds. Dorrestjin et al. [12] did some work on the decomposition of the methoxide group on a phenol and the OH interaction with MeO, Fig. 4b. They reported that 93% of the time the OH would be interacting with the free-electron pair on MeO. This implies that it could be beneficial for the components to fragment from dimethoxybenzene into methoxyphenol and CH_4 at elevated temperatures (750 °C).

The compounds shown in Fig. 3c and d have similar curve trajectories; they both decrease steadily after peaking at around 500 °C. The energy related to further degradation of them should be quite similar, as is expected for these types of compounds, based on the BDE and the mechanism for further degradation previously reported by Liu et al. [19]. One compound that diverges from the others is component **20**, which is non-detectable at 750 °C. Component **20** is non-phenolic and has adjacent dimethoxy groups; see Table 2. Component **15** is an insect
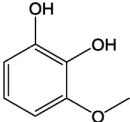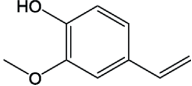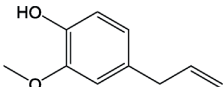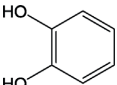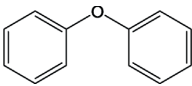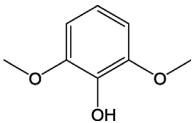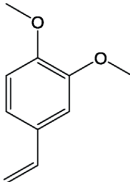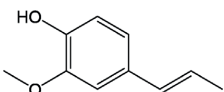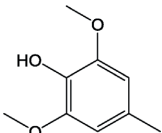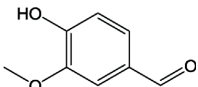
Table 2

All integrated compounds from the pyrogram across all the different isothermal pyrolysis temperatures, see supplementary for pyrograms.

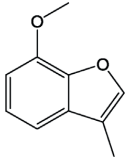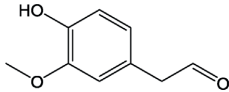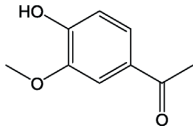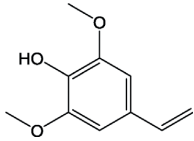| Peak No.	Structure	IUPAC name	RT (min)	M$^+\cdot$ (m/z)
1		ethanoic acid	8.90	60
2		methylbenzene	10.68	92
3	Unknown	not identified	17.23	74
4		ethenylbenzene	19.57	104
5		furan-2-carbaldehyde	20.01	96
6		1*H*-indene	24.86	116
7		phenol	26.45	94116
8		2-methoxyphenol	27.51	124116
9		2-methylphenol	28.06	108
10		4-methylphenol	29.06	108
11		naphthalene	29.43	206
12		2-methoxy-4-methylphenol	30.58	138
13		1-(2-hydroxy-5-methyphenyl)ethanone	33.51	152

Table 2 *(continued)*

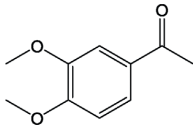| Peak No.	Structure	IUPAC name	RT (min)	M$^+ \cdot$ (m/z)
14		3-methoxy-1,2-benzenediol	35.36	140
15		4-ethenyl-2-methoxyphenol	35.59	150
16		2-methoxy-4-(prop-2-enyl)phenol	36.64	164
17		benzene-1,2-diol	36.79	110
18		1,1′-oxydibenzene	36.91	170
19		2,6-dimethoxyphenol	37.77	154
20		4-ethenyl-1,2-dimethoxybenzene	39.02	164
21	Superimposed	not identified	39.25	154
22		2-methoxy-4-[(E)-prop-1-enyl]phenol	41.29	164
23		2,6-dimethoxy-4-methylphenol	41.88	168
24		4-hydroxy-3-methoxybenzaldehyde	42.00	152
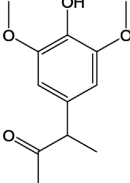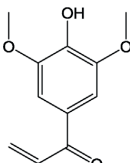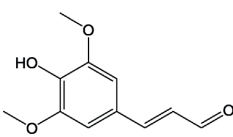
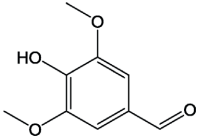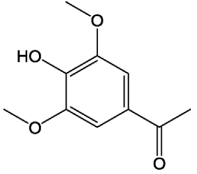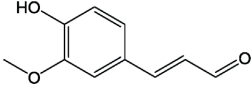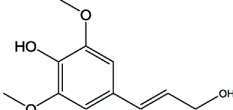*(continued on next page)*

Table 2 *(continued)*

Peak No.	Structure	IUPAC name	RT (min)	$M^+ \cdot$ (m/z)
25		7-methoxy-3-methyl-1-benzofuran	43.02	162
26		2-(4-hydroxy-3-methoxyphenyl)acetaldehyde	44.73	166
27	Unknown	not identified	45.37	182
28		1-(4-hydroxy-3-methoxyphenyl)ethanone	45.87	166
29		4-ethenyl-2,6-dimethoxyphenol	48.10	180
30		1-(3,4-dimethoxyphenyl)ethanone	48.30	180
31		2,6-dimethoxy-4-prop-2-enylphenol	49.10	194
32		1-(4-hydroxy-3-methoxyphenyl)prop-2-en-1-one	50.58	178
33	Superimposed	not identified	50.93	-
34		2,6-dimethoxy-4-[(E)-prop-1-enyl]phenol	51.65	194
35	Unknown	not identified	53.37	192
36	Unknown	not identified	54.51	194

(continued on next page)

217

Table 2 *(continued)*

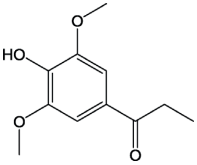| Peak No.	Structure	IUPAC name	RT (min)	$M^+ \cdot$ (m/z)
37		4-hydroxy-3,5-dimethoxybenzaldehyde	55.68	182
38	Unknown	not identified	57.76	196
39	Unknown	not identified	58.76	208
40		1-(4-hydroxy-3,5-dimethoxyphenyl)ethanone	58.98	196
41		(E)-3-(4-hydroxy-3-methoxyphenyl)prop-2-enal	60.42	178
42		4-[(E)-3-hydroxyprop-1-enyl]-2,6-dimethoxyphenol	60.98	210
43		1-(4-hydroxy-3,5-dimethoxyphenyl)propan-1-one	62.66	210
44		3-(4-hydroxy-3,5-dimethoxyphenyl)butan-2-one	62.94	224
45		1-(4-hydroxy-3,5-dimethoxyphenyl)prop-2-en-1-one	63.33	208
46		(E)-3-(4-hydroxy-3,5-dimethoxyphenyl)prop-2-enal	72.48	208

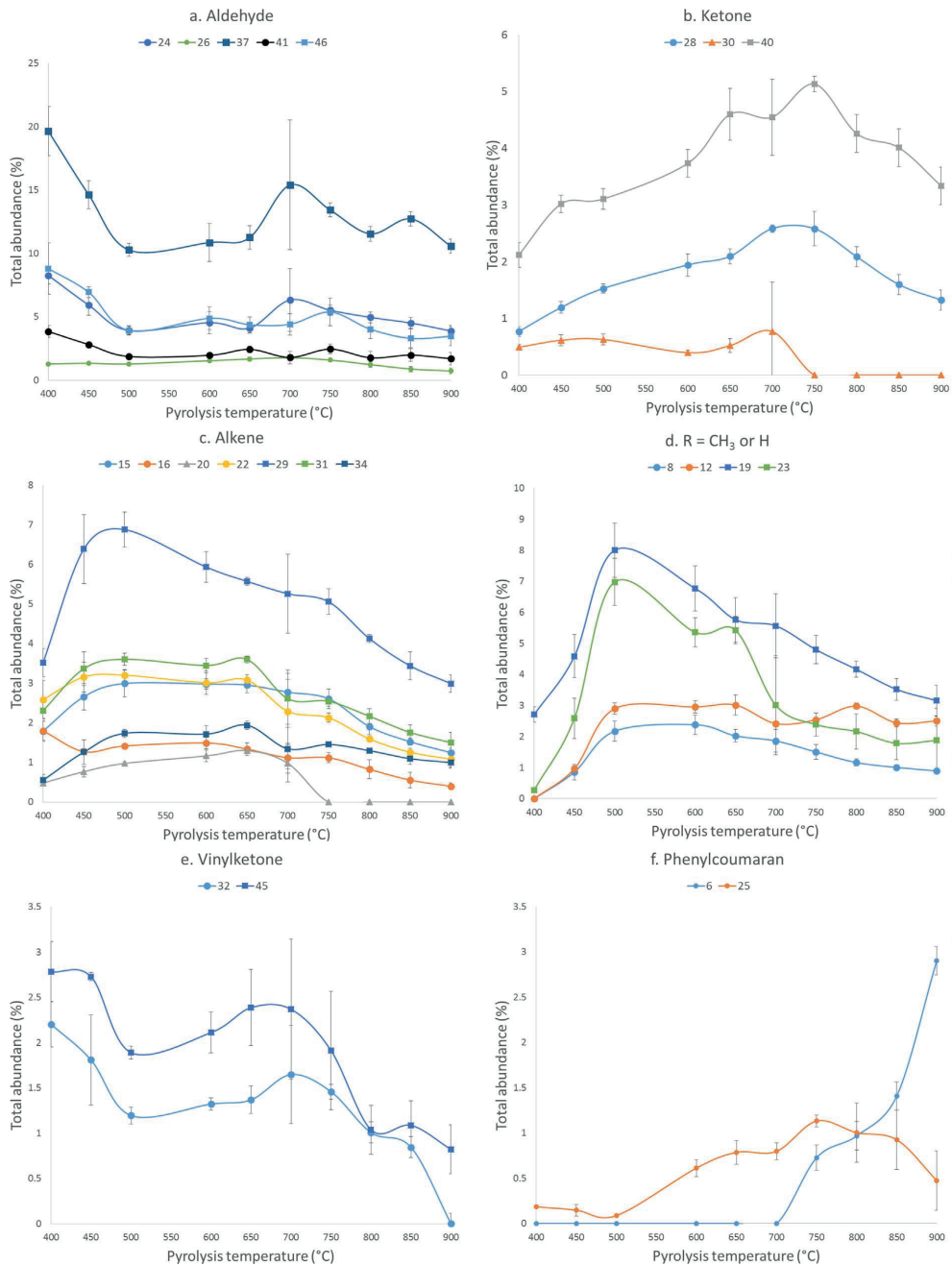**Fig. 3.** Relative amounts of selected compounds as a function of isothermal pyrolysis temperature. The components are separated into each graph according to their functionality on the C-1, a) aldehydes, b) ketones, c) alkenes, d) R = CH$_3$/H, e) vinylketones and f) phenylcoumaran. Symbols depicted represent ■ = S-unit, ● = G-unit, ▲ = Dimethoxyphenol compounds. The error bars show the difference of three aliquots.
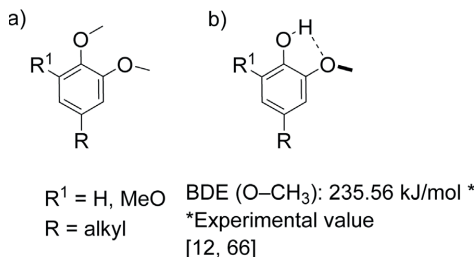
Fig. 4. a) Hydrogen interaction between O and H. b) Dimethoxyphenol compounds [12,66].
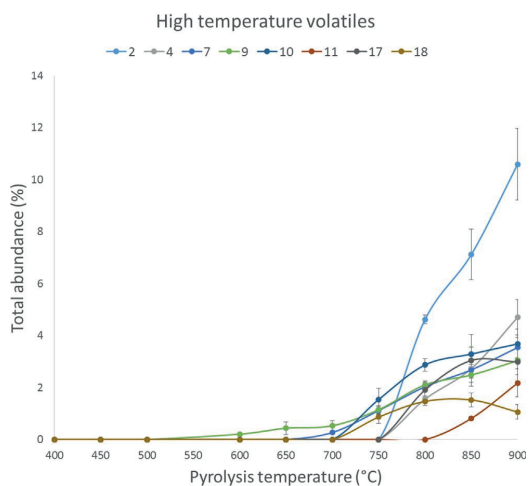

Fig. 5. Relative amount of selected high temperature volatiles as a function of pyrolysis temperature.

pheromone of Red palm weevil (*Rhynchophorus ferrugineus*) in addition to being a flavoring agent from buckwheat [67,68]. Component **29** is another medicinal interesting component. It has been shown to inhibit initiation and progression of gastric tumor in mice [69]. All components in Fig. 3d have been shown to exhibit both antioxidant and antibacterial effects [70,71].

Fig. 3e, shows the curve trajectory for two compounds, **32** and **45**, which correspond to the G- and S-units with vinyl ketone side chains. These structures are interesting because the simplest formation of them would be a "retro-ene" type reaction from the β–β bonding pattern, as previously published by Akazawa et al. [21]. The homolytical cleavage of the same bonding pattern yields a more complex and stepwise mechanism as published by Elder [29] with BDE's of 273.50–339.30 kJ/mol.

Fig. 3f shows two compounds, **6** and **25**, related to the phenylcoumaran coupling in lignin, more specifically the α-O-4 and β-5 cross coupling. The C_{β}–C_{ar-5} BDE is calculated to be one of the strongest bonds in lignin linkage (685.97 kJ/mol) by Parthasarathi et al. [9]. The homolysis of this bond therefore seems unlikely. On the other hand the C_{α}–C_{β} and C_{α}–O–C_{ar-4} BDE is calculated by Younker et al. [30] to be incrementally lower (246.69 and 175.73 kJ/mol, respectively). A publication by Huang et al. [72] focuses on the theoretical homolysis of this linkage through four different pathways. Neither of these mentioned pathways can account for the methyl in γ-position.

Fig. 5 show the formation of volatile compounds that evolve at a high temperatures. These compounds are often associated with

secondary reactions and char formation in thermal degradation of biomass [27,45,73,74]. From the figure, it seems that they mainly evolve from 700 °C, with a few exceptions. Representable structures of these compounds can be seen in Table 2. The inverted trend is also reflected in the decrease of volatile products from Fig. 3, as previously mentioned. To determine if the high temperature components are products from further decomposition of the pyrolyzate or if it is directly degraded from the lignin macromolecule it is necessary to perform analyses with total quantification.

4. Conclusions

We have studied the composition of birch MWL over a temperature range (400–900 °C) of isothermal flash pyrolysis. The components with the same sidechain functionality were observed to have similar temperature profiles. The variation in relative amount of lignin monomers at different isothermal temperatures shows that it is possible to control this with respect to the composition of the pyrolyzate. This open up for more efficient extraction of several high value products. In this study, seven interesting high value compounds were identified which in total amounted to around 45% of the pyrolyzate at 500 °C. Scale-up of such a process is challenging since heat transfer is difficult at large scale, but technologies such as Fluid-bed pyrolyzers give good and consistent performance. However, small biomass particle sizes are needed to achieve high heating rates, meaning that the milling step is important [75]. While the Bjorkman method for lignin isolation probably is not economic at large scale, there exists other methods such as removal of carbohydrates by enzymatic saccharification which would make it possible to valorize both the carbohydrate and lignin fractions of birch in an integrated biorefinery process [76].

Appendix A. Supplementary data

Supplementary data associated with this article can be found, in the online version, at http://dx.doi.org/10.1016/j.jaap.2017.08.003.

References

[1] M. FitzPatrick, P. Champagne, M.F. Cunningham, R.A. Whitney, A biorefinery processing perspective: treatment of lignocellulosic materials for the production of value-added products, Bioresour. Technol. 101 (2010) 8915–8922.
[2] S. Czernik, A.V. Bridgwater, Overview of applications of biomass fast pyrolysis oil, Energy Fuels 18 (2004) 590–598.
[3] A.V. Bridgwater, Renewable fuels and chemicals by thermal processing of biomass, Chem. Eng. J. (Amsterdam Neth.) 91 (2003) 87–102.
[4] M.Y. Balakshin, E.A. Capanema, Comprehensive structural analysis of biorefinery lignins with a quantitative ^{13}C NMR approach, RSC Adv. 5 (2015) 87187–87199.
[5] J. Zhao, W. Xiuwen, J. Hu, Q. Liu, D. Shen, R. Xiao, Thermal degradation of softwood lignin and hardwood lignin by TG-FTIR and Py-GC/MS, Polym. Degrad. Stab. 108 (2014) 133–138.
[6] A.E. Harman-Ware, M. Crocker, A.P. Kaur, M.S. Meier, D. Kato, B. Lynn, Pyrolysis–GC/MS of sinapyl and coniferyl alcohol, J. Anal. Appl. Pyrolysis 99 (2013) 161–169.
[7] D.J. Nowakowski, A.V. Bridgwater, D.C. Elliott, D. Meier, P. de Wild, Lignin fast pyrolysis: results from an international collaboration, J. Anal. Appl. Pyrolysis 88 (2010) 53–72.
[8] J.L. Wen, S.L. Sun, B.L. Xue, R.C. Sun, Quantitative structures and thermal properties of birch lignins after ionic liquid pretreatment, J. Agric. Food. Chem. 61 (2013) 635–645.
[9] R. Parthasarathi, R.A. Romero, A. Redondo, S. Gnanakaran, Theoretical study of the remarkably diverse linkages in lignin, J. Phys. Chem. Lett. 2 (2011) 2660–2666.
[10] T. Elder, A. Beste, Density functional theory study of the concerted pyrolysis mechanism for lignin models, Energy Fuels 28 (2014) 5229–5235.
[11] A. Beste, A.C. Buchanan, Kinetic analysis of the phenyl-shift reaction in β-O-4 lignin model compounds: a computational study, J. Org. Chem. 76 (2011) 2195–2203.
[12] E. Dorrestijn, P. Mulder, The radical-induced decomposition of 2-methoxyphenol, J.

Chem. Soc. Perkin Trans. 2 (1999) 777–780.

[13] K.H. Kim, X. Bai, R.C. Brown, Pyrolysis mechanisms of methoxy substituted α-O-4 lignin dimeric model compounds and detection of free radicals using electron paramagnetic resonance analysis, J. Anal. Appl. Pyrolysis 110 (2014) 254–263.

[14] T. Kotake, H. Kawamoto, S. Saka, Pyrolytic formation of monomers from hardwood lignin as studied from the reactivities of the primary products, J. Anal. Appl. Pyrolysis 113 (2015) 57–64.

[15] T. He, Y. Zhang, Y. Zhu, W. Wen, Y. Pan, J. Wu, J. Wu, Pyrolysis mechanism study of lignin model compounds by synchrotron vacuum ultraviolet photoionization mass spectrometry, Energy Fuels 30 (2016) 2204–2208.

[16] M. Akazawa, Y. Kojima, Y. Kato, Effect of pyrolysis temperature on the pyrolytic degradation mechanism of β-aryl ether linkages, J. Anal. Appl. Pyrolysis 118 (2016) 164–174.

[17] C. Liu, Y. Deng, S. Wu, M. Lei, J. Liang, Experimental and theoretical analysis of the pyrolysis mechanism of a dimeric lignin model compound with α-O-4 linkage, BioResources 11 (2016) 3626–3636.

[18] M. Wang, C. Liu, Theoretic studies on decomposition mechanism of o-methoxy phenethyl phenyl ether: primary and secondary reactions, J. Anal. Appl. Pyrolysis 117 (2016) 325–333.

[19] C. Liu, Y. Deng, S. Wu, H. Mou, J. Liang, M. Lei, Study on the pyrolysis mechanism of three guaiacyl-type lignin monomeric model compounds, J. Anal. Appl. Pyrolysis 118 (2016) 123–129.

[20] J. Huang, C. He, G. Pan, H. Tong, A theoretical research on pyrolysis reactions mechanism of coumarone-contained lignin model compound, Comput. Theor. Chem. 1091 (2016) 92–98.

[21] M. Akazawa, Y. Kato, Y. Kojima, Application of two resinols as lignin dimer models to characterize reaction mechanisms during pyrolysis, J. Anal. Appl. Pyrolysis 122 (2016) 355–364.

[22] S. Wang, B. Ru, G. Dai, Z. Shi, J. Zhou, Z. Luo, M. Ni, K. Cen, Mechanism study on the pyrolysis of a synthetic β-O-4 dimer as lignin model compound, Proc. Combust. Inst. 36 (2017) 2225–2233.

[23] C. Amen-Chen, H. Pakdel, C. Roy, Production of monomeric phenols by thermo-chemical conversion of biomass: a review, Bioresour. Technol. 79 (2001) 277–299.

[24] T. Watanabe, H. Kawamoto, S. Saka, Radical chain reactions in pyrolytic cleavage of the ether linkages of lignin model dimers and a trimer, Holzforschung 63 (2009) 424–430.

[25] M.W. Jarvis, J.W. Daily, H.-H. Carstensen, A.M. Dean, S. Sharma, D.C. Dayton, D.J. Robichaud, M.R. Nimlos, Direct detection of products from the pyrolysis of 2-phenethyl phenyl ether, J. Phys. Chem. A 115 (2011) 428–438.

[26] H. Kawamoto, M. Ryoritani, S. Saka, Different pyrolytic cleavage mechanisms of β-ether bond depending on the side-chain structure of lignin dimers, J. Anal. Appl. Pyrolysis 81 (2008) 88–94.

[27] H. Kawamoto, S. Horigoshi, S. Saka, Pyrolysis reactions of various lignin model dimers, J.Wood Sci. 53 (2007) 168–174.

[28] L. Munk, A.K. Sitarz, D.C. Kalyani, J.D. Mikkelsen, A.S. Meyer, Can laccases catalyze bond cleavage in lignin? Biotechnol. Adv. 33 (2015) 13–24.

[29] T. Elder, Bond dissociation enthalpies of apinoresinol lignin model compound, Energy Fuels 28 (2014) 1175–1182.

[30] J.M. Younker, A. Beste, A.C. Buchanan Iii, Computational study of bond dissociation enthalpies for lignin model compounds: β-5 arylcoumaran, Chem. Phys. Lett. 545 (2012) 100–106.

[31] S. Kim, S.C. Chmely, M.R. Nimlos, Y.J. Bomble, T.D. Foust, R.S. Paton, G.T. Beckham, Computational study about bond dissociation enthalpies for a large range of native and modified lignins, J. Phys. Chem. Lett. 2 (2011) 2846–2852.

[32] A.M. Azeez, D. Meier, J. Odermatt, Temperature dependence of fast pyrolysis volatile products from European and African biomasses, J. Anal. Appl. Pyrolysis 90 (2011) 81–92.

[33] J. Lede, F. Blanchard, O. Boutin, Radiant flash pyrolysis of cellulose pellets: products and mechanisms involved in transient and steady state conditions, Fuel 81 (2002) 1269–1279.

[34] J. Scheirs, G. Camino, W. Tumiatti, Overview of water evolution during the thermal degradation of cellulose, Eur. Polym. J. 37 (2001) 933–942.

[35] F.-X. Collard, J. Blin, A. Bensakhria, J. Valette, Influence of impregnated metal on the pyrolysis conversion of biomass constituents, J. Anal. Appl. Pyrolysis 95 (2012) 213–226.

[36] V. Mamleev, S. Bourbigot, M. Le Bras, J. Yvon, The facts and hypotheses relating to the phenomenological model of cellulose pyrolysis, J. Anal. Appl. Pyrolysis 84 (2009) 1–17.

[37] M. Van de Velden, J. Baeyens, A. Brems, B. Janssens, R. Dewil, Fundamentals, kinetics and endothermicity of the biomass pyrolysis reaction, Renew. Energy 35 (2010) 232–242.

[38] C.A. Mullen, A.A. Boateng, Characterization of water insoluble solids isolated from various biomass fast pyrolysis oils, J. Anal. Appl. Pyrolysis 90 (2011) 197–203.

[39] E. Jakab, O. Faix, F. Till, Thermal decomposition of milled wood lignins studied by thermogravimetry/mass spectrometry, J. Anal. Appl. Pyrolysis 40 (41) (1997) 171–186.

[40] T. Hosoya, H. Kawamoto, S. Saka, Pyrolysis behaviors of wood and its constituent polymers at gasification temperature, J. Anal. Appl. Pyrolysis 78 (2007) 328–336.

[41] L. Wei, S. Xu, L. Zhang, H. Zhang, C. Liu, H. Zhu, S. Liu, Characteristics of fast pyrolysis of biomass in a free fall reactor, Fuel Process. Technol. 87 (2006) 863–871.

[42] P. Morf, P. Hasler, T. Nussbaumer, Mechanisms and kinetics of homogeneous secondary reactions of tar from continuous pyrolysis of wood chips, Fuel 81 (2002)

[43] F.-X. Collard, J. Blin, A review on pyrolysis of biomass constituents: mechanisms and composition of the products obtained from the conversion of cellulose, hemi-celluloses and lignin, Renew. Sustain. Energy Rev. 38 (2014) 594–608.

[44] R.J. Evans, T.A. Milne, Molecular characterization of the pyrolysis of biomass, Energy Fuels 1 (1987) 123–137.

[45] T. Hosoya, H. Kawamoto, S. Saka, Role of methoxyl group in char formation from lignin-related compounds, J. Anal. Appl. Pyrolysis 84 (2009) 79–83.

[46] J.A. Moulijn, M. Makkee, A.V. Diepen, Chapter 7, Processes for the Conversion of Biomass, second edition, John Wiley & Sons Inc., Chichester, West Sussex, United Kingdom, 2013, pp. 221–248.

[47] V. Vivekanand, E.F. Olsen, V.G.H. Eijsink, S.J. Horn, Effect of different steam explosion conditions on methane potential and enzymatic saccharification of birch, Bioresour. Technol. 127 (2013) 343–349.

[48] J.R. Obst, T.K. Kirk, Isolation of lignin, Methods Enzymol. 161 (1988) 3–12.

[49] A. Bjorkman, Finely divided wood. I. Extraction of lignin with neutral solvents, Sven. Papperstidn. 59 (1956) 477–485.

[50] J.C. del Rio, P. Prinsen, E.M. Cadena, A.T. Martinez, A. Gutierrez, J. Rencoret, Lignin-carbohydrate complexes from sisal (*Agave sisalana*) and abaca (*Musa textilis*): chemical composition and structural modifications during the isolation process, Planta 243 (2016) 1143–1158.

[51] L. Shuai, M.T. Amiri, Y.M. Questell-Santiago, F. Heroguel, Y. Li, H. Kim, R. Meilan, C. Chapple, J. Ralph, J.S. Luterbacher, Formaldehyde stabilization facilitates lignin monomer production during biomass depolymerization, Science (Washington, DC, U.S.) 354 (2016) 329–333.

[52] R.B. Santos, E.A. Capanema, M.Y. Balakshin, H.-m. Chang, H. Jameel, Lignin structural variation in hardwood species, J. Agric. Food Chem. 60 (2012) 4923–4930.

[53] A. González-Sarrías, L. Li, N.P. Seeram, Anticancer effects of maple syrup phenolics and extracts on proliferation apoptosis, and cell cycle arrest of human colon cells, J. Funct. Foods 4 (2012) 185–196.

[54] E. Van den Worm, C.J. Beukelman, A.J.J. Van den Berg, B.H. Kroes, R.P. Labadie, H. Van Dijk, Effects of methoxylation of apocynin and analogs on the inhibition of reactive oxygen species production by stimulated human neutrophils, Eur. J. Pharmacol. 433 (2001) 225–230.

[55] K.T. Beggs, K.A. Glendining, N.M. Marechal, V. Vergoz, I. Nakamura, K.N. Slessor, A.R. Mercer, Queen pheromone modulates brain dopamine function in worker honey bees, Proc. Natl. Acad. Sci. U. S. A. 104 (2007) 2460–2464.

[56] V. Vergoz, H.A. Schreurs, A.R. Mercer, Queen pheromone blocks aversive learning in young worker bees, Science 317 (2007) 384.

[57] K.T. Beggs, A.R. Mercer, Dopamine receptor activation by honey bee queen pheromone, Curr. Biol. 19 (2009) 1206–1209.

[58] D.Y. Curtin, M.J. Hurwitz, Free radical rearrangements in the decarbonylation of aldehydes[1a], J. Am. Chem. Soc. 74 (1952) 5381–5387.

[59] A.F. Parsons, Chapter 4.4, Fragmentation Reactions, Blackwell Science, Malden, MA, 2000, pp. 72–74.

[60] M. Akazawa, Y. Kojima, Y. Kato, Effect of pyrolysis temperature on the pyrolytic degradation mechanism of β-aryl ether linkages, J. Anal. Appl. Pyrolysis 118 (2016) 164–174.

[61] A. Beste, A.C. Buchanan III, P.F. Britt, B.C. Hathorn, R.J. Harrison, Kinetic analysis of the pyrolysis of phenethyl phenyl ether: computational prediction of α/β-selectivities, J. Phys. Chem. A 111 (2007) 12118–12126.

[62] R. Ray, Ajay M. Shah, NADPH oxidase and endothelial cell function, Clin. Sci. 109 (2005) 217.

[63] Y. Steffen, C. Gruber, T. Schewe, H. Sies, Mono-O-methylated flavanols and other flavonols as inhibitors of endothelial NADPH oxidase, Arch. Biochem. Biophys. 469 (2008) 209–219.

[64] Y.-Y. Qin, M. Li, X. Feng, J. Wang, L. Cao, X.-K. Shen, J. Chen, M. Sun, R. Sheng, F. Han, Z.-H. Qin, Combined NADPH and the NOX inhibitor apocynin provides greater anti-inflammatory and neuroprotective effects in a mouse model of stroke, Free Radic. Biol. Med. 104 (2017) 333–345.

[65] D.-K. Dang, E.-J. Shin, Y. Nam, S. Ryoo, J.H. Jeong, C.-G. Jang, T. Nabeshima, J.-S. Hong, H.-C. Kim, Apocynin prevents mitochondrial burdens, microglial activation, and pro-apoptosis induced by a toxic dose of methamphetamine in the striatum of mice via inhibition of p47phox activation by ERK, J. Neuroinflammation 13 (2016) 12.

[66] M.M. Suryan, S.A. Kafafi, S.E. Stein, Dissociation of substituted anisoles: substituent effects on bond strengths, J. Am. Chem. Soc. 111 (1989) 4594–4600.

[67] N.E. Gunawardena, F. Kern, E. Janssen, C. Meegoda, D. Schäfer, O. Vostrowsky, H.J. Bestmann, Host attractants for Red Weevil, *Rhynchophorus ferrugineus*: Identification, electrophysiological activity, and laboratory bioassay, J. Chem. Ecol. 24 (1998) 425–437.

[68] D. Janes, D. Kantar, S. Kreft, H. Prosen, Identification of buckwheat (*Fagopyrum esculentum* Moench) aroma compounds with GC–MS, Food Chem. 112 (2008) 120–124.

[69] D. Cao, J. Jiang, T. Tsukamoto, R. Liu, L. Ma, Z. Jia, F. Kong, M. Oshima, X. Cao, Canolol inhibits gastric tumors initiation and progression through COX-2/PGE2 pathway in K19-C2mE transgenic mice, PLoS One 10 (2015) e0120938.

[70] J.-F. Yang, C.-H. Yang, M.-T. Liang, Z.-J. Gao, Y.-W. Wu, L.-Y. Chuang, Chemical composition, antioxidant, and antibacterial activity of wood vinegar from *Litchi chinensis*, Molecules 21 (2016) 1150.

[71] S.-N. Sun, X.-F. Cao, F. Xu, R.-C. Sun, G.L. Jones, Structural features and antioxidant activities of lignins from steam-exploded bamboo (*Phyllostachys pubescens*), J. Agric.

Food Chem. 62 (2014) 5939–5947.

[72] J. Huang, C. He, G. Pan, H. Tong, A theoretical research on pyrolysis reactions mechanism of coumarone-contained lignin model compound, Comput. Theor. Chem. 1091 (2016) 92–98.

[73] M. Asmadi, H. Kawamoto, S. Saka, Thermal reactivities of catechols/pyrogallols and cresols/xylenols as lignin pyrolysis intermediates, J. Anal. Appl. Pyrolysis 92 (2011) 76–87.

[74] M. Asmadi, H. Kawamoto, S. Saka, Gas- and solid/liquid-phase reactions during

pyrolysis of softwood and hardwood lignins, J. Anal. Appl. Pyrolysis 92 (2011) 417–425.

[75] A.V. Bridgwater, Review of fast pyrolysis of biomass and product upgrading, Biomass Bioenergy 38 (2012) 68–94.

[76] D.C. Kalyani, T. Fakin, S.J. Horn, R. Tschentscher, Valorisation of woody biomass by combining enzymatic saccharification and pyrolysis, Green Chem. 19 (2017) 3302–3312, http://dx.doi.org/10.1039/C7GC00936D.
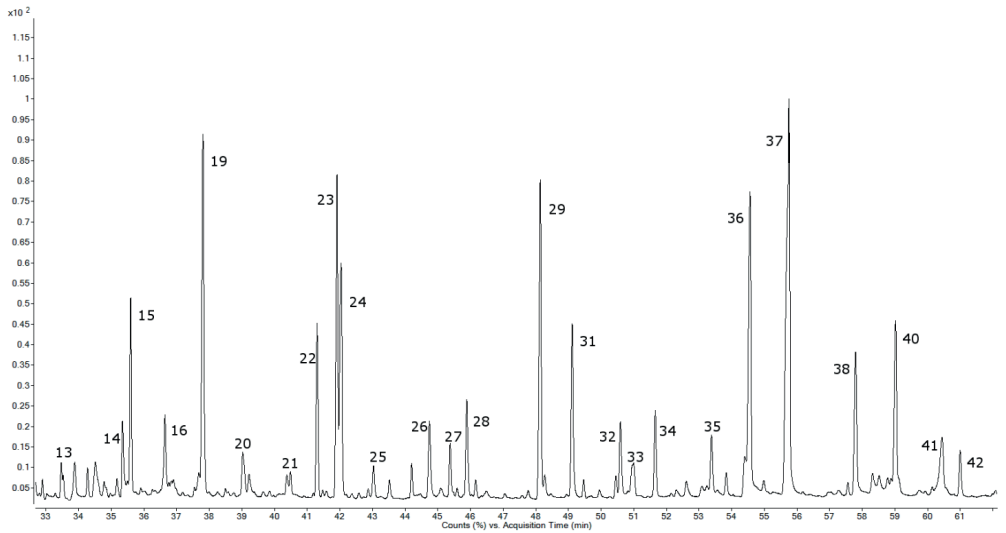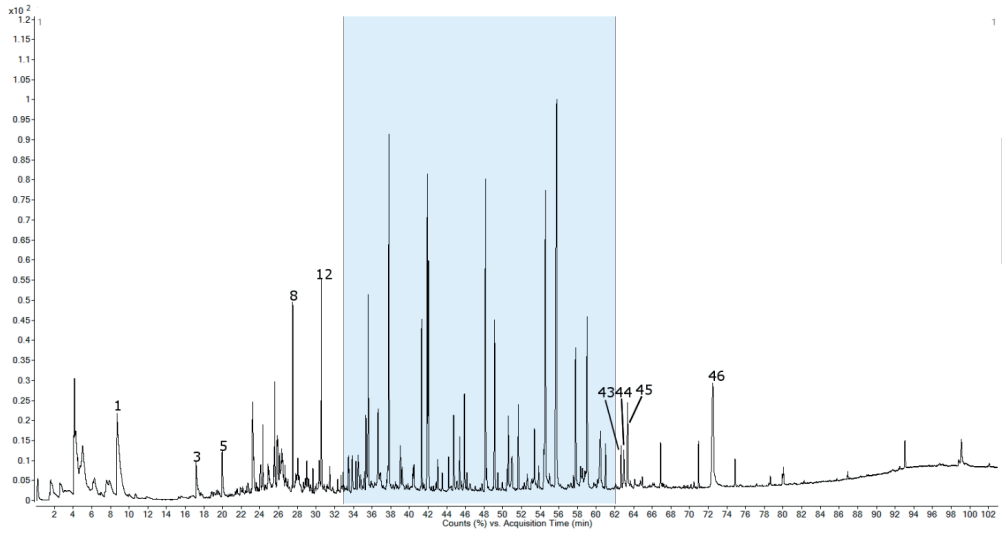
Supplementary

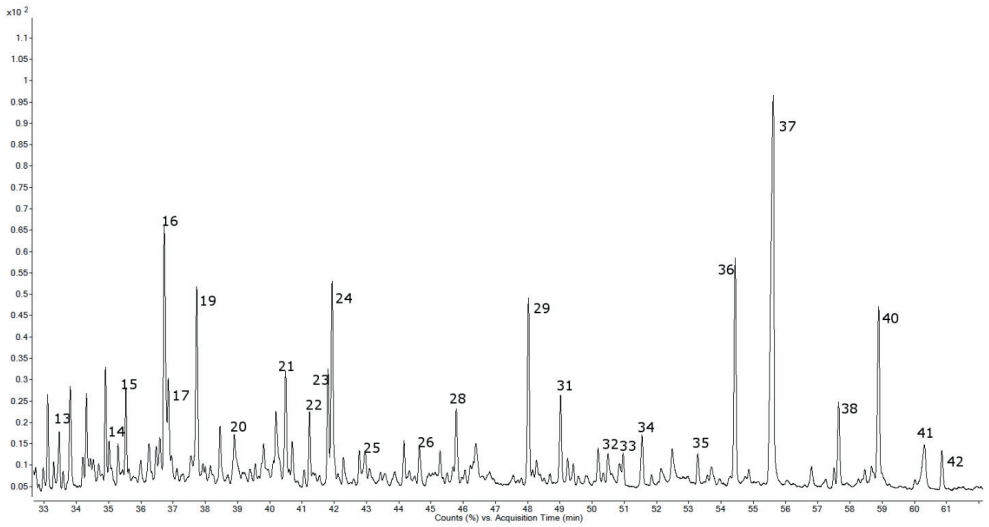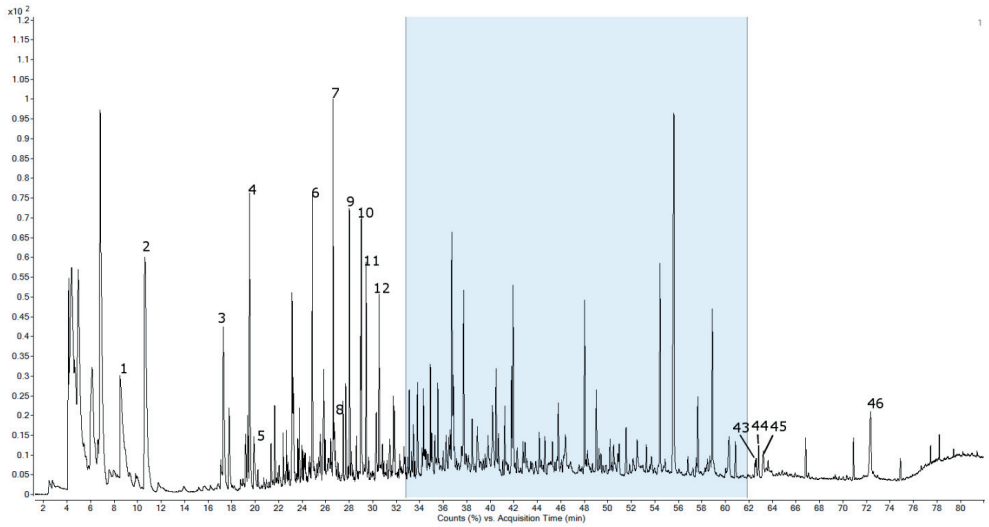Numbers on the peaks refers to peak number in Table 2.

Pyrogram pyrolysis temperature 400 °C
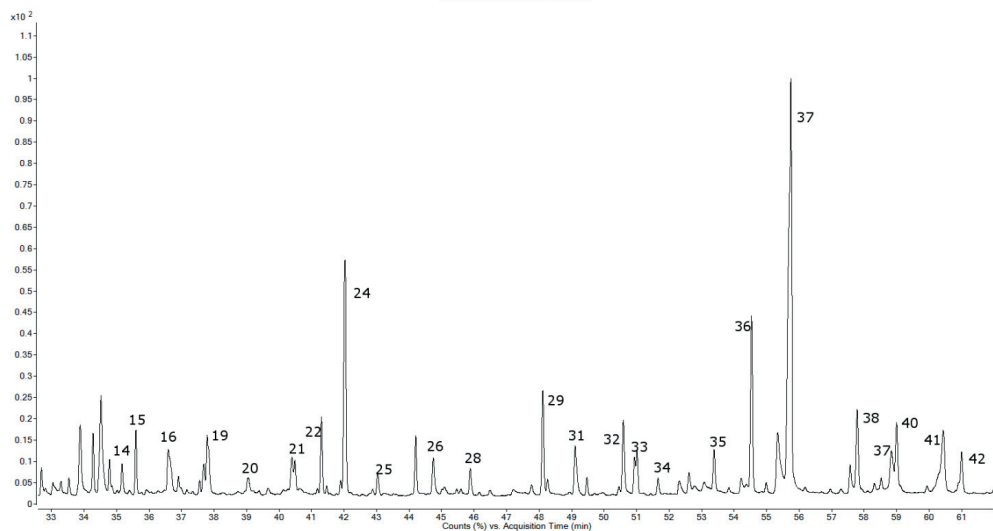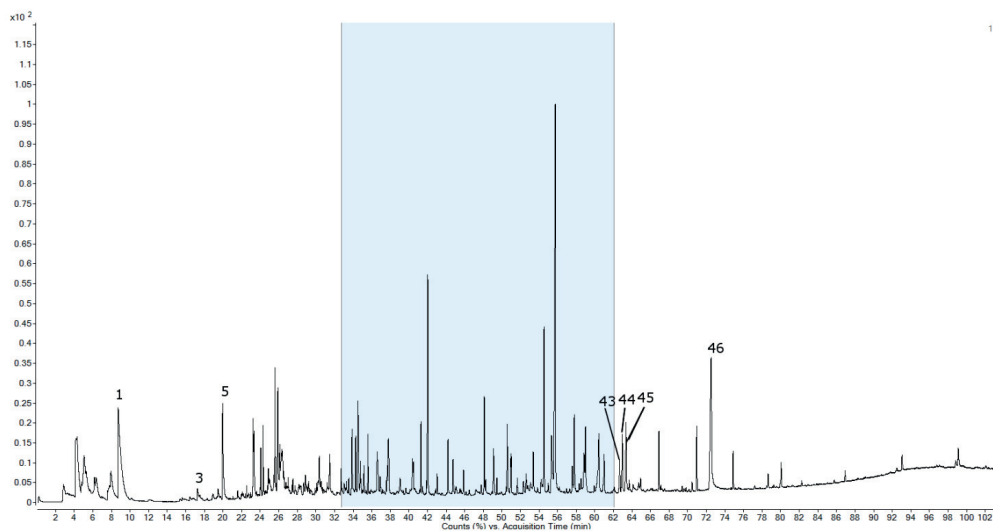
Pyrogram pyrolysis temperature 600 °C

Pyrogram pyrolysis temperature 900 °C

Paper II

Characterization of pseudo-lignin from steam exploded birch

Ida Aarum[*], Hanne Devle, Dag Ekeberg, Svein J. Horn and Yngve Stenstrøm

ACS OMEGA

Article

# Characterization of Pseudo-Lignin from Steam Exploded Birch

Ida Aarum,* Hanne Devle, Dag Ekeberg, Svein J. Horn, and Yngve Stenstrøm

Faculty of Chemistry, Biotechnology and Food Science, Norwegian University of Life Sciences, P.O. Box 5003, N-1432 Ås, Norway

S Supporting Information

ABSTRACT: There is a growing interest in a more wholesome utilization of biomass as the need for greener chemistry and non-mineral oil-based products increases. Lignin is the largest renewable resource for aromatic chemicals, which is found in all types of lignocellulosic biomass. Steam-explosion of lignocellulosic biomass is a useful pretreatment technique to make the polymeric material more available for processing. However, this heat-based pretreatment is known to result in the formation of pseudo-lignin, a lignin-like polymer made from carbohydrate degradation products. In this work, we have analyzed steam-exploded birch with a varying severity factor (3.1−5.0) by pyrolysis−gas chromatography−mass spectrometry, 2D-NMR, and Fourier transform infrared spectroscopy. The main results reveal a consumption of acetic acid at higher temperatures, with the increase of furan components in the pyrolyzate. The IR and NMR spectral data support these results, and there is a reason to believe that the conditions for humin formation are accomplished under steam explosion. Pseudo-lignin seems to be a humin-like compound.
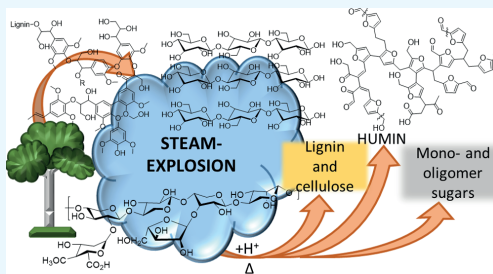
INTRODUCTION

Total utilization of lignocellulosic biomass and conversion into a range of valuable products is a central goal in biorefining and green chemistry. This renewable material has the potential to replace depleting fossil resources for the production of energy, chemicals, and fuels.[1−3] Lignin is the most abundant renewable aromatic polymer on the planet and is found in all types of lignocellulosic biomass. However, in the pulp and paper industry and the emerging cellulosic ethanol industry, lignin is considered to be a waste product and is currently mostly burned to generate process heat.[4−8] For biochemical production of ethanol, a pretreatment of the lignocellulosic biomass is needed to make the carbohydrates accessible for enzymes. Steam explosion (SE) is a treatment with a high industrial potential, as it has a low cost for energy and does not need addition of other chemicals than steam, thereby producing no extra waste.[9−11] SE is both a chemical and physical treatment. It hydrolyses the hemicellulose into soluble monomers and oligomers and makes the cellulose fibers much more accessible for further degradation with enzymes.[12−14] The lignin and cellulose part is not expected to be significantly altered during SE, but as several other authors have noticed, the β-O-4 bonds in lignin are degraded with increasing pretreatment severity.[15] For SE, the severity factor can be calculated as log R_0[16] that includes both temperature (T °C) and residence time (rt) as variables

$$\log R_0 = \log(\text{rt} \times e^{T-100/14.75})$$

Interestingly, several studies show an increase of Klason lignin (KL) content after SE.[17,18] This increase has been attributed to the formation of pseudo-lignin during pretreat-

ment.[19] Recently, several studies have attempted to identify the structure of pseudo-lignin, as it has been shown to hamper the enzymatic hydrolysis of cellulose.[17−23] The general pseudo-lignin definition is broad and diffuse and the most accepted one states that it is "an aromatic material that yields a positive Klason lignin value that is not derived from native lignin."[19] The KL analysis is however only a crude method, as it just measures the increase of nonhydrolysable residues after acid hydrolysis, and is therefore not a proper identification test.[18]

SE treatment of hardwoods releases acetic acid from the hemicellulose, which leads to pH drop and drives the autohydrolysis.[24,25] The acetic acid is generated from the acetylated carbohydrates, mainly xylans, and it can accumulate to a pH of 3.[26] Both time and temperature in SE have an effect on the release of acetic acid. Li et al. showed that this relationship is almost linear under hydrolysis with increasing time and temperature.[27]

With the combined effects of high temperature and pressure in addition to the low pH under SE, several side reactions can take place. The cleavage of the β-O-4 bonding pattern in lignin has been reported by Li et al.[28] at pH 3, but the cleavage also happens at a higher pH as reported by Yelle et al.[29] A study of Glasser and Wright[30] shows that the MW of lignin decreases during SE treatment at severities above log R_0 4.2.

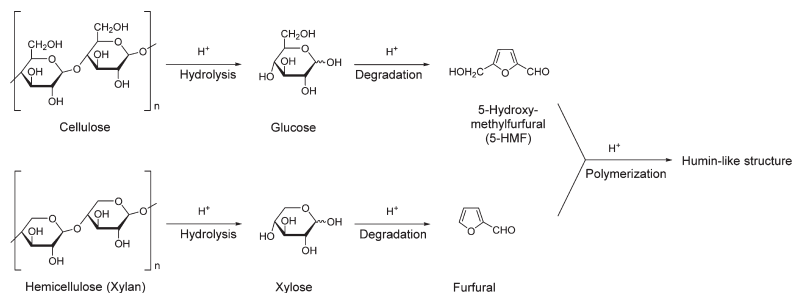The formation of 5-hydroxymethylfurfural (5-HMF) from carbohydrates are reported by several groups, as a degradation

Scheme 1. Overview of Reaction Pathway of Cellulose and Hemicellulose into Furan Components and Humin-Like Structures (Modified from Li et al.)[25]

product of C6 sugars such as glucose in cellulose, Scheme 1.[22,25]

Additionally, there is formation of furfural from C5 sugars such as xylose from xylan. Generally, C6 sugars are more stable than C5 sugars during high-temperature pretreatments. These furan-like components can under certain conditions form a polymer structure called humin, Figure 1. Humins are an

Figure 1. Humin structures derived from (A) glucose and (B) xylose (van Zandvoort et al.).[33]

organic compound class which are insoluble in water at all pH's. The term is used in two related contexts, soil and carbohydrate chemistry. Humins from carbohydrates are produced under dehydration of sugars, the subsequent formaldehydes, and 5-HMF form further polymers.[31,32] van Zandvoort et al. found that the furan and phenol compounds formed under acid-catalyzed dehydration of sugars are a part of the humin structure formation.[33] Patil et al. showed the direct formation of humins from glucose, fructose, and 5-HMF as a condensation product.[34,35] In addition, Tuercke et al. did a microreactor synthesis of 5-HMF from dehydrating fructose, where it polymerized into a humin structure.[36] A different group, Date

et al. reduced 5-HMF with Pd/C and formaldehyde and made a crystalline structure of 22.4 nm size.[37]

The byproduct called pseudo-lignin apparent in the increase of KL content is formed under SE-treatment with identical conditions to what is needed for the formation of humins. The aim of this study was to investigate this unknown byproduct with pyrolysis–gas chromatography–mass spectrometry (GC–MS), 2D-NMR, and Fourier transform infrared spectroscopy (FT-IR) for characterization and identifications of similarities between pseudo-lignin and the humins.

■ RESULTS AND DISCUSSION

Table 1 shows that the KL content (% KL) increased with the severity of the SE, from 22% in untreated birch to 40−42% at
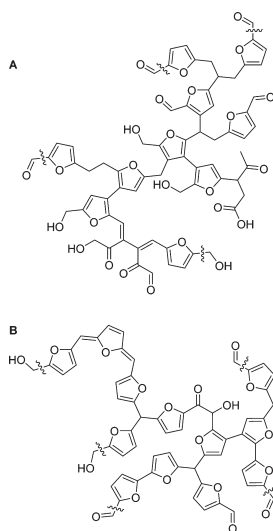
Table 1. SE Conditions and KL Content from Birch Wood[a]

severity factor	pretreatment condition	KL content (%)
	untreated	22
3.1	170 °C—10 min	23
3.4	180 °C—10 min	24
3.6	190 °C—10 min	25
3.9	200 °C—10 min	28
3.9	210 °C—5 min	30
4.2	210 °C—10 min	32
4.2	220 °C—5 min	32
4.4	210 °C—15 min	32
4.5	220 °C—10 min	37
4.5	230 °C—5 min	37
4.7	220 °C—15 min	42
4.8	230 °C—10 min	41
5.0	230 °C—15 min	40

[a]KL analysis were carried out in triplicates.

the most severe pretreatment conditions. The estimated increase of KL as an effect of xylan loss has been calculated to be 25%; this work has been described by Vivekanand et al.[18] In an effort to characterize this pseudo-lignin the samples were analyzed by fractionated pyrolysis and 2D-NMR.

2D-NMR Heteronuclear Single Quantum Coherence (HSQC). NMR experiments of the solvable fraction of untreated and severely pretreated (log R_0 4.7) birch before pyrolysis show the change in both aliphatic (Figure 2) and aromatic (Figure 3) regions. In the aliphatic area (Figure 2), from 2.6/45.0 to 5.3/115.0 ppm, the most noticeable difference is around the proton peaks of the β-O-4 bonding pattern. The
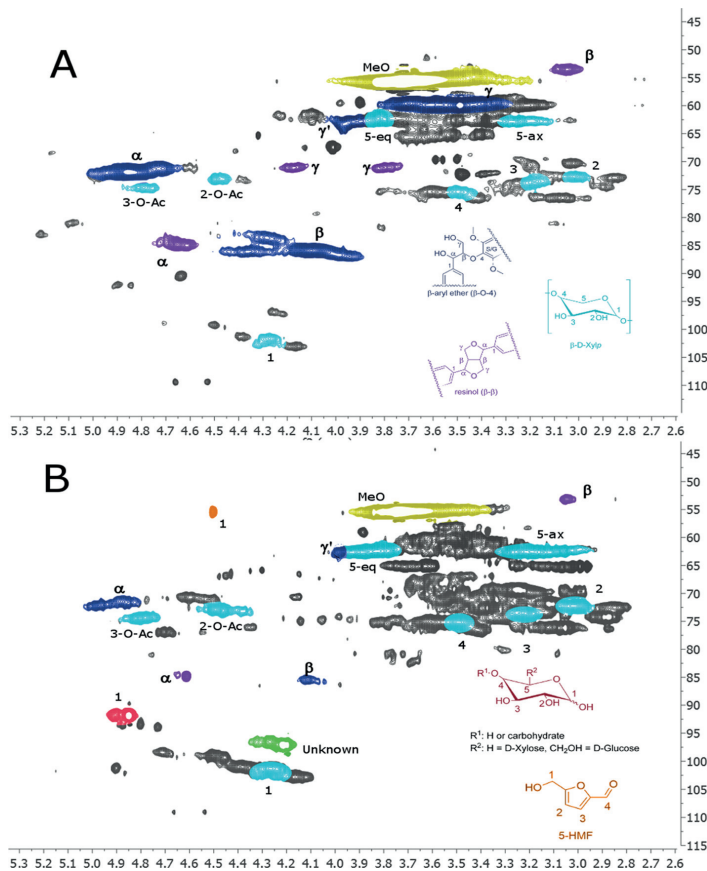
Figure 2. HSQC of lignocellulosic biomass at (A) untreated and (B) severity factor 4.7 (220 °C—15 min), focused on aliphatic region.

α-H shifts to the left and the signal is lower for the SE sample than untreated birch. The β-H signal has a similar pattern. In addition, the γ-H and γ-H′ (ox) disappears nearly completely after SE. Overall, this indicates that the β-O-4 bonding fragments with the pretreatment. Interestingly, this happens even at the lowest severity conditions in these pretreatment experiments, at 170 °C 10 min (Figure S1), even before the KL amount increases. This means that the changes in the NMR spectrum are not directly related to the accumulation of KL. Increasing the SE severity factor only results in limited alterations in the NMR spectra, while the KL content increases. Therefore, the byproduct formed under SE is not dissolvable in any of the three deuterated solvents used in this study.

The main change in the NMR spectra is the emersion of xylan peaks. These are visible in the spectrum (Figure 2) at 4.27/101, 3.88/3.17/63.0, 3.50/75.0, 3.25/74.0, and 3.0/72.5 ppm. The two peaks at 4.80/74.10 and 4.50/72.80 ppm is β-D-Xylp acetylated in position C-3 and C-2, respectively.

The peaks at 4.85/93.0 and 4.90/93.0 ppm are actually the anomeric carbon in D-xylose and D-glucose, respectively. These peaks are detectable in even the lowest SE-treatment, but the signal intensity is stronger at high severity factor such as 4.7 as

ppm. This means that carbohydrates are released, most likely from fragmentation of lignin—carbohydrate complexes, cellulose, and hemicellulose under SE as a result of depolymerization of lignocellulosic biomass.

In the aromatic region (Figure 3), there is also an immediate change in the NMR spectra at lowest SE. The G_2 and G_6 shifts disappear and only the G_5 and $S_{2,6}$ are left (Figure 3). With the increasing SE-treatment, there is a new area that becomes stronger in the aromatic region right below the $S_{2,6}$ region. An additional change in the aromatic region with the increasing SE-treatment is a shift in the $S_{2,6}$ peak. In the untreated version (Figure S2), there is an "iceberg" shape and with increasing treatment the top peak shifts toward the lower proton area. This small shift in $S_{2,6}$ corresponds to the difference in the enantiomer versions erythro and threo as shown by Schmid and Bardet et al.[38,39] This is in compliance with hydrolysis in α-position in β-O-4, as the signals shifts from racemic to thermodynamic stable enantiomer signals.

In the SE-treated spectra in both regions (Figures 2 and 3), there are peaks that correlates with the 5-HMF, at shift values, 4.5/56.5, 6.6/110.1, and 7.5/125.0. The peaks have a low
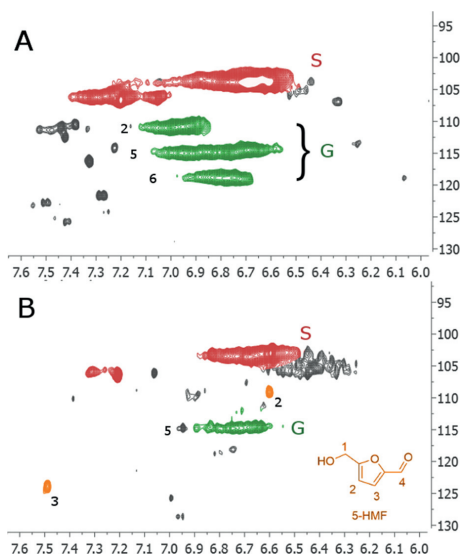
Figure 3. HSQC of lignocellulosic biomass at (A) untreated and (B) severity factor 4.7 (220 °C—15 min), focused on aromatic region.
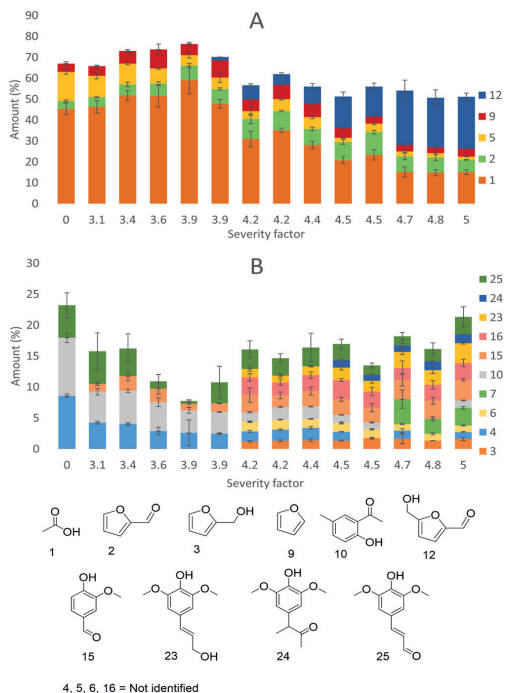

Figure 4. Amount and structure of several components in the pyrolyzate at 350 °C, as a function of severity factors of SE. The amounts are the average of normalization with standard deviation of three replicates. (A) Components of major amounts and (B) components of minor amounts.

intensity, meaning that there is a low concentration of 5-HMF dissolved in the sample.

Pyrolysis–GC–MS. The fractionated temperatures in the pyrolysis was determined based on previous results, Aarum et al. and Jurak,[40,41] as the carbohydrates will be mostly valorized at 350 °C and then subsequently pyrolysis at 600 °C would yield the lignin fraction. This turned out to be a mostly correct assumption, as the 350 °C pyrogram contained small amounts of lignin components. The amount of lignin at 350 °C does increase with the SE-treatment, which is a result of the hydrolysis of the β-O-4 bond in lignin at higher severities.

All detected components after pyrolysis–GC–MS are described in Table S1. At 350 °C, the pyrolyzate is mainly composed of the most volatile products such as acetic acid (**1**), small furan-like rings (**2**, **3**, **9**, and **12**), and some lignin structures (**10**, **15**, **23**, **24**, and **25**), see Figure 4.

The pyrolyzate at 350 °C has an increase of lignin products such as **15** (4-hydroxy-3-methoxybenzaldehyde, vanilin), **23** (4-[(E)-3-hydroxyprop-1-enyl]-2,6-dimethoxyphenol), and **24** (3-(4-hydroxy-3,5-dimethoxyphenyl)butan-2-one), with the increasing severity of the SE-treatment, Figure 4. The increase of volatile lignin components means that the polymer is more fragmented, which corresponds to the hydrolysis and cleavage of the β-O-4 bond as described in other works.[28,30,42] In the pyrolyzate at 350 °C, there is a significant increase of 5-HMF **12**, first detected (1.5%) with a severity factor of 3.9 at a temperature of 210 °C and a rt of 5 min. In untreated wood samples, this compound was not detected at all. The amount of 5-HMF thereafter increased to approximately 25% at a severity factor 4.5, 4.8, and 5.0 (230 °C, all rts). HMF is a typical dehydration product of C6 sugars.

The four main components that decrease at 350 °C are **1** (acetic acid), **4** (unknown m/z 114), **5** (unknown m/z 114), and **10** (unknown m/z 152). Components **4** and **5** have the same molecular mass, but display distinctly different

fragmentation patterns in their mass spectra and are therefore evidently not the same compound.

The amount of acetic acid increases (45−59%) until a severity factor of 3.9 (210 °C, 5 min), from which point the amount decreases (59−15%). The increase and subsequent loss of **1** has been previously reported by Sunqvist et al., where they observed consumption of acetic acid by water extraction using a temperature around 200 °C.[26] Formation of **12** in the pyrolyzate coincides with the consumption of **1** at a severity factor of 3.9. This can explain that production of **12** is a building block in the formation of humins that also need acid, as shown in Figure 5 and Scheme 1.

Using the pyrolysis temperature (at 600 °C, shown in Figure 6), there is mainly a decrease of **1**. The other lignin components that increase in amounts are **13** (2,6-dimethoxyphenol), **36** (2-methoxyphenol), **37** (2-methylphenol), **40** (2-methoxy-4-methylphenol), and **49** (2,6-dimethoxy-4-methylphenol). The three lignin components that are decreasing in amounts are **21** (3,5-dimethoxy-4-hydroxybenzaldehyde), **22** (unknown m/z 196), and **25** (3,5-dimethoxy-4-hydroxycinnamaldehyde).

In general, we have observed a trend of decreasing amounts of aldehydes and lignin's with shorter side chains in the C-4 position with the increasing severity factor. The β-O-4 bonding pattern can undergo hydrolysis at both hydroxyl groups on the side chain C-4. However, the α-hydroxyl gives the most stable
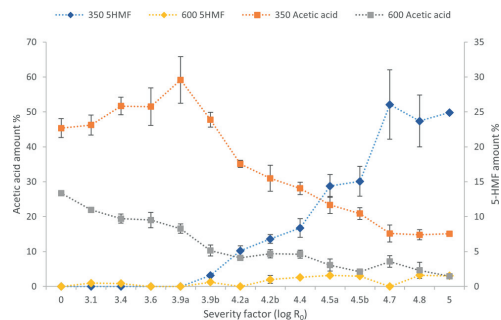
Figure 5. 5-HMF and acetic acid pyrolyzate content, (3.9a) 200 °C—10 min, (3.9b) 210 °C—5 min, (4.2a) 220 °C—5 min, (4.2b) 210 °C—10 min, (4.5a) 230 °C—5 min, (4.5b) 220 °C—10 min, 0 is untreated biomass).
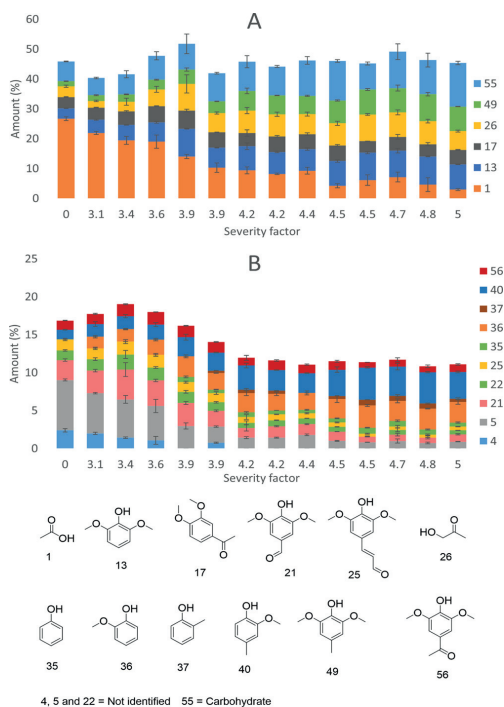

Figure 6. Amount and structure of several components in the pyrolyzate at 600 °C, at different severity factors of SE. The amounts are the average of a normalization with standard deviation of three replicates. (A) Components of major amounts and (B) components of minor amounts.

intermediate cation. This carbocation intermediate is subsequently open for nucleophilic attack, rearrangement, or both, Scheme 2. The changes seen in the pyrolyzate composition is mostly related to the α-carbon on the side chain, with a general decrease in number of oxygen atoms.

Because there are little or no changes in the phenyl content in the pyrolyzate, there is a reason to believe that pseudo-lignin does not contain this structure in a large amount. On the other hand, there is a significant increase of component 12 (5-HMF) and other furan-components in the pyrolyzate with the increase of the severity factor. 5-HMF is visible in the NMR, but the intensity of the peaks are low and do not correspond to the increase seen in the pyrolyzate. There are also several other components appearing with log R_0 3.9 in the pyrolyzate such as: 2 (furfural), 3 (2-furanmethanol), and 7 (2,5-furandicarboxaldehyde). These compounds are related to the pyrolytic cleavage of humins as shown by van Zandvoort et al.[33] We propose that the byproduct formed by SE, called pseudo-lignin, corresponds to humin because of the furan polymer structure that was found. According to van Zandvoort et al.[33] and Patil and Lund,[35] the formation of humins from carbohydrates takes place under harsh conditions, for example, high temperature and acidic pH. The acetic acid released is consumed in forming the humin polymer; therefore, after pyrolysis, the acid content drops and the depolymerized humin increases with furan-like components in the pyrolyzate.

To support that humins are formed under SE-treatment, FT-IR spectra were recorded (Figures S3 and S4). The untreated samples had IR transmittance at 1722, 1655, and 1594 cm^{-1}, but in the treated sample (severity factor 4.7 (220 °C, 15 min)), there is instead transmittance at 1711, 1605, and 1515 cm^{-1}. These results are in agreement to IR of humins as described by van Zandvoort et al.[33] Baccile et al.[46] did structural characterization of hydrothermal carbon spheres, revealing a structure and bonding pattern similar to the proposed humin structure (Figure 1). These carbon spheres were accumulated from carbohydrates and raw biomass with temperatures between 160 and 220 °C. The solid-state NMR of the unsolvable part showed a clear furan-ring polymeric structure, very similar in structure as suggested by van Zandvoort et al.[33] Tuercke et al.[36] acid catalyzed (0.1 M HCl) dehydration of fructose into 5-HMF, but noticed that at temperatures from 200 °C the yield started to decline. They found that this was caused by the formation of humin and other insoluble polymeric byproducts.

To summarize, the changes in NMR spectra do not correlate with the increase in the KL content and therefore is not consistent with the structure of pseudo-lignin, but they confirm the release of several monomeric carbohydrates, some 5-HMF, and hydrolysis of lignin. The SE-temperature of 200–210 °C is a critical temperature for SE-treatment of biomass. This is the temperature where the inhibition of enzymes and formation of pseudo-lignin escalates. At the severity factor above 3.9 (210 °C), there is a decrease of acetic acid in the pyrolyzate. We believe the acetic acid is consumed as a result of polymerization with furan components to form humins. Several furan components, especially 5-HMF, are increasing in the pyrolyzate with SE-treatment. There are also small amounts of this that are visible in the liquid NMR fraction, but the intensity does not correspond to the amount in pyrolyzate. This strongly indicates that 5-HMF is bound in a polymeric molecule not solvable in NMR solvents. These furan-like components are known to be related to humin structures. The conditions under SE are conducive for the synthesis of these humins, with acid, heat, and water. Therefore, pseudo-lignin as the byproduct formed during the SE-treatment of birch seems be a type of humin structure and not a more condensed lignin structure.

Scheme 2. Reaction Pathways under SE of Lignin that Might Take Place[a]
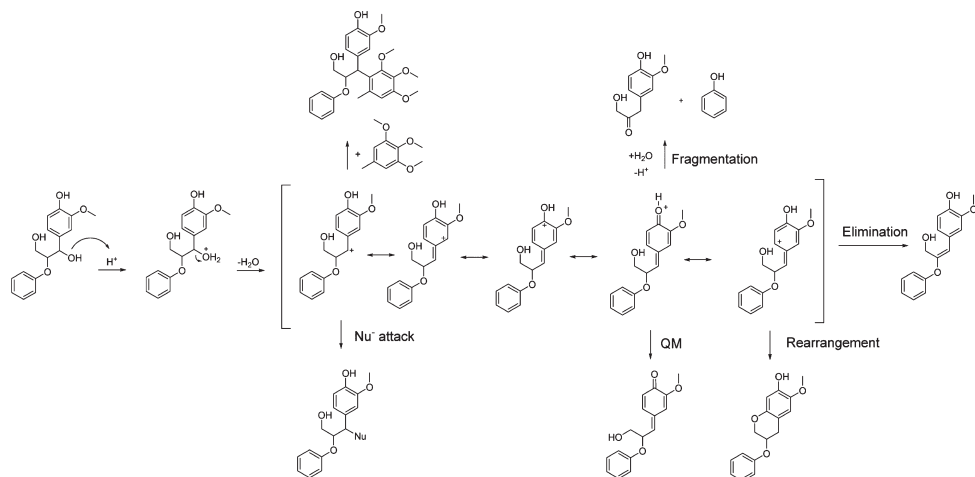
[a]The first resonance structure is open for a nucleophilic attack, Li et al.[43] and Shimada et al.[44] The fragmentation reaction in the fourth resonance form is calculated to be exothermic by Sturgeon et al.[45] QM is the formation of the quinone methide-structure. The rearrangement in the fifth resonance would yield flavonoid-like structures as detected by Rasmussen et al.[21]

■ METHODS

Materials. Birch (*Betula pubescens*) stem wood without bark was pretreated with SE.[18] The list of standards are listed in Supporting Information and is used for retention validation of components.[40] The hemicellulose 4-O-methyl-D-glucurono-D-xylan and cellulose (powder) were acquired from Sigma-Aldrich (Steinheim, Germany). The milling was done with a Retsch GmbH 100PM (Haan, Germany) instrument with zirconium balls (ZrO_2) at 350 rpm, for 12 h with 15 min on/off increments.

Steam Explosion. The SE was done on birch stem wood at several different temperatures (170−230 °C with a 10 °C increment) and resident times (rt, 5, 10, and 15 min), see Table 1. The pretreatment was performed at the SE facility, at Norwegian University of Life Sciences (NMBU) in Ås, designed by Cambi AS. Three hundred grams of dry matter of milled birch was added to preheated pressure chambers (10 min). SE at temperatures of 170−200 °C was only done with 10 min rt.[18] These samples were dried and stored in room temperature, before applying the powder to the pyrolysis filament, with a micropipette designed for powder. The Klason-lignin analysis was carried out in triplicates.

Pyrolysis−GC−MS. The flash filament Pyrola 2000 pyrolyzer (Pyrol AB, Lund, Sweden) was coupled to a GC−MS (7890B-7000C triple quadrupole GC−MS instrument from Agilent technologies) to characterize the volatile pyrolyzate generated from fast pyrolysis of birch samples. The GCMS method and identification was done as previously described, with a capillary column (TraceGOLD TG-1710MS 60 m, ID 0.25 mm, and 0.25 μm film thickness, Thermo Fisher Scientific).[40] The total pyrolysis time is 2 s, with a heating time of 8 ms, which is injected on-line to the GC with a total run time of 76.4 min. The pyrolysis was a fractionated pyrolysis which is, according to IUPAC system, "pyrolysis in which the sample is pyrolyzed at different temperatures at different times to study a special fraction of the sample"[47] and in this case at

350 and 600 °C, before each GC-run. The amounts of each component are a normalization by maximum peak area and therefore only represent the change in the composition as a function of the SE-treatment. Each pyrolysis has been performed in three replicates, and the value shown is the average with corresponding standard deviation.

2D-NMR HSQC. For the preparation of NMR samples, three different deuterated solvents were tested, DMSO-d_6, DMF-d_4, and acetic acid-d_4. Generally, all of the different solvents resulted in similar spectra. NMR spectra with DMSO-d_6 as the solvent were chosen to present in this study because DMSO is known to be a good solvent for lignin materials. DMF-d_6 gave a somewhat better spectra resolution but was not used, as the gain was small. The NMR spectra were recorded on a Bruker Ascend 400 spectrometer (400 MHz) as previously described.[40] The SE-treated material was ball-milled after drying and dissolved in the deuterated solvent for 5 min. Then, they were filtered through glass wool, to remove any unsolved particles, directly into the NMR-tube.

Fourier Transform Infrared Spectroscopy. The IR spectra were recorded on an Agilent technologies FTIR 5500 (single reflection diamond attenuated total reflection-cell), with the solid powder after SE-treatment, drying, and milling. The resultant IR spectra consist of 32 co-added interferograms recorded at 8 cm^{-1} resolution in the 4000−650 cm^{-1} wavelength region.

■ ASSOCIATED CONTENT

Ⓢ Supporting Information

The Supporting Information is available free of charge on the ACS Publications website at DOI: 10.1021/acsomega.8b00381.

> HSQC spectrum of birch biomass treated with steam-explosion at a severity factor of 3.1 (170 °C—10 min); topographical visualization of untreated and treated biomass (220 °C—5 min); FTIR-spectrum of untreated, treated biomass (220 °C, 15 min), cellulose, and

hemicellulose overlaid; FT-IR-spectra of untreated and steam-exploded at severity factor 4.7 (220 °C—15 min); HSQC of 5-HMF in DMSO-d_6; and all detected components from fractionated py-GC-MS at 350 and 600 °C (PDF)

■ AUTHOR INFORMATION

Corresponding Author

*E-mail: ida.aarum@nmbu.no (I.A.).

ORCID ⊙

Ida Aarum: 0000-0002-9035-494X

Notes

The authors declare no competing financial interest.

■ REFERENCES

(1) Hamelinck, C. N.; van Hooijdonk, G.; Faaij, A. P. C. Ethanol from lignocellulosic biomass: techno-economic performance in short-, middle- and long-term. *Biomass Bioenergy* **2005**, *28*, 384−410.

(2) Pan, X.; Xie, D.; Gilkes, N.; Gregg, D. J.; Saddler, J. N. Strategies to enhance the enzymatic hydrolysis of pretreated softwood with high residual lignin content. *Appl. Biochem. Biotechnol.* **2005**, *124*, 1069−1080.

(3) Alvira, P.; Tomás-Pejó, E.; Ballesteros, M.; Negro, M. J. Pretreatment technologies for an efficient bioethanol production process based on enzymatic hydrolysis: A review. *Bioresour. Technol.* **2010**, *101*, 4851−4861.

(4) Sette, M.; Wechselberger, R.; Crestini, C. Elucidation of Lignin Structure by Quantitative 2D NMR. *Chem.—Eur. J.* **2011**, *17*, 9529−9535.

(5) Zhang, L.; Gellerstedt, G. Quantitative 2D HSQC NMR determination of polymer structures by selecting suitable internal standard references. *Magn. Reson. Chem.* **2007**, *45*, 37−45.

(6) Capanema, E. A.; Balakshin, M. Y.; Kadla, J. F. A Comprehensive Approach for Quantitative Lignin Characterization by NMR Spectroscopy. *J. Agric. Food Chem.* **2004**, *52*, 1850−1860.

(7) Adler, E. Lignin chemistry—past, present and future. *Wood Sci. Technol.* **1977**, *11*, 169−218.

(8) Alekseev, O. A.; Shamsutdinov, M. É.; Kutyshev, F. K.; Kostochko, A. V. Combustion and Heat Properties of Lignin−Containing Fuels. *Combust., Explos. Shock Waves* **2001**, *37*, 67−71.

(9) Carvalheiro, F.; Duarte, L. C.; Girio, F. M. Hemicellulose biorefineries: a review on biomass pretreatments. *J. Sci. Ind. Res.* **2008**, *67*, 849−864.

(10) Holtzapple, M. T.; Humphrey, A. E.; Taylor, J. D. Energy requirements for the size reduction of poplar and aspen wood. *Biotechnol. Bioeng.* **1989**, *33*, 207−210.

(11) Jacquet, N.; Maniet, G.; Vanderghem, C.; Delvigne, F.; Richel, A. Application of Steam Explosion as Pretreatment on Lignocellulosic Material: A Review. *Ind. Eng. Chem. Res.* **2015**, *54*, 2593−2598.

(12) Chen, H.; Fu, X. Industrial technologies for bioethanol production from lignocellulosic biomass. *Renewable Sustainable Energy Rev.* **2016**, *57*, 468−478.

(13) Li, Y.; Liu, W.; Hou, Q.; Han, S.; Wang, Y.; Zhou, D. Release of Acetic Acid and Its Effect on the Dissolution of Carbohydrates in the Autohydrolysis Pretreatment of Poplar Prior to Chemi-Thermomechanical Pulping. *Ind. Eng. Chem. Res.* **2014**, *53*, 8366−8371.

(14) Chen, X.; Lawoko, M.; van Heiningen, A. Kinetics and mechanism of autohydrolysis of hardwoods. *Bioresour. Technol.* **2010**, *101*, 7812−7819.

(15) Heikkinen, H.; Elder, T.; Maaheimo, H.; Rovio, S.; Rahikainen, J.; Kruus, K.; Tamminen, T. Impact of Steam Explosion on the Wheat Straw Lignin Structure Studied by Solution-State Nuclear Magnetic Resonance and Density Functional Methods. *J. Agric. Food Chem.* **2014**, *62*, 10437−10444.

(16) Overend, R. P.; Chornet, E.; Gascoigne, J. A. Fractionation of Lignocellulosics by Steam-Aqueous Pretreatments [and Discussion]. *Philos. Trans. R. Soc., A* **1987**, *321*, 523−536.

(17) Hu, F.; Jung, S.; Ragauskas, A. Impact of Pseudolignin versus Dilute Acid-Pretreated Lignin on Enzymatic Hydrolysis of Cellulose. *ACS Sustainable Chem. Eng.* **2013**, *1*, 62−65.

(18) Vivekanand, V.; Olsen, E. F.; Eijsink, V. G. H.; Horn, S. J. Effect of different steam explosion conditions on methane potential and enzymatic saccharification of birch. *Bioresour. Technol.* **2013**, *127*, 343−349.

(19) Hu, F.; Jung, S.; Ragauskas, A. Pseudo-lignin formation and its impact on enzymatic hydrolysis. *Bioresour. Technol.* **2012**, *117*, 7−12.

(20) Xianzhi, M.; Ragauskas, A. Pseudo-Lignin Formation during Dilute acid Pretreatment for Cellulosic Ethanol. *Recent Adv. Petrochem. Sci.* **2017**, *1*, 555551.

(21) Rasmussen, H.; Tanner, D.; Sørensen, H. R.; Meyer, A. S. New degradation compounds from lignocellulosic biomass pretreatment: routes for formation of potent oligophenolic enzyme inhibitors. *Green Chem.* **2017**, *19*, 464−473.

(22) Sannigrahi, P.; Kim, D. H.; Jung, S.; Ragauskas, A. Pseudo-lignin and pretreatment chemistry. *Energy Environ. Sci.* **2011**, *4*, 1306−1310.

(23) Jönsson, L. J.; Alriksson, B.; Nilvebrant, N.-O. Bioconversion of lignocellulose: inhibitors and detoxification. *Biotechnol. Biofuels* **2013**, *6*, 16.

(24) Rissanen, J. V.; Grénman, H.; Willför, S.; Murzin, D. Y.; Salmi, T. Spruce Hemicellulose for Chemicals Using Aqueous Extraction: Kinetics, Mass Transfer, and Modeling. *Ind. Eng. Chem. Res.* **2014**, *53*, 6341−6350.

(25) Li, J.; Henriksson, G.; Gellerstedt, G. Carbohydrate reactions during high-temperature steam treatment of aspen wood. *Appl. Biochem. Biotechnol.* **2005**, *125*, 175−188.

(26) Sundqvist, B.; Karlsson, O.; Westermark, U. Determination of formic-acid and acetic acid concentrations formed during hydrothermal treatment of birch wood and its relation to colour, strength and hardness. *Wood Sci. Technol.* **2006**, *40*, 549−561.

(27) Li, J.; Henriksson, G.; Gellerstedt, G. Lignin depolymerization/repolymerization and its critical role for delignification of aspen wood by steam explosion. *Bioresour. Technol.* **2007**, *98*, 3061−3068.

(28) Li, S.; Lundquist, K.; Westermark, U. Cleavage of arylglycerol β-aryl ethers under neutral and acid conditions. *Nord. Pulp Pap. Res. J.* **2000**, *15*, 292−299.

(29) Yelle, D. J.; Kaparaju, P.; Hunt, C. G.; Hirth, K.; Kim, H.; Ralph, J.; Felby, C. Two-Dimensional NMR Evidence for Cleavage of Lignin and Xylan Substituents in Wheat Straw Through Hydrothermal Pretreatment and Enzymatic Hydrolysis. *BioEnergy Res.* **2013**, *6*, 211−221.

(30) Glasser, W. G.; Wright, R. S. Steam-assisted biomass fractionation. 2. Fractionation behavior of various biomass resources. *Biomass Bioenergy* **1998**, *14*, 219−235.

(31) van Putten, R.-J.; van der Waal, J. C.; de Jong, E.; Rasrendra, C. B.; Heeres, H. J.; de Vries, J. G. Hydroxymethylfurfural, A Versatile Platform Chemical Made from Renewable Resources. *Chem. Rev.* **2013**, *113*, 1499−1597.

(32) Rice, J. A. HUMIN. *Soil Sci.* **2001**, *166*, 848−857.

(33) van Zandvoort, I.; Wang, Y.; Rasrendra, C. B.; van Eck, E. R. H.; Bruijnincx, P. C. A.; Heeres, H. J.; Weckhuysen, B. M. Formation, Molecular Structure, and Morphology of Humins in Biomass Conversion: Influence of Feedstock and Processing Conditions. *ChemSusChem* **2013**, *6*, 1745−1758.

(34) Patil, S. K. R.; Heltzel, J.; Lund, C. R. F. Comparison of Structural Features of Humins Formed Catalytically from Glucose, Fructose, and 5-Hydroxymethylfurfuraldehyde. *Energy Fuels* **2012**, *26*, 5281−5293.

(35) Patil, S. K. R.; Lund, C. R. F. Formation and Growth of Humins via Aldol Addition and Condensation during Acid-Catalyzed Conversion of 5-Hydroxymethylfurfural. *Energy Fuels* **2011**, *25*, 4745−4755.

(36) Tuercke, T.; Panic, S.; Loebbecke, S. Microreactor Process for the Optimized Synthesis of 5-Hydroxymethylfurfural: A Promising Building Block Obtained by Catalytic Dehydration of Fructose. *Chem. Eng. Technol.* **2009**, *32*, 1815−1822.

(37) Date, N. S.; Biradar, N. S.; Chikate, R. C.; Rode, C. V. Effect of Reduction Protocol of Pd Catalysts on Product Distribution in Furfural Hydrogenation. *ChemistrySelect* **2017**, *2*, 24−32.

(38) Schmid, G. H. Determination of erythro and threo configurations by nuclear magnetic resonance spectroscopy. *Can. J. Chem.* **1968**, *46*, 3415−3418.

(39) Bardet, M.; Lundquist, K.; Parkås, J.; Robert, D.; von Unge, S. 13C assignments of the carbon atoms in the aromatic rings of lignin model compounds of the arylglycerol *β*-aryl ether type. *Magn. Reson. Chem.* **2006**, *44*, 976−979.

(40) Aarum, I.; Devle, H.; Ekeberg, D.; Horn, S. J.; Stenstrøm, Y. The effect of flash pyrolysis temperature on compositional variability of pyrolyzates from birch lignin. *J. Anal. Appl. Pyrolysis* **2017**, *127*, 211−222.

(41) Jurak, E. *How Mushrooms Feed on Compost: Conversion of Carbohydrates and Linin in Industrial Wheat Straw Based Compost Enabling the Growth of Agaricus bisporus*, 1st ed.; Wageningen University: Wageningen, 2015; pp 130−131.

(42) Mosier, N.; Wyman, C.; Dale, B.; Elander, R.; Lee, Y. Y.; Holtzapple, M.; Ladisch, M. Features of promising technologies for pretreatment of lignocellulosic biomass. *Bioresour. Technol.* **2005**, *96*, 673−686.

(43) Li, J.; Henriksson, G.; Gellerstedt, G. Lignin depolymerization/repolymerization and its critical role for delignification of aspen wood by steam explosion. *Bioresour. Technol.* **2007**, *98*, 3061−3068.

(44) Shimada, K.; Hosoya, S.; Ikeda, T. Condensation Reactions of Softwood and Hardwood Lignin Model Compounds Under Organic Acid Cooking Conditions. *J. Wood Chem. Technol.* **1997**, *17*, 57−72.

(45) Sturgeon, M. R.; Kim, S.; Lawrence, K.; Paton, R. S.; Chmely, S. C.; Nimlos, M.; Foust, T. D.; Beckham, G. T. A Mechanistic Investigation of Acid-Catalyzed Cleavage of Aryl-Ether Linkages: Implications for Lignin Depolymerization in Acidic Environments. *ACS Sustainable Chem. Eng.* **2014**, *2*, 472−485.

(46) Baccile, N.; Laurent, G.; Babonneau, F.; Fayon, F.; Titirici, M.-M.; Antonietti, M. Structural Characterization of Hydrothermal Carbon Spheres by Advanced Solid-State MAS 13C NMR Investigations. *J. Phys. Chem. C* **2009**, *113*, 9644−9654.

(47) Uden, P. C. Nomenclature and terminology for analytical pyrolysis (IUPAC Recommendations 1993). *Pure Appl. Chem.* **1993**, *65*, 2405−2409.

Supporting information

Characterization of pseudo-lignin from steam exploded birch

Authors: Ida Aarum,*,[†] Hanne Devle,[†] Dag Ekeberg,[†] Svein J. Horn,[†] and Yngve Stenstrøm[†]

[†]Faculty of Chemistry, Biotechnology and Food Science, Norwegian University of Life Sciences,

P.O. Box 5003, N-1432, Ås, Norway

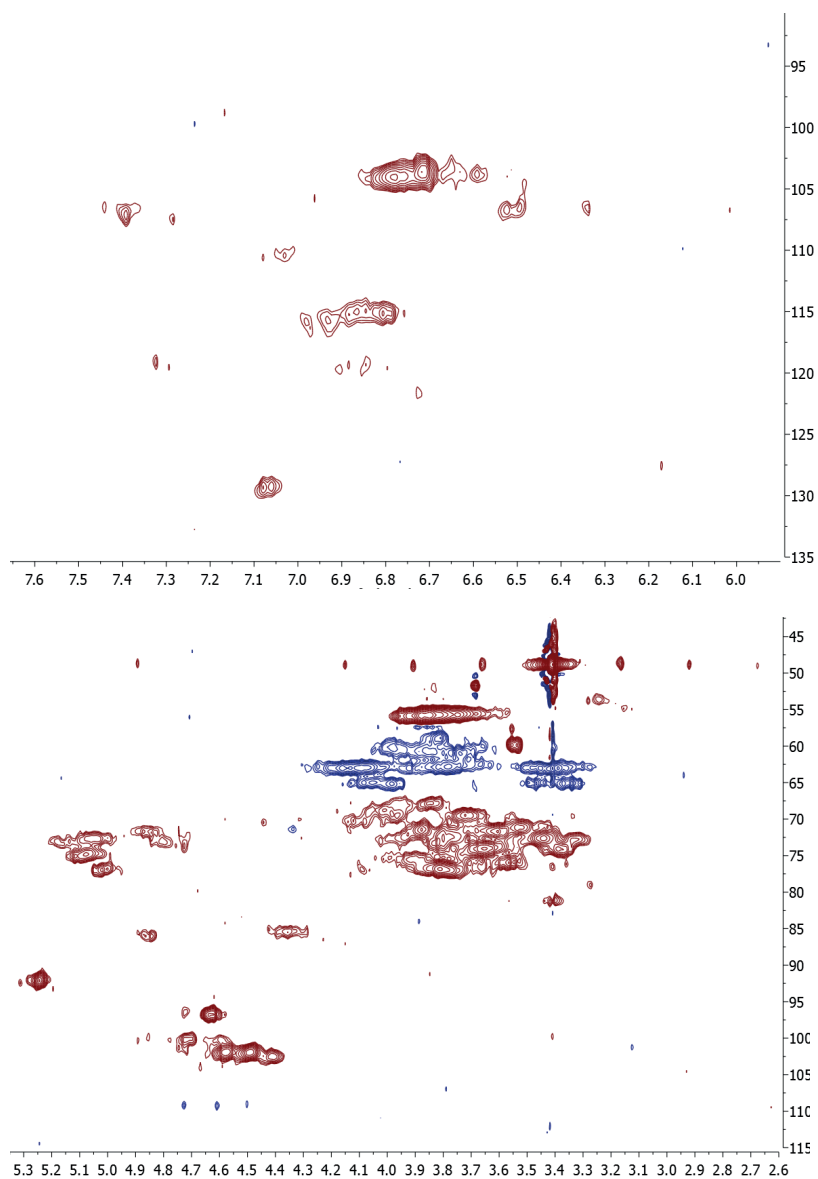It includes 12 pages with 5 figures and 1 table.

Figure S1. HSQC of SE-treated biomass of severity factor of 3.1 (170 °C – 10 min) in acetic acid-d_4. The shift values are slightly more upshift than with DMSO-d_6. The spectra are focused on aromatic region (above) and aliphatic region (below).
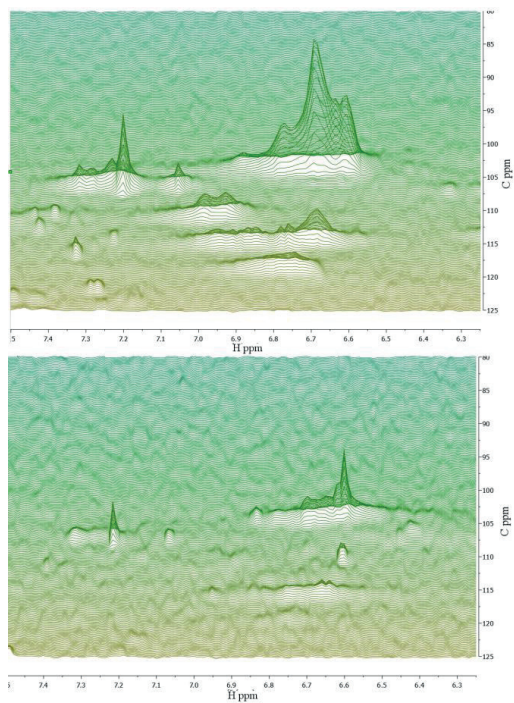
Figure S2. Topographic visualization of lignocellulosic biomass at untreated (above) and severity 4.7 (220 °C – 15 min) (below), focused on aromatic region.
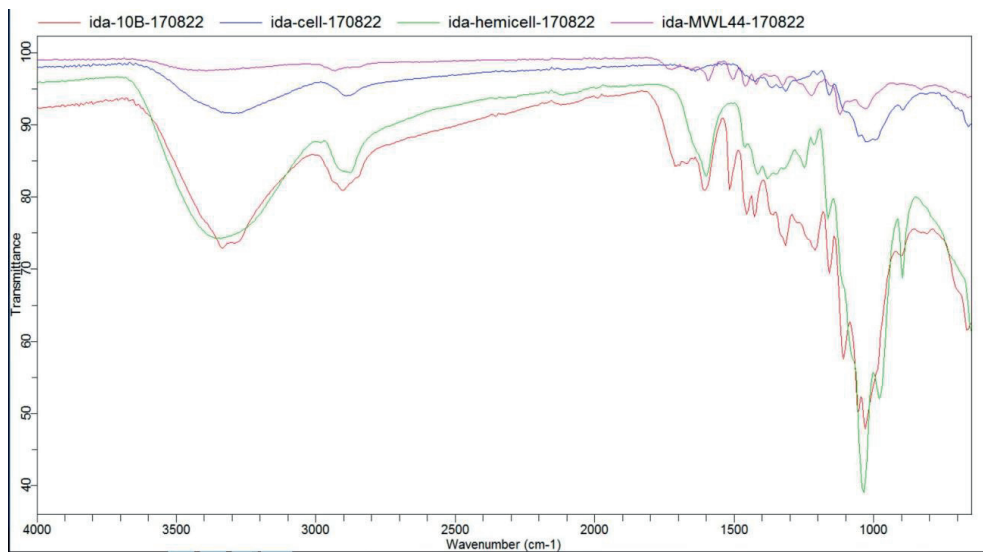
Figure S3. FTIR of milledwood lignin (red), cellulose (blue), hemicellulose (xylan, green) and

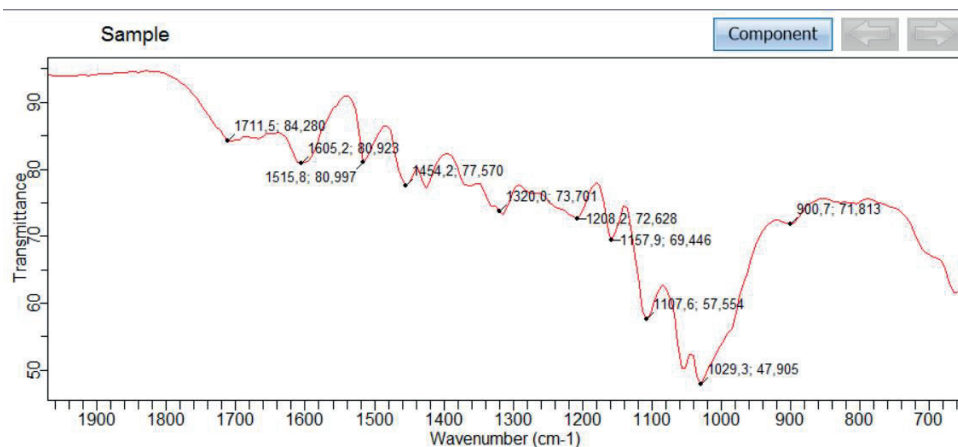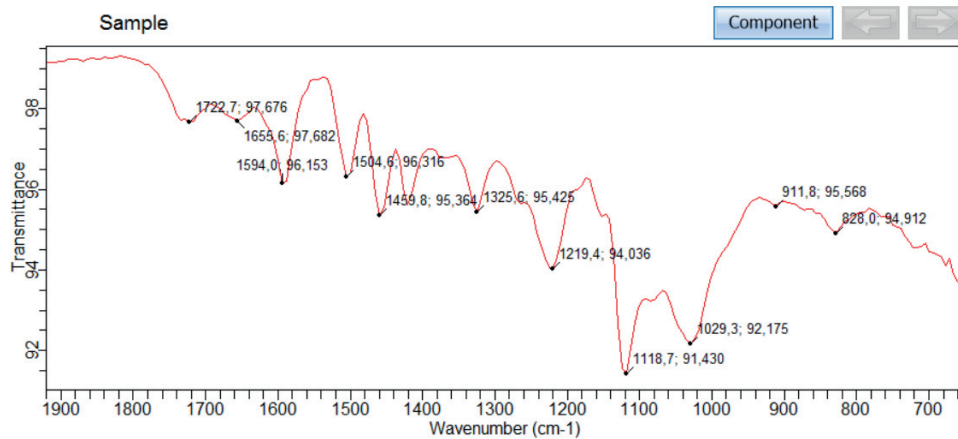se-treated biomass (220 °C, 15 min, purple)

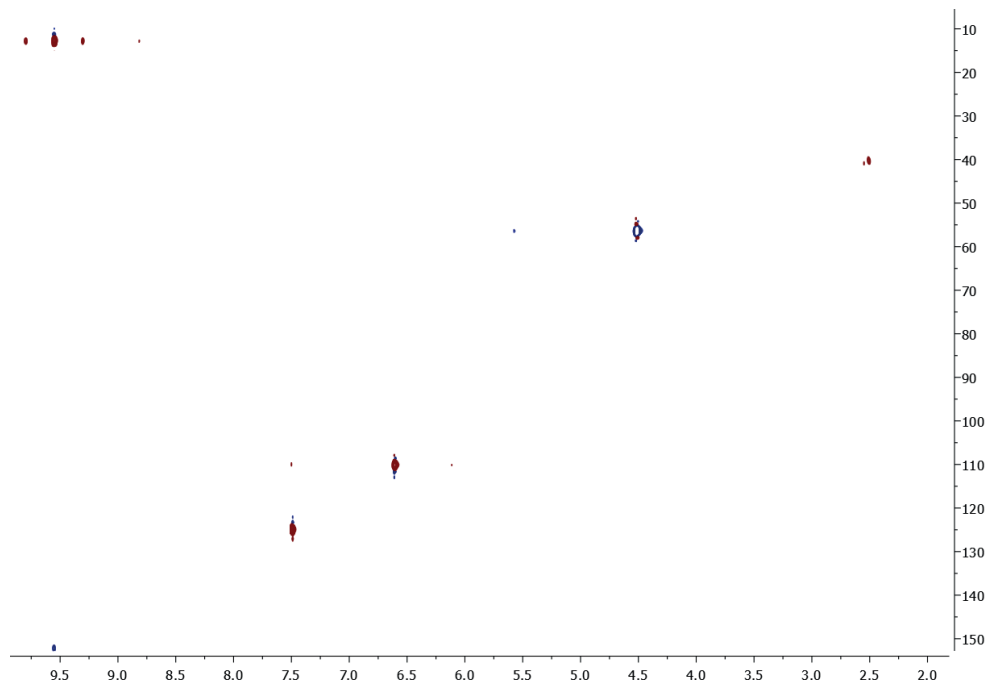**Figure S4.** FT-IR of untreated biomass (above) and SE –treated with log R_0 4.7 (below), focused in on 700 cm^{-1} to 2000 cm^{-1}.
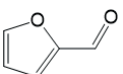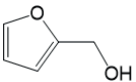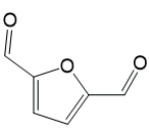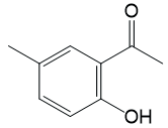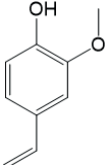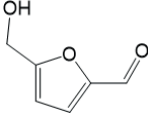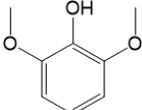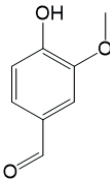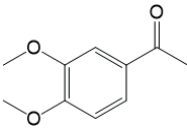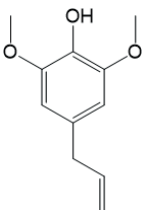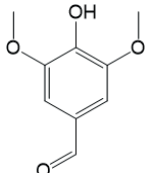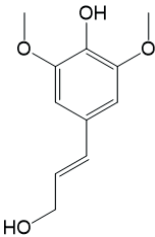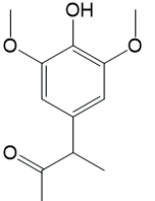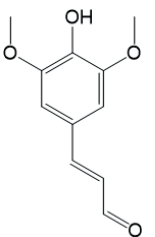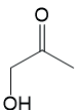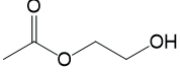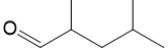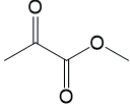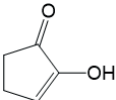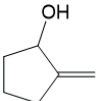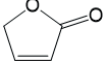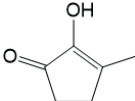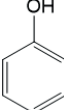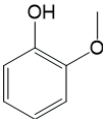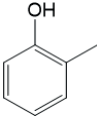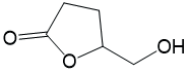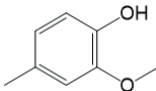
Figure S5. HSQC of 5-HMF standard in DMSO-d$_6$.

Table S1. Detected components from py-GC-MS at 350 and 600 °C.

ID	Name	$M^{+\cdot}$	Retention time (min)	Structure
1	Acetic acid	60	7.99	
2	Furfural	96	19.58	
3	2-Furanmethanol	98	21.22	
4	Not identified[1]	114	23.98	
5	Not identified	114	25.21	
6	Not identified	128	27.35	
7	2,5-Furandicarboxaldehyde	124	28.35	
8	Not identified	-	29.68	
9	Furan	68	30.93	
10	Not identified	152	33.87	
11	2-Methoxy-4-vinylphenol	150	35.05	

---

[1]

| 12 | 5-Hydroxymethyl furfural | 126 | 35.94 |

| 13 | 2,6-Dimethoxyphenol | 154 | 37.14 |

| 14 | Carbohydrate | 180 | 39.72 |

| 15 | 4-Hydroxy-3-methoxybenzaldehyde | 152 | 41.27 |

| 16 | Not identified | -- | 43.4 |

| 17 | 1-(3,4-dimethoxyphenyl)ethanone | 180 | 47.35 |

| 18 | Carbohydrate | 180 | 51.48 |
| 19 | Not identified | 166 | 51.79 |

| 20 | 4-Allyl-2,6-dimethoxyphenol | 194 | 53.75 |

| 21 | 4-Hydroxy-3,5-dimethoxybenzaldehyde | 182 | 54.79 |

| 22 | Not identified | 196 | 56.9 |

23	4-[(E)-3-hydroxyprop-1-enyl]-2,6-dimethoxyphenol	210	60.07	
24	3-(4-hydroxy-3,5-dimethoxyphenyl)butan-2-one	224	62.02	
25	3,5-Dimethoxy-4-hydroxycinnamaldehyde	208	70	
26	1-hydroxy-2-propanone	74	9.31	
27	1,2-Ethanediol, monoacetate	104	16.53	
28	Pentanal, 2,4-dimethyl-	114	18.48	
29	Propanoic acid, 2-oxo-, methyl ester	102	18.74	

30	2-Hydroxy-2-cyclopenten-1-one	98	23.24	
31	2-Methylene cyclopentanol	98	23.66	
32	2-Furanone	84	24.48	
33	Not identified	112	25.77	
34	2-Hydroxy-3-methyl-2-cyclopenten-1-one	112	25.89	
35	Phenol	94	26.31	
36	Phenol-2-methoxy-	124	27.14	
37	Phenol-2-methyl-	108	27.66	
38	5-Hydroxymethyldihydrofuran-2-one	116	28.9	
39	Not identified	--	29.95	
40	2-Methoxy-4-methylphenol	138	30.14	

| 41 | Coeluting | 114/152 | 32.38 |
| 42 | Not identified | -- | 32.64 |

| 43 | 4-Ethyl-2-methoxyphenol | 152 | 32.95 |
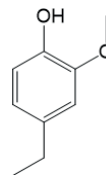
44	Not identified	164	36.06
		138/	
45	Coeluting	164/	38.39
		180	
46	Not identified	144	38.95
47	Carbohydrate	244	39.71

| 48 | 2-methoxy-4-(1-propenyl)phenol | 164 | 40.66 |

| 49 | 2,6-Dimethoxy-4-methylphenol | 168 | 41.18 |

| 50 | 2-Methoxy-4-propylphenol | 166 | 43.97 |

| 51 | 5-tert-butylbenzene-1,2,3-triol | 182 | 44.69 |

| 52 | 1-(4-Hydroxy-3-methoxyphenyl)ethanone | 166 | 45.13 |

| 53 | Not identified | 194 | 48.33 |
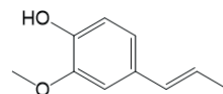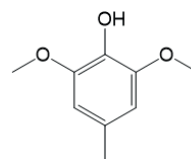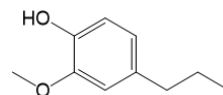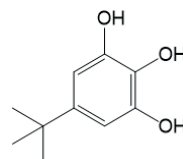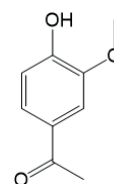
54	Not identified	194	50.87
55	Carbohydrate	180	51.55
56	1-(4-Hydroxy-3,5-dimethoxyphenyl)ethanone	196	58.12
57	1-(4-Hydroxy-3,5-dimethoxyphenyl)propan-1-one	210	61.77
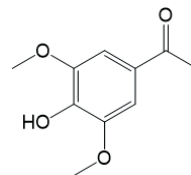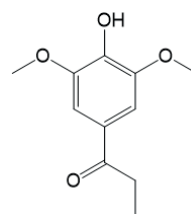
Paper III

Effect of steam explosion on spruce wood

Ida Aarum[*], Hanne Devle, Dag Ekeberg, Svein J. Horn and Yngve Stenstrøm

Impact of milled wood lignin purifications on spruce lignocellulose

Authors: Ida Aarum[†]*, Anders Solli[†], Hördur Gunnarsson[†], Dayanand Kalyani[†], Hanne Devle[†], Dag Ekeberg[†] and Yngve Stenstrøm[†]

[†]Faculty of Chemistry, Biotechnology and Food Science, Norwegian University of Life Sciences, P.O. Box 5003, N-1432 Ås, Norway

*Corresponding author, telephone: +47 67232471, email: ida.aarum@nmbu.no orcID 0000-0002-9035-494X

Abstract

The increasing energy and chemical needs have to be covered by renewable resources such as biomass, in the near future. Steam-explosion is a green pretreatment for utilizing biomass, but it produces a byproduct, pseudo-lignin. By comparing purified (milled wood lignin) and unpurified samples after steam explosion with pyrolysis-GC-MS, the components of pseudo-lignin should be evident. 2D NMR HSQC was also conducted on the purified samples, in addition to compositional analysis after steam explosion. After steam-explosion there is about 6 wt% of pseudo-lignin, and the pyrolysis show an increase of diol benzenes and furan components in the unpurified samples, which is associated with pseudo-lignin.

Introduction

As the need for more renewable sources of chemicals and energy keeps increasing, a sustainable conversion of biomass is more important. This conversion of biomass into high value products is a challenge as the refining process often degrades at least one of the three constituent (cellulose, hemicellulose and lignin), steam explosion in this case will decompose hemicellulose (Carvalheiro et al. 2008).

Steam explosion (SE) is a cheap, environmentally friendly pretreatment, which only uses small amounts of chemicals, other than water. It hydrolyses the hemicellulose into water-soluble oligomers and monomers (Carvalheiro et al. 2008; Chen and Fu 2016; Jacquet et al. 2015; Li et al. 2014). The cellulose get a higher crystalline index with SE below 200 °C as only the amorphous areas are degraded, but above 200 °C the fibers also starts to deform (Schultz et al. 1983; Steinbach et al. 2017). The lignin will also dissociate into smaller components, by hydrolysis under SE (Heikkinen et al. 2014). SE will in addition produce a by-product, denoted pseudo-lignin, and is defined as the increase of mass in Klason lignin (Hu et al. 2012). Pseudo-lignin obstructs enzymatic degradation of cellulose (Hu et al. 2013; Rasmussen et al. 2017; Vivekanand et al. 2013; Xianzhi and Ragauskas 2017) inhibiting further conversion of lignin and cellulose into high value products. For this reason alone, it is important to identify the chemical structure of pseudo-lignin, so that it can be avoided or handled downstream. The SE intensity is estimated by use of a severity factor model ($\log R_0$), whereas the parameters are temperature and time (Jacquet and Richel 2017; Overend et al. 1987).

As the definition of pseudo-lignin states that it is an increase of Klason lignin mass, it cannot just be lignin reacting with itself. The only two other possibilities are that either the holocellulose is degraded and reacts with the lignin to make a "different"-lignin or the

holocellulose is degraded and then polymerizes into a new polymer. If the degraded product reacts with lignin, the most likely position for this is the α-position of the alky-chain. Lignin will hydrolyze under SE causing the formation of a resonance-stabilized carbocation and the α-positioned cation will then be susceptible for nucleophilic attack (Scheme 1). This should give a shift in the ppm of α-H in a β-O-4 bond of lignin, which will be visible in the NMR spectrum as the lignin solubility does not change.
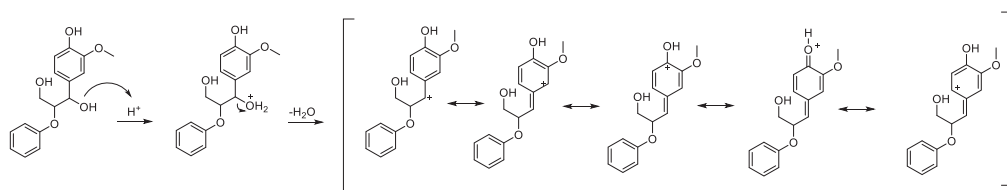
Scheme 1. Hydrolysis reaction of lignin and the resonance structures of the corresponding carbon cation formed (Aarum et al. 2018).

The option of degrading holocellulose being polymerized, is already documented in carbohydrate chemistry, into a product called humin (Rice 2001; van Putten et al. 2013). Humin is an organic polymer that is not soluble at any pH. The conditions for formation of humin are under mild acidic water together with heat (160 – 340 °C). For hardwoods SE is done using only water, but acetic acid will be released from the hemicellulose (auto hydrolysis), and the pH have been documented to decrease to around 3 (Sundqvist et al. 2006). Softwoods do not have acetic acid in the hemicellulose and SE is often done with a mild acidic presoaking, for example with 0.1 M H_2SO_4. These acidic conditions for hard- and softwood, including the heat under SE, is very comparable to the conditions for humin formation.

Milled wood lignin purification (MWLp) is a method of extraction and purifying lignin from wood, without altering the lignin structure at all (Brauns 1962). It is a technique that results in a lignin product known to be the closest to native lignin. Other techniques comparable to MWL are Ionic Liquids (ILs) extraction and Enzymatic Mild Acidolysis Lignin (EMAL) (Ventura et

al. 2017; Wu and Argyropoulos 2003). After SE, the MWLp will extract the lignin that has the same solubility properties as native lignin. The difference between purified and non-purified samples will then show the effect SE has on the residue left after pretreatment.

Fractionated pyrolysis is a technique where the same sample is pyrolyzed several times with increasing pyrolysis temperatures and each pyrolyzate is directly analyzed using GC-MS (Uden 1993). This will give different fractions of sample to analyze at specific volatile temperatures. It is important that the heating and cooling in the pyrolysis system has a fast rate to reduce secondary reactions in the pyrolysis (Asmadi et al. 2011; Bridgwater 2012; Collard and Blin 2014).

Purified samples are expected to be a uniformed lignin fraction, where carbohydrates and eventual pseudo-lignin has been removed. Carbohydrates in the unpurified samples will be mostly burned off in the fractionated pyrolysis, so that it is possible to analyze the remaining part. The difference in the pyrograms will then show the effect SE has on lignin and the holocellulose part of the biomass. Any byproducts such as pseudo-lignin or structural changes to the lignin should therefore be visible in the difference between the pyrograms, with increasing SE severity. The aim of this study was to see the effect of the purification on SE samples from Norway spruce stem wood and identify the differences. This is done by comparing the pyrograms of SE samples before and after purification with the MWLp method.

Materials and method

Raw materials

Norway spruce stem wood without bark were shredded (20-30 mm chips) and dried using a drum dryer, then milled to pass a sieve of 6 mm (SM2000, Retsch, Haan, Germany), and stored at room temperature. The dry matter content (DM) of the milled material was 85-90%.

The milled samples were pretreated with SE whereas one part was purified with milled wood lignin (MWL). The second part of the pretreated samples was the unpurified samples. These were then rinsed with ion exchanged water (RO-water) until clear (2 g dry weight, 1.5 L), to remove residue acids and small components. The samples were then freeze-dried (Alpha 2-4 LDplus, Christ Gmbh) for 72 h, before grinding in a planetary ball mill (Planetary Ball Mill PM100, Retsch Gmbh, Haan, Germany), with zirconium oxide (ZrO_2) balls. Each sample was ball milled at 350 rpm for 16 hours with 15 minutes interval and 15 minutes recess. The pulverized samples were then washed with acetone in a Soxhlet for 3-6 h until visually clear then dried in room temperature for 16 h.

All samples were dried and stored at room temperature, before applying the powder to the pyrolysis filament, with a sample handler for powdered substances (PyrolAB, Sweden).

The list of standards (Table S1) are described in a previously publication, used for retention validation of components (Aarum et al. 2017).

Mild acid catalysis and steam explosion

For mild acid catalysis, the spruce sample was presoaked at room temperature in the appropriate concentration of dilute sulfuric acid H_2SO_4 solution at 0.5% solids (w/w) for overnight. Pretreatment was performed as described previously, (Vivekanand et al. 2013) using the steam explosion facility designed by Cambi AS, Asker, Norway. Three hundred grams dry matter (DM) of dilute sulfuric acid treated spruce biomass was added to the pressure vessel for different pretreatment conditions. The spruce was pretreated at various temperature (180, 190, 200 and 210 °C) using a 5 and 10 min residence time. Prior to each pretreatment the pressure vessel was preheated for 10 min at the temperature to be used for pretreatment. The pretreated

fractions were stored at 4 °C. The dry matter (DM) content of the SE samples was in the range of 20-31%.

Moisture and ash content

The moisture content of untreated and pretreated spruce samples was determined by a Metrohmn Karl Fischer titrator (Florida, USA). Ash content was determined by a NREL method (A. Sluiter 2008), weighing samples before and after heating in a furnace at temperature of 550 °C for 3 h.

Compositional and carbohydrate analysis

Analyses of the sugars and lignin content in spruce wood samples before and after steam explosion (whole slurry) were carried out according to NREL/TP-510-42618 (A. Sluiter 2004). In short, the dry grinded spruce samples and sugar recovery standards (glucose, arabinose, mannitol, galactose and xylose) was exposed to 72% (w/w) H_2SO_4 at 30 °C for 60 min and then further hydrolyzed in 4% (w/w) H_2SO_4 at 121 °C in an autoclave for 60 min. After complete hydrolysis, the hydrolysates were filtered through filter (4 μm, Sigma Aldrich) and diluted with deionized water. The hydrolysates were stored at -20 °C. For the structural carbohydrate determination, sugar analysis was performed with a Dionex ICS3000 High-Performance Anion-Exchange Chromatography (HPAEC) system (Dionex, Sunnyvale, CA, USA) equipped with a pulsed amperometric detector (PAD), a CarboPac-PA1 2 × 250 mm analytical column, and a CarboPac PA1 2 × 50 mm guard column. As eluent Milli-Q water was used with a flow rate of 0.250 mL/min. The column temperature was 30 °C and the total run time 35 min.

Milled Wood Lignin

The steam exploded samples were purified with milled wood lignin method (MWL) (Bjorkman 1956; Obst and Kirk 1988) and stored in room temperature before analyzing with py-GC-MS. These samples were not rinsed before purification.

The SE samples were first dried over 48 h, in a desiccator (1 atm) with red silica gel and phosphorous pentoxide (P_4O_{10}) as a drying agent. The samples were then ball milled as stated above with 10 grams. To remove unwanted extractives from the wood powder the samples were first treated with acetone (60 mL) in a Soxhlet extractor for 4 h. The samples were dried overnight (minimum 16 h) in a desiccator. Then the samples were extracted with 1,4-dioxane and deionized water (70 mL, 96:4% v/v) for 6 h. This solution was diluted with water to precipitate the lignin before vacuum distillation. When the solution was approximately 20 mL a second portion of water was added (75 mL), before continuing the evaporation. This was repeated 2 more times until all the 1,4-dioxane was replaced and the mixture was freeze-dried to give crude MWL (MWLc).

The MWLc was dissolved in 90% acetic acid, filtered (Qualitative filter paper 303, 5 – 13 µm, VWR) by suction filtration using a Büchner funnel and precipitated into deionized water. The precipitate was evaporated again with vacuum distillation, and washed 3 times with water, before freeze-drying. The final step was the dissolution into 1,2-dichloroethane and ethanol (2:1, v/v%), filtration by suction filtration, precipitation into diethyl ether, evaporation with water wash and lastly freeze-drying to give pure MWL (MWLp). The samples were stored in a desiccator at room temperature.

Pyrolysis-GC-MS

The MWL samples was analyzed on an online flash filament Pyrola 2000 pyrolyzer (Pyrol AB, Lund, Sweden) that was coupled to a GC-MS (7890B-7000C Triple Quadrupole GC-MS instrument from Agilent technologies) to characterize the volatile pyrolyzate generated from fast pyrolysis of spruce samples. The GC-MS method and identification was done as previously described, with a capillary column (TraceGOLD TG-1710MS 60 m, ID 0.25 mm and 0.25 µm film thickness, Thermo Fisher Scientific), list of standards and NIST14 library (Aarum et al. 2017). For the unpurified samples the Pyrola 2000 was connected to a different GC-MS (Trace 1310-ISQ-QD, Thermo Scientific), with the same column (TG-1701MS, Thermo Scientific).

Pyrolysis of the purified samples was an isothermal pyrolysis at 600 °C. Total pyrolysis time was 2 s, with a heating time of 8 ms, before entering the GC. For the unpurified samples, pyrolysis was a fractionated pyrolysis (Uden 1993) at temperatures 350 and 600 °C, before each GCMS-analysis. For this to be representative, it is of utmost importance that the amount of secondary pyrolysis reactions occurring is not significant or non-existing, which is achieved with a fast heating rate and time (175 000 °C/s, 8 ms). The amounts of each component were normalized and therefore represent the change in composition as a function of SE-severity. Each pyrolysis has been performed in three replicates, and the values shown (Figure 1-7) are the average with corresponding standard deviation.

2D-NMR Heteronuclear Single Quantum Coherence (HSQC)

The NMR spectra were recorded on a Bruker Ascend 400 spectrometer (400 MHz), with a 5 mm PABBO-probe. The HSQC were run with DMSO-d_6 as a solvent with 60 mg of MWLp sample in 0.5 mL. The NMR spectra were recorded with a width of 0 – 10 ppm in ^1H and 0 – 165 ppm in ^{13}C, number of scans were 128 at 27 °C for both dimensions. The relaxation time

for ^{1}H-^{13}C was 1.5 s and the FID decay dimensions 2048 and 256, with 120 scans at 27 °C

(Aarum et al. 2017). The NMR experiments were done in triplicates.

Results and Discussion

Composition of wood samples

The compositional and carbohydrate analysis (Table S1) were used to calculate the amount of

pseudo-lignin generated under SE, Table 1. The calculation takes into account the loss of

total biomass from hydrolysis of hemicellulose represented as mannose and xylose. For the

first SE sample the estimated pseudo-lignin is a negative value (-0.4%) as the model over

estimates the amount of observed lignin.

Table 1. Effect of SE severities factor on biomass composition, and estimated pseudo-lignin. Amounts are expressed as percentage of dry matter. The amount of carbohydrate were calculated using the mass of anhydrous sugar.

Severity factor (log R_0)	Observed carbohydrates (man/xyl, %)[a]	Carbohydrate loss (man/xyl, %)[b]	Remaining biomass (%)[c]	Estimated lignin (%)[d]	Observed lignin (%)[e]	Pseudo-lignin (%)
—	15.2	0.0	100.0	31.2	31.2	0.0
3.1	11.7	4.0	96.0	32.5	32.1	-0.4
3.3	11.0	4.7	95.3	32.7	33.2	0.5
3.4	9.2	6.6	93.4	33.4	34.1	0.7
3.6	7.4	8.4	91.6	34.1	34.8	0.7
3.6	6.8	9.0	91.0	34.3	35.7	1.4
3.9	5.0	10.7	89.3	35.0	37.2	2.2
3.9	5.8	10.0	90.0	34.7	39.0	4.3
4.2	4.0	11.7	88.3	35.3	41.7	6.4

[a.] The amount of all components are expressed as percentage of dry matter. The amount of carbohydrates (mannose = man and xylose =xyl) was calculated using the mass of anhydrous sugar, from protocol NREL/TP-510-42618, (A. Sluiter 2004).
[b.] Assuming that the reduction of carbohydrates content during SE is due to loss of carbohydrates from the biomass (and not pseudo-lignin formation), the loss of carbohydrates can be estimated based on xylan content before (15.2 g) and after pretreatment: 15.2 = X + (100 - X)*Y/100 where X = carbohydrate loss and Y = observed carbohydrate content after pretreatment.

c. Calculated as 100 – carbohydrate loss.
d. Calculated as lignin content in non-treated spruce (31.2 g) divided by remaining biomass (Z): 31.2/(Z/100).
e. Lignin content was measured following the protocol from NREL/TP-510-42618, (A. Sluiter 2004).

Purified samples

The MWL extracted samples analyzed with semi-quantitative 2D-NMR (HSQC), (Sette et al. 2011) show a strong decrease in the β-O-4 bonding pattern (43.4 – 14.8%, Table 2), with increasing SE-severity (Heikkinen et al. 2014).

With the decreasing β-O-4 bonding pattern, there was a small increase of the other two bonding patterns, β-β and β-5/α-O-4 (3.60 – 4.36% and 10.5 – 17.0%, respectively), Table 2. The most noticeable difference in the spectra is the increase of the soluble carbohydrate fraction after even the lowest severity SE (180 °C, 5 min). In the anomeric area between 90.0/4.0 until 110/5.3 ppm there is an upsurge of signals. In addition, the corresponding carbohydrate signals (C2-C6) between 65.0/2.80 and 85.0/4.30 all have the same signal increase. By running a few standards (Table S2), we have denoted some of the shifts to be anomeric carbon in different carbohydrates (C1) in both acetal and hemiacetal from hemicellulose carbohydrates (galactoglucomannan, GGM), full assignment is given in Table S1. The anomeric carbon (C1) in galactose (Gal1, 91.9/4.92 ppm), glucose (Glu1, 92.2/4.87 ppm) and mannose (Man1, 93.9/4.88) are not visible in the untreated MWL sample. At severity factor 3.1 the reducing end Gal1, Glu1 and Man1 increases to 18.6, 23.5 and 60.5, respectively per 100 aromatic (G2-signal). This continues to increase until 85.6, 34.0 and 188.9 at severity factor 4.2. These samples are isolated with MWL and should contain only minor amounts of carbohydrates; this means that some of holocellulose has been hydrolyzed into smaller polymers or oligomers that is then isolated with the lignin. Hemicellulose is expected to hydrolyze, and if so will be extracted with the first liquid fraction after SE. This means that the hemicellulose is hydrolyzed in random places and not from the end, first to smaller polymers, then oligomers and in the end

into water soluble di- and monomers (Biermann et al. 1984; Garrote et al. 1999). This is confirmed by the fact that the intensity of the hemiacetal signal increases with SE-severity, meaning it must include a large number of reducing ends.

Table 2. Amount of the three most abundant lignin bonding patterns β-O-4, β-5, and β- β in [%], as an effect of SE-severity. The signal intensity is per 100 G2-signals, with standard deviation of three replicates.

Severity factor	β-O-4	β-5/α-O-4	β-β
-	43.4 ± 0.3	10.5 ± 0.1	3.60 ± 0.16
3.1	34.4 ± 0.3	12.5 ± 0.1	3.20 ± 0.14
3.3	26.7 ± 1.7	14.3 ± 0.3	3.73 ± 0.26
3.4	31.8 ± 0.8	12.9 ± 0.2	2.70 ± 0.36
3.6	23.7 ± 0.7	14.6 ± 0.3	3.43 ± 0.12
3.6	19.4 ± 0.4	16.2 ± 0.1	4.07 ± 0.05
3.9	19.3 ± 0.7	15.5 ± 0.4	3.57 ± 0.14
3.9	15.2 ± 1.4	17.2 ± 0.4	3.45 ± 0.38
4.2	14.8 ± 1.9	17.0 ± 0.7	4.36 ± 0.29

The pyrolysis of MWL purified samples reflected the change from the NMR spectra, as most of the lignin components where detected in equal amounts at all SE-severities, Figure 1. The major observed change was the increase of 2-methoxy-4-methylphenol and the decrease of 4-hydroxy-3-methoxy-benzaldehyd (vanillin). This decrease of oxygen in lignin is expected as lignin also undergoes hydrolysis in SE, especially in the β-O-4 bond, Table 2. This is confirmed with the HSQC-spectra, where a decreasing signal intensity can be seen.

There is little change in the composition with increasing SE-severity, with the exception of the hydrolysis for the purified samples. This means that either the lignin changes very little or that

the only one type of lignin is extracted and the hydrolyzed carbohydrates are too large for water fractionation.

A few new components do accumulate in the pyrograms after SE, component 2-furanaldehyde, 1,2-cyclopentadione, 5-methyl-2-furaldehyde and 2-hydroxy-3-methyl-2-cyclopenten-1-one (Figure 2). All of these components are furan-like components (Date et al. 2017; Steinbach et al. 2017) resulting from degradation of carbohydrates.
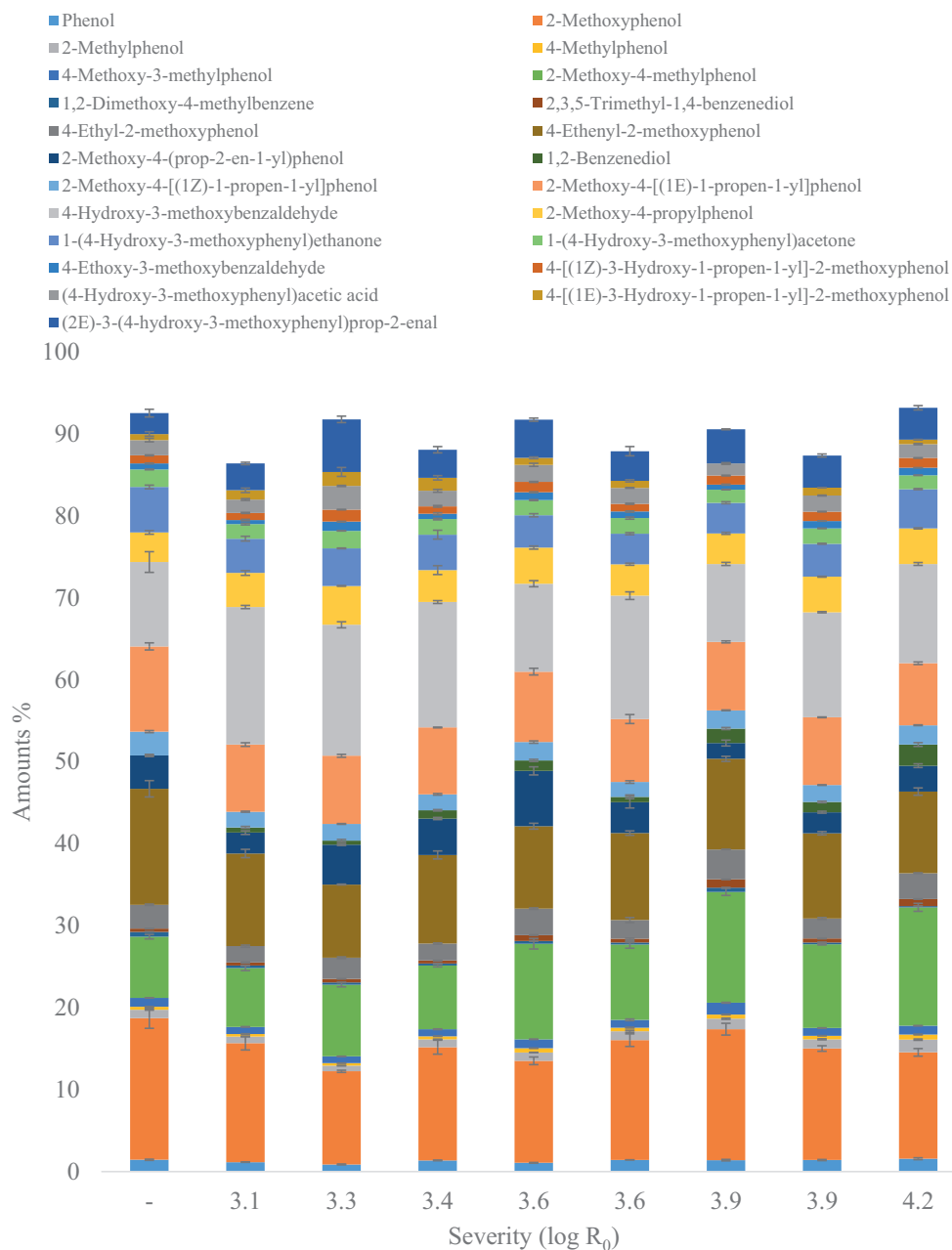
Figure 1. Amount of all lignin components in MWL-isolated samples from py-GC-MS, non-lignin components are not shown and are less than 15 %. The SE-samples with

13

identical log R_0 are placed with the low-high temperature from left to right. Pyrolysis temperature was 600 °C and the samples were run in triplicates.
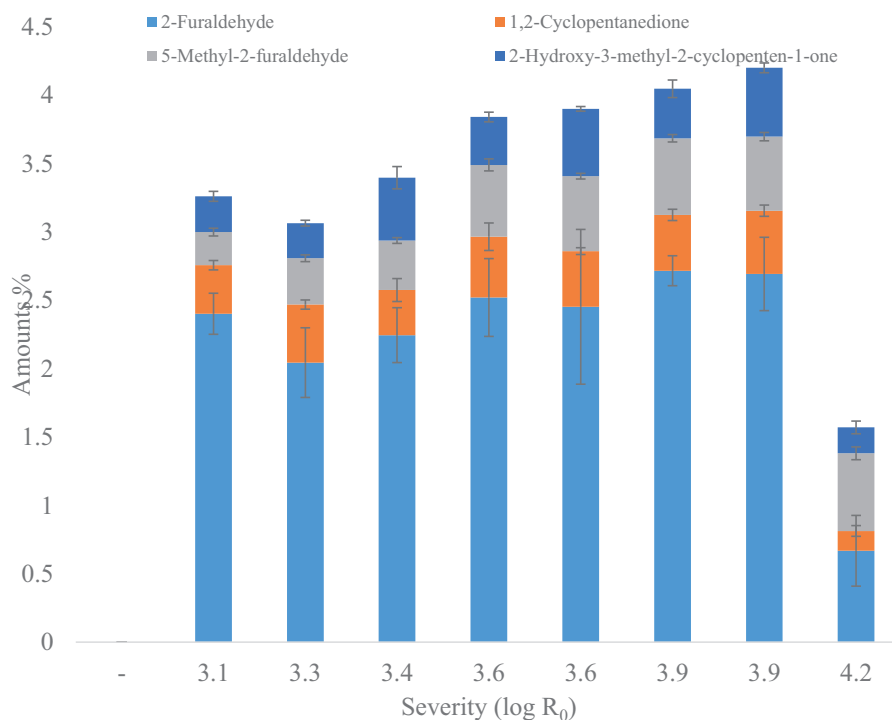
Figure 2. Amounts of furan and degraded furan components in MWL-isolated samples from py-GC-MS, not identified components are not shown and is less than 7%. The SE-samples with identical log R_0 are placed with the low-high temperature from left to right. Pyrolysis temperature was 600 °C and the samples were done in triplicates.

Unpurified samples

The first observation from the pyrograms were the increased complexity of the chromatograms, prior to purification. The matrix complexity including the cellulose and hemicellulose in the pyrolysis, could be circumvented by the use of fractionated pyrolysis. The 350 °C pyrolysis is

mainly performed to reduce the amount of carbohydrates, giving a decreased sample complexity. This is in accord with previous observation regarding the structure of carbohydrates (weak acetal bonding) (Aarum et al. 2018; Jurak 2015).

We found seven components that were unidentified and not present in the purified samples. Two of these could originate from hemicellulose as they match the molecular ions and fragmentation pattern of a previous work done on pyrolysis of hemicellulose (Table S3) (Gomez-Pardo and d'Angelo 1991; Ohnishi and Katō 1977), but it was non-conclusive as there was too few fragmentation peaks (only 3 in each mass spectra).

Pyrogram 350 °C

In the 350 °C analysis there is little changes in amount of the lignin derivatives with increasing SE-severity (Figure 3). One of the reasons is that SE will hydrolyze the lignin into smaller polymers. The degree of hydrolyzed lignin will increase with SE-severity. 3-(4-hydroxy-3-methoxyphenyl)prop-2-enal is a pyrolytic degradation component of lignin, since this decreases (13 – 3%) with increasing SE, this means that the lignin bonding pattern responsible for making coniferyl aldehyde under pyrolysis have been degraded with SE-severity. In the same way 1-(4-hydroxy-3-methoxyphenyl)butan-1-one (1 – 7%) and 2-methoxy-4-propylphenol (2 – 6%) increases, with SE-severity as a result of hydrolysis removing oxygen in general.
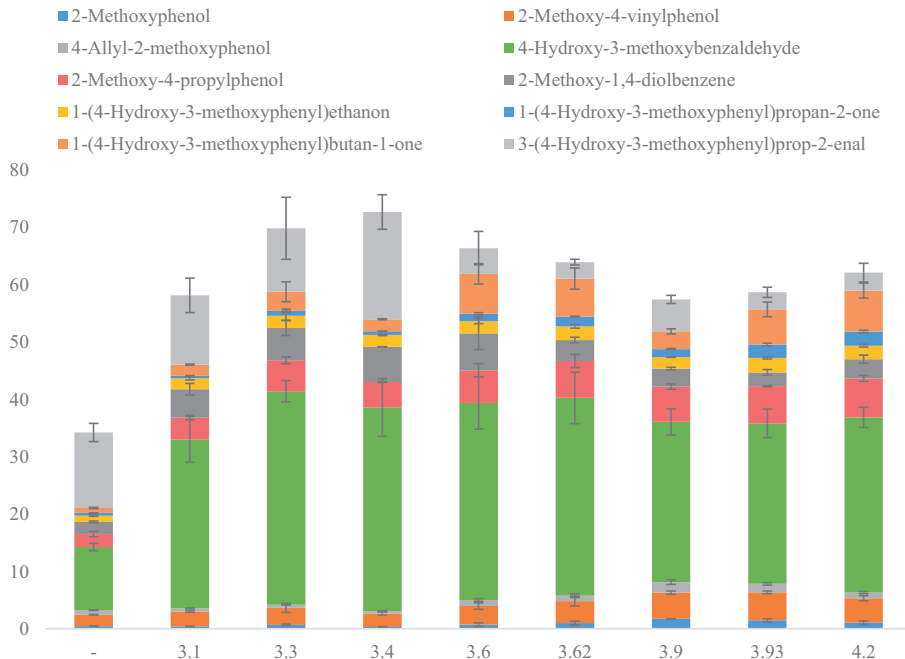
Figure 3. Benzene components from 350 °C fractionated pyrolysis, the samples were done in triplicates. The SE-samples with identical log R_0 are placed with the low-high temperature from left to right

Especially noteworthy is the change of vanillin amounts that increase from 11% in untreated samples to a stable level, 31% ±3, throughout the SE samples. This is different from the purified samples, where there was a sudden increase from 10% in untreated to 16% in log R_0 3.1 (Figure 1). However, with increasing SE the vanillin amount then continually decreases (16 – 12%). The most obvious explanation for this is that this is dependent on the extraction method. Apparently, the MWL purification method gives less vanillin, this could mean that the vanillin is directly involved in lignin-carbohydrate-complex (LCC) and by isolating lignin (and removing carbohydrates) we reduce the amount of vanillin in the pyrograms. The sudden increase of vanillin in both methods indicates that when the biomass is hydrolyzed under SE,

the LCC's and amorphous areas are most likely hydrolyzed into soluble components and give rise to more vanillin than normal in the lignin partition.

The components from the 350 °C pyrogram that did not include a six-membered aromatic moiety are shown in Figure 4. All of these components are normal pyrolysis degradation products from biomass, such as 5-hydroxymethylfurfural (5-HMF). However, there is a steady increase of 5-HMF (9 – 20%) and decrease of acetic acid (19 – 2%) with increasing SE. This means that there is a generation of 5-HMF under SE.

Figure 4. Non-benzene components from 350 °C fractionated pyrolysis on the unpurified samples, the samples were done in triplicates. The SE-samples with identical log R_0 are placed with the low-high temperature from left to right.

Pyrogram 600 °C

From the pyrograms at 600 °C (Figure 5 and Figure 6) the lignin component amounts are relatively stable. This means that very little changes in the core lignin, except that it becomes

more volatile, as showed with the increase of lignin components in the 350 °C pyrogram. The exceptions are 4-methyl-1,2-benzdiol and 3-methyl-1,2-benzdiol that both increase with SE-severity, 1 – 9% and 1 – 3%, respectively. The increase in amounts of these two different diols is interesting together with the increase of 5-HMF previously described. Since pseudo-lignin is defined as an increase in Klason lignin weight, it cannot stem from lignin reacting with itself in any form, as this will not increase the mass of Klason-lignin. The only possible weight increase comes from either; i) a degraded carbohydrate by-product formed under SE that can withstand strong acidic hydrolysis, or ii) a nucleophilic attack on lignin by a degraded carbohydrate, which can withstand the same conditions.

Early research in carbohydrate chemistry has studied the degradation of carbohydrates under mild acidic water conditions. As far back as 1910, the first mechanism of acid degradation was published (Nef 1910). Later this has been studied in more detail. The major feature of the mechanism is he degradation of carbohydrate (D-fructose) into 5-HMF (Li et al. 2005; Moye 1966; Sun et al. 2016). A documented by-product formed when carbohydrates are heated in a dilute acidic environment, is a furan polymer called humin. This is in particular the case with temperatures from 200 °C and above (Mednick 1962; Newth 1951). There have been some research into the structure of humins using NMR, but this has been done with a solid-state probe (Baccile et al. 2009; Herzfeld et al. 2011). Since the humins are not soluble at any pH or in organic solvents, mild acidic conversion gives a furan polymeric structure (van Zandvoort et al. 2015). An additional publication on the formation of humin with a 1,2,4-trihydroxybenzene as a supplement, gave a substantially higher crystal growth (van Zandvoort et al. 2013).

Differences

In both the purified and unpurified samples there is only small changes to the benzene component amount, with increasing SE-severity, only vanillin can be identified as a major product. For the purified samples a steady increase can be seen after the SE treatment (log R_0 3.2), while for the unpurified samples the amount is unchanged. In addition there is an emerging amounts of diols, 2-methoxy-1,4-benzediol (350 °C, Figure 3) and 4-methyl-1,2-benzediol (600 °C, Figure 5) in the unpurified samples. Based on the calculation of estimated and observed lignin in the samples there was an unnatural increase of observed lignin of about 6 % (Table 1). This is the denoted pseudo-lignin. The comparison of py-GC-MS from purified and unpurified samples show that pseudo-lignin is mostly removed in the purification step (MWLp), as the amounts of non-benzene components are low (less than 10% including non-identified components).

In the non-benzene components there are a significant change in the py-GC-MS results. There is an increase of 5-HMF and the two diols in py-GC-MS as an effect of SE-severity. The 5-HMF can also undergo conversion into 1,2,4-trihydroxybenzene. This happens mostly in the temperature range of 290 – 350 °C (Luijkx et al. 1993). In this case a strong acid (H_2SO_4) was utilized and even in diluted form (0.5% solids w/w) this will increase the degradation of holocellulose much faster than with autohydrolysis (release of acetic acid from hemicellulose in hardwoods, (Chen et al. 2010; Li et al. 2014)). Sulfuric acid has a dissociation constant pK_{a1} of -3, in addition to hygroscopic properties, this will push the hydrolysis reaction forward and the degradation will be more significant than autohydrolysis. This strong acid will then also help to further degrade lignin and furans into the diol benzenes. These two types of aromatic components can then polymerize into a new polymer, *i.e.* pseudo-lignin with some structural variations from pseudo-lignin of autohydrolysis. The formation of pseudo-lignin is rather the

degradation of carbohydrates into furans, such as 5-HMF, with further degradation into a humin-like structure.

Legend:
- 4-Methylphenol
- 3-Methylphenol
- 2-Methoxy-4-methylphenol
- 3,4-Dimethylphenol
- 4-Ethyl-2-methoxyphenol
- 2-Methoxy-4-vinylphenol
- 4-Allyl-2-methoxypheno
- 1,2-Benzenediol
- 2-Methoxy-4-(1-propenyl)phenol
- 3-Methyl-1,2-benzenediol
- 3-Methoxy-5-methylphenol
- 4-Methyl-1,2-benzenediol
- 2-Methoxy-4-(1-propenyl)phenol
- 4-Hydroxy-3-methoxybenzaldehyde
- 2-Methoxy-4-propylphenol
- 1-(4-Hydroxy-3-methoxyphenyl)ethanon
- 1-(4-Hydroxy-3-methoxyphenyl)-2-propanone
- 4-(1-Hydroxyallyl)-2-methoxyphenol
- 4-Hydroxy-3-methoxybenzenepropanol

Figure 5. Benzene components from 600 °C fractionated pyrolysis, the samples were done in triplicates. The SE-samples with identical log R_0 are placed with the low-high temperature from left to right

For the non-benzene components Figure 6, the biggest change is the abrupt decrease of acetic acid (19 – 2%), a small increase of 5-HMF (9 – 13%) and the increase of 2-hydroxy-3-methyl-2-cyclopenten-1-one (3 – 5%).
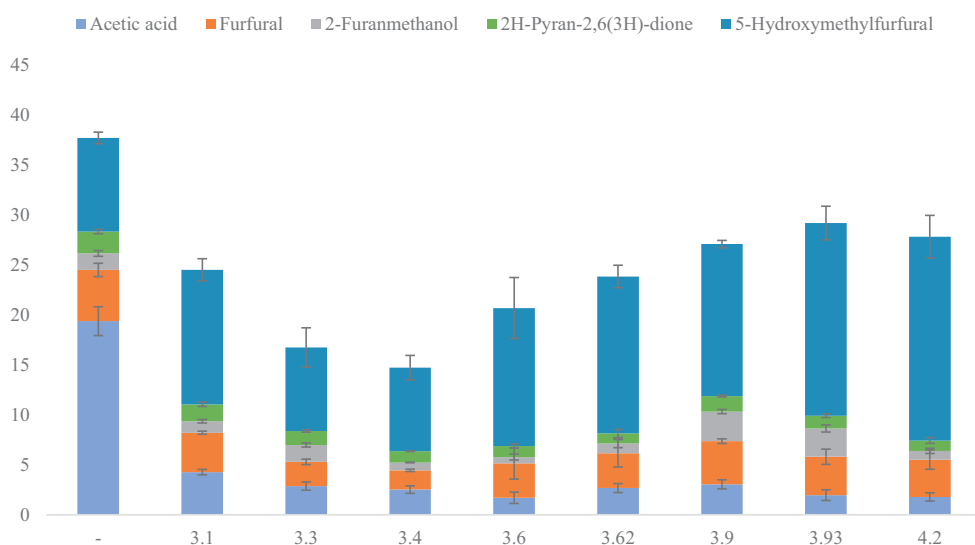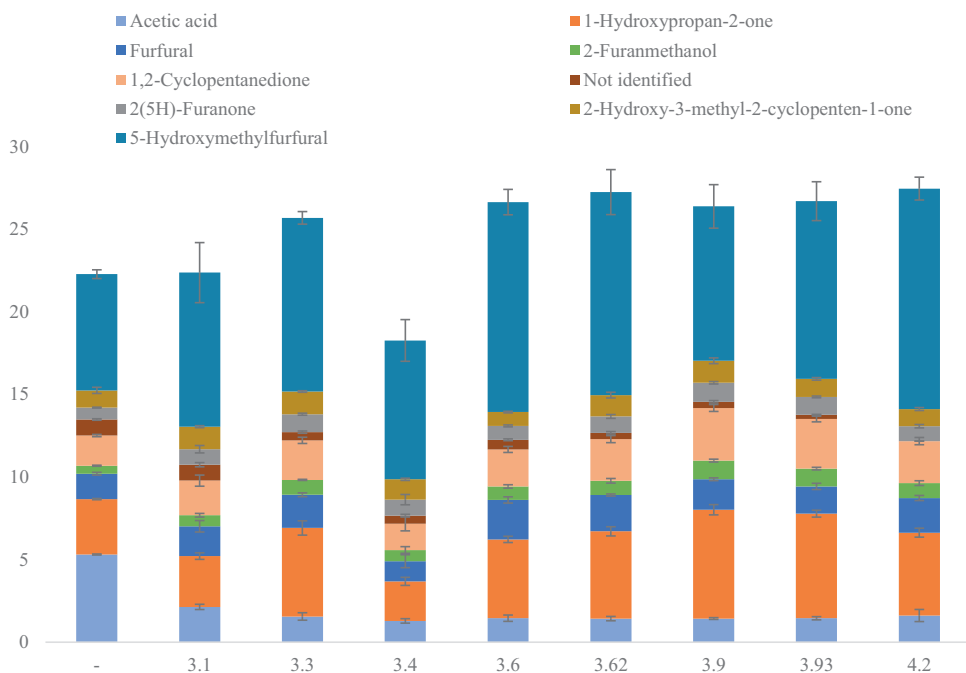

Figure 6. Non-benzene components from 600 °C fractionated pyrolysis on the unpurified samples, the samples were done in triplicates. The SE-samples with identical log R_0 are placed with the low-high temperature from left to right

Conclusions

With SE and increasing severity factor the lignin and holocellulose is degraded into smaller polymers. This yields more carbohydrate impurities in the MWLp than untreated wood. Interestingly the results implies that LCC are mostly connected to lignin through vanillin type

units. The difference between the purified and unpurified samples show some insight into the pseudo-lignin structure, it mostly contains furans and diols.

Acknowledgment

References

A. Sluiter BH, R. Ruiz, C. Scarlata, J. Sluiter, D. Templeton (2004) Determination of Structural Carbohydrates and Lignin in Biomass [Electronic Resource]. National Renewable Energy Laboratory, Laboratory Analytical Procedure (LAP)

A. Sluiter BH, R. Ruiz, C. Scarlata, J. Sluiter, D. Templeton (2008) Determination of Ash in Biomass [Electronic Resource]. National Renewable Energy Laboratory, Laboratory Analytical Procedure (LAP)

Aarum I, Devle H, Ekeberg D, Horn SJ, Stenstrøm Y (2017) The effect of flash pyrolysis temperature on compositional variability of pyrolyzates from birch lignin J Anal Appl Pyrolysis 127:211-222 doi:http://dx.doi.org/10.1016/j.jaap.2017.08.003

Aarum I, Devle H, Ekeberg D, Horn SJ, Stenstrøm Y (2018) Characterization of Pseudo-Lignin from Steam Exploded Birch ACS Omega 3:4924-4931 doi:10.1021/acsomega.8b00381

Asmadi M, Kawamoto H, Saka S (2011) Gas- and solid/liquid-phase reactions during pyrolysis of softwood and hardwood lignins J Anal Appl Pyrolysis 92:417-425 doi:10.1016/j.jaap.2011.08.003

Baccile N, Laurent G, Babonneau F, Fayon F, Titirici M-M, Antonietti M (2009) Structural Characterization of Hydrothermal Carbon Spheres by Advanced Solid-State MAS 13C NMR Investigations The Journal of Physical Chemistry C 113:9644-9654 doi:10.1021/jp901582x

Biermann CJ, Schultz TP, McGinnia GD (1984) Rapid Steam Hydrolysis/Extraction of Mixed Hardwoods as a Biomass Pretreatment J Wood Chem Technol 4:111-128 doi:10.1080/02773818408062286

Bjorkman A (1956) Finely divided wood. I. Extraction of lignin with neutral solvents Sven Papperstidn 59:477-485

Brauns FE (1962) Soluble Native Lignin, Milled Wood Lignin, Synthetic Lignin, and the Structure of Lignin vol 16. doi:10.1515/hfsg.1962.16.4.97

Bridgwater AV (2012) Review of fast pyrolysis of biomass and product upgrading Biomass Bioenergy 38:68-94 doi:https://doi.org/10.1016/j.biombioe.2011.01.048

Carvalheiro F, Duarte LC, Girio FM (2008) Hemicellulose biorefineries: a review on biomass pretreatments J Sci Ind Res 67:849-864

Chen H, Fu X (2016) Industrial technologies for bioethanol production from lignocellulosic biomass Renew Sustainable Energy Rev 57:468-478 doi:https://doi.org/10.1016/j.rser.2015.12.069

Chen X, Lawoko M, Heiningen Av (2010) Kinetics and mechanism of autohydrolysis of hardwoods Bioresour Technol 101:7812-7819 doi:10.1016/j.biortech.2010.05.006

Collard F-X, Blin J (2014) A review on pyrolysis of biomass constituents: Mechanisms and composition of the products obtained from the conversion of cellulose, hemicelluloses and lignin Renew Sustainable Energy Rev 38:594-608 doi:10.1016/j.rser.2014.06.013

Date NS, Biradar NS, Chikate RC, Rode CV (2017) Effect of Reduction Protocol of Pd Catalysts on Product Distribution in Furfural Hydrogenation ChemistrySelect 2:24-32 doi:10.1002/slct.201601790

Garrote G, Domínguez H, Parajó JC (1999) Hydrothermal processing of lignocellulosic materials Holz als Roh- und Werkstoff 57:191-202 doi:10.1007/s001070050039

Gomez-Pardo D, d'Angelo J (1991) Revision of structure of a "C56O3" substance generated in the pyrolysis of biomass materials Tetrahedron Lett 32:3067-3068 doi:https://doi.org/10.1016/0040-4039(91)80690-8

Heikkinen H, Elder T, Maaheimo H, Rovio S, Rahikainen J, Kruus K, Tamminen T (2014) Impact of Steam Explosion on the Wheat Straw Lignin Structure Studied by Solution-State Nuclear Magnetic Resonance and Density Functional Methods J Agric Food Chem 62:10437-10444 doi:10.1021/jf504622j

Herzfeld J, Rand D, Matsuki Y, Daviso E, Mak-Jurkauskas M, Mamajanov I (2011) Molecular structure of humin and melanoidin via solid state NMR J Phys Chem B 115:5741-5745 doi:10.1021/jp1119662

Hu F, Jung S, Ragauskas A (2012) Pseudo-lignin formation and its impact on enzymatic hydrolysis Bioresour Technol 117:7-12 doi:http://dx.doi.org/10.1016/j.biortech.2012.04.037

Hu F, Jung S, Ragauskas A (2013) Impact of Pseudolignin versus Dilute Acid-Pretreated Lignin on Enzymatic Hydrolysis of Cellulose ACS Sustainable Chem Eng 1:62-65 doi:10.1021/sc300032j

Jacquet N, Maniet G, Vanderghem C, Delvigne F, Richel A (2015) Application of Steam Explosion as Pretreatment on Lignocellulosic Material: A Review Industrial & Engineering Chemistry Research 54:2593-2598 doi:10.1021/ie503151g

Jacquet N, Richel A (2017) Adaptation of Severity Factor Model According to the Operating Parameter Variations Which Occur During Steam Explosion Process. In: Ruiz HA, Hedegaard Thomsen M, Trajano HL (eds) Hydrothermal Processing in Biorefineries: Production of Bioethanol and High Added-Value Compounds of Second and Third Generation Biomass. Springer International Publishing, Cham, pp 333-351. doi:10.1007/978-3-319-56457-9_13

Jurak E (2015) How mushrooms feed on compost: conversion of carbohydrates and linin in industrial wheat straw based compost enabling the growth of Agaricus bisporus. Wageningen University

Li J, Henriksson G, Gellerstedt G (2005) Carbohydrate reactions during high-temperature steam treatment of aspen wood Appl Biochem Biotechnol 125:175 doi:10.1385/ABAB:125:3:175

Li Y, Liu W, Hou Q, Han S, Wang Y, Zhou D (2014) Release of Acetic Acid and Its Effect on the Dissolution of Carbohydrates in the Autohydrolysis Pretreatment of Poplar Prior to Chemi-Thermomechanical Pulping Industrial & Engineering Chemistry Research 53:8366-8371 doi:10.1021/ie500637a

Luijkx GCA, van Rantwijk F, van Bekkum H (1993) Hydrothermal formation of 1,2,4-benzenetriol from 5-hydroxymethyl-2-furaldehyde and d-fructose Carbohydr Res 242:131-139 doi:https://doi.org/10.1016/0008-6215(93)80027-C

Mednick ML (1962) The Acid-Base-Catalyzed Conversion of Aldohexose into 5-(Hydroxymethyl)-2-furfural2 The Journal of Organic Chemistry 27:398-403 doi:10.1021/jo01049a013

Moye C (1966) The formation of 5-hydroxymethylfurfural from hexoses Aust J Chem 19:2317-2320 doi:https://doi.org/10.1071/CH9662317

Nef JU (1910) Dissoziationsvorgänge in der Zuckergruppe. Über das Verhalten der Zuckerarten gegen Ätzalkalien Justus Liebigs Annalen der Chemie 376:1-119 doi:doi:10.1002/jlac.19103760102

Newth FH (1951) The Formation of Furan Compounds from Hexoses. In: Hudso CS, Canto SM (eds) Advances in Carbohydrate Chemistry, vol 6. Academic Press, pp 83-106. doi:https://doi.org/10.1016/S0096-5332(08)60064-8

Obst JR, Kirk TK (1988) Isolation of lignin Methods Enzymol 161:3-12

Ohnishi A, Katō K (1977) Beiträge zur Tabakforschung International/Contributions to Tobacco Research 9:147-152 doi:https://doi.org/10.2478/cttr-2013-0439

Overend RP, Chornet E, Gascoigne JA (1987) Fractionation of Lignocellulosics by Steam-Aqueous Pretreatments [and Discussion] Philosophical Transactions of the Royal Society of London A: Mathematical, Physical and Engineering Sciences 321:523-536

Rasmussen H, Tanner D, Sorensen HR, Meyer AS (2017) New degradation compounds from lignocellulosic biomass pretreatment: routes for formation of potent oligophenolic enzyme inhibitors Green Chemistry 19:464-473 doi:10.1039/C6GC01809B

Rice JA (2001) HUMIN Soil Science 166:848-857

Schultz TP, Biermann CJ, McGinnis GD (1983) Steam explosion of mixed hardwood chips as a biomass pretreatment Industrial & Engineering Chemistry Product Research and Development 22:344-348 doi:10.1021/i300010a034

Sette M, Wechselberger R, Crestini C (2011) Elucidation of Lignin Structure by Quantitative 2D NMR Chemistry - A European Journal 17:9529-9535 doi:10.1002/chem.201003045

Steinbach D, Kruse A, Sauer J (2017) Pretreatment technologies of lignocellulosic biomass in water in view of furfural and 5-hydroxymethylfurfural production- A review Biomass Conversion and Biorefinery:1-28 doi:10.1007/s13399-017-0243-0

Sun Y, Liu P, Liu Z (2016) Catalytic conversion of carbohydrates to 5-hydroxymethylfurfural from the waste liquid of acid hydrolysis NCC Carbohydr Polym 142:177-182 doi:https://doi.org/10.1016/j.carbpol.2016.01.053

Sundqvist B, Karlsson O, Westermark U (2006) Determination of formic-acid and acetic acid concentrations formed during hydrothermal treatment of birch wood and its relation to colour, strength and hardness Wood Science and Technology 40:549-561 doi:10.1007/s00226-006-0071-z

Uden PC (1993) Nomenclature and terminology for analytical pyrolysis (IUPAC Recommendations 1993) Pure Appl Chem 65:2405-2409 doi:10.1351/pac199365112405

van Putten R-J, van der Waal JC, de Jong E, Rasrendra CB, Heeres HJ, de Vries JG (2013) Hydroxymethylfurfural, A Versatile Platform Chemical Made from Renewable Resources Chem Rev 113:1499-1597 doi:10.1021/cr300182k

van Zandvoort I, Koers EJ, Weingarth M, Bruijnincx PCA, Baldus M, Weckhuysen BM (2015) Structural characterization of 13C-enriched humins and alkali-treated 13C humins by 2D solid-state NMR Green Chemistry 17:4383-4392 doi:10.1039/C5GC00327J

van Zandvoort I, Wang Y, Rasrendra CB, van Eck ERH, Bruijnincx PCA, Heeres HJ, Weckhuysen BM (2013) Formation, Molecular Structure, and Morphology of Humins in Biomass Conversion: Influence of Feedstock and Processing Conditions ChemSusChem 6:1745-1758 doi:10.1002/cssc.201300332

Ventura SPM, e Silva FA, Quental MV, Mondal D, Freire MG, Coutinho JAP (2017) Ionic-Liquid-Mediated Extraction and Separation Processes for Bioactive Compounds: Past, Present, and Future Trends Chem Rev 117:6984-7052 doi:10.1021/acs.chemrev.6b00550

Vivekanand V, Olsen EF, Eijsink VGH, Horn SJ (2013) Effect of different steam explosion conditions on methane potential and enzymatic saccharification of birch Bioresour Technol 127:343-349 doi:http://dx.doi.org/10.1016/j.biortech.2012.09.118

Wu S, Argyropoulos DS (2003) An improved method for isolating lignin in high yield and purity J Pulp Pap Sci 29:235-240

Xianzhi M, Ragauskas A (2017) Pseudo-Lignin Formation during Dilute acid Pretreatment for Cellulosic Ethanol Recent Adv Petrochem Sci 1:1-5 doi:10.19080/RAPSCI.2017.01.555551

Supplementary
Impact of milled wood lignin purifications on spruce lignocellulose

Authors: Ida Aarum[†]*, Anders Solli[†], Hördur Gunnarsson[†], Dayanand Kalyani[†], Hanne Devle[†], Dag Ekeberg[†] and Yngve Stenstrøm[†]

[†]Faculty of Chemistry, Biotechnology and Food Science, Norwegian University of Life Sciences, P.O. Box 5003, N-1432 Ås, Norway

*Corresponding author, telephone: +47 67232471, email: ida.aarum@nmbu.no orcID 0000-0002-9035-494X

Table S1. Compositional and carbohydrate analysis of steam exploded spruce. The amount of all components are expressed as percentage of dry matter. The amount of carbohydrates were calculated using the mass of anhydrous sugar.

Severity factor (log R_0)	Glucan (%)	Arabinan (%)	Mannan (%)	Galactan (%)	Xylan (%)	Lignin (%)	Moisture (%)
—	44.6	1.6	10	1.5	5.2	31.2	8.9
3.1	37.3	1	6.7	1.2	5	32.1	76.7
3.3	37.4	0.8	5.9	1	5.1	33.2	74.4
3.4	36.1	0.8	5.2	0.9	4	34.1	76.5
3.6	38	0.6	4.2	0.7	3.2	34.8	76
3.6	37.2	0.8	3.7	0.6	3.1	35.7	74.9
3.9	38.2	0.6	2.4	0.4	2.6	37.2	75.1
3.9	37.9	0.5	2.9	0.3	2.9	39	74.1
4.2	39.7	0.3	2.2	0.2	1.8	41.7	75.3

Table S2. List of standards used for GC-MS analysis.

Standard	Retention time (min)	M$^+$(m/z)
2-methoxyphenol	27.652	109.0
2-methylphenol	28.482	108.0
4-methylphenol	29.478	107.0
3-methylphenol	29.482	108.0
2-methoxy-5-methylphenol	30.482	123.0
1-(2-hydroxy-5-methylphenyl)ethanone	33.900	135.0
3-methoxy-1,2-benzenediol	36.066	140.0
2-methoxy-4-(2-propenyl)phenol	37.192	164.0
2-methoxy-4-propylphenol-	37.274	137.0
1,2,4-trimethoxybenzene	37.767	153.0
1,2-dihydroxybenzene	38.120	110.0
2,6-dimethoxyphenol	38.379	154.0
1,2,3-trimethoxy-5-methylbenzene	38.549	182.0
2-methoxy-4-(1E-propenyl)phenol	39.481	164.0
2-methoxy-4-(1Z-propenyl)phenol	42.185	164.0
3,5-dimethoxy-4-hydroxytoluene	42.705	168.0
3-methoxy-4-hydroxybenzaldehyde	43.225	152.0
3-methoxy-4-hydroxyacetophenone	46.973	151.0
1-(3,4-dimethoxyphenyl)ethanone	49.585	165.0
2,6-dimethoxy-4-(2-propenyl)phenol	50.198	194.0
1-(3-hydroxy-4-methoxyphenyl)ethanone	51.504	151.0
4-hydroxy-3,5-dimethoxybenzaldehyde	57.303	182.0
1-(4-hydroxy-3,5-dimethoxyphenyl)ethanone	60.761	181.0

Table S3. Mass spectrometry fragmentation pattern of the two possible hemicellulose indicators.

Component	RT	m/z	relative intensity	m/z	relative intensity	m/z	relative intensity
Not identified 1	23.01	114	25	86	80	55	100
Not identified 2	24.17	114	100	58	80	57	35

Table S4. Assignment of ^{13}C-^{1}H correlations in HSQC spectra of untreated spruce (MWLp), severity factor 3.1 and severity factor 4.2.

Label	δ_C/δ_H [ppm]	Assignment
C_β	53.1/3.44	$C_\beta - H_\beta$ in phenylcoumarane substructures (C)
B_β	53.4/3.06	$C_\beta - H_\beta$ in resinol substructures (B)
F_β	55.0/2.75	$C_\beta - H_\beta$ in diphenylethane substructures (F)
MeO	55.3/3.74	C – H in methoxyls
A_γ	59.8/3.3-3.7	$C_\gamma - H_\gamma$ in β-O-4' substructures (A)
C_γ	62.5/3.7	$C_\gamma - H_\gamma$ in phenylcoumarane substructures (C)
A_α	71.1/4.7	$C_\alpha - H_\alpha$ in β-O-4' substructures (A)
A_β	83.8/4.27	$C_\beta - H_\beta$ in β-O-4' substructures (A)
B_α	84.7/4.6	$C_\alpha - H_\alpha$ in resinol substructures (B)
C_α	86.9/5.46	$C_\alpha - H_\alpha$ in phenylcoumarane substructures (C)
G_2	110.9/6.98	$C_2 - H_2$ in guaiacyl units (G)
G_5	115/6.8	$C_5 - H_5$ in guaiacyl units (G)
G_6	119/6.8	$C_6 - H_6$ in guaiacyl units (G)
Gal1	91.9/4.9	$C_1 - H_1$ in galactose with reducing end
Glu1	92.2/4.9	$C_1 - H_1$ in glucose with reducing end
Man1	93.9/4.9	$C_1 - H_1$ in mannose with reducing end
F3	109.4/6.6	$C_3 - H_3$ in 5-hydroxymethylfuran (F)
F6	55.7/4.5	$C_6 - H_6$ in 5-hydroxymethylfuran (F)
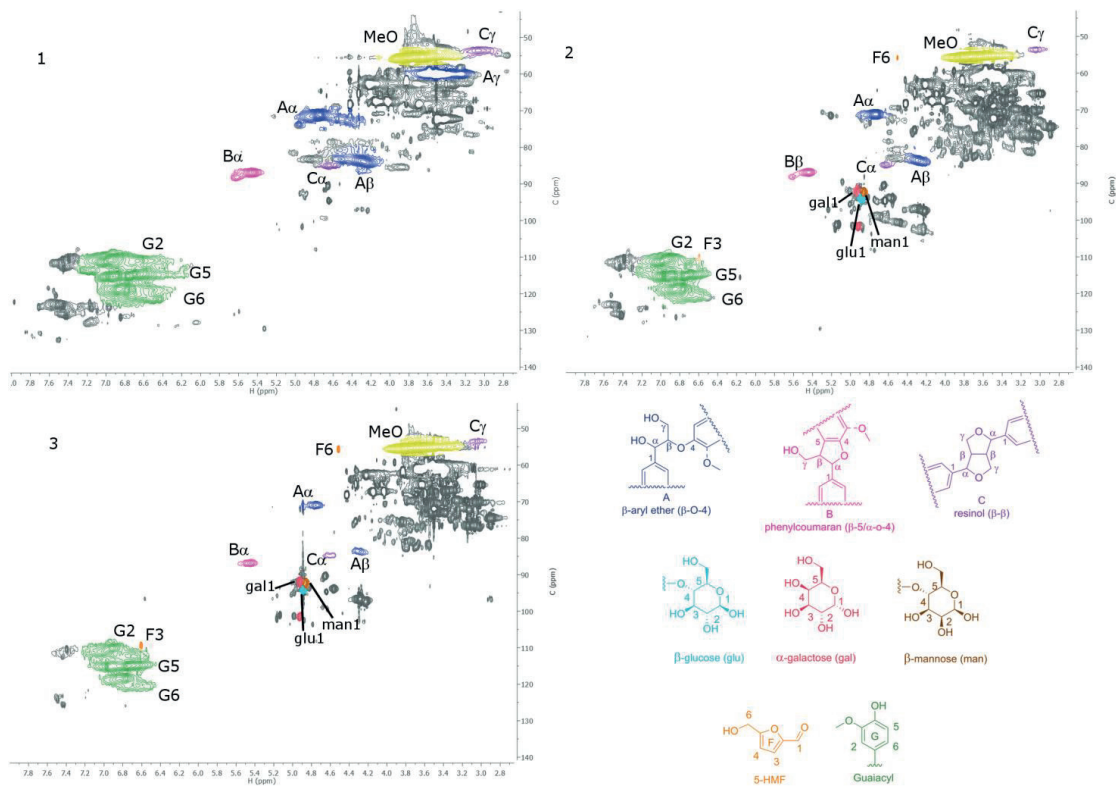
Figure S1. HSQC spectra of untreated spruce (MWLp, 1), severity factor 3.1 (2) and severity factor 4.2 (3). Focused on area 8.0 – 2.65 ^{1}H and 140.8 – 43.0 ^{13}C.

Paper IV

Effects of pH on steam explosion extraction of acetylated galactoglucomannan from Norway spruce.

Leszek Michalak, Ida Aarum, Svein Halvor Knutsen, Bjørge Westereng*

Effects of pH on steam explosion extraction of acetylated galactoglucomannan from Norway spruce.

Leszek Michalak[1], Svein Halvor Knutsen[2], Ida Aarum[1], Bjørge Westereng[1*]

[1] Faculty of Chemistry, Biotechnology and Food Science, Norwegian University of Life Sciences, Ås, Norway

[2] Nofima, Norwegian Institute of Food, Fishery and Aquaculture Research, PB 210, N-1431 Ås, Norway

* Corresponding author, bjorwe@nmbu.no

Keywords:

Steam explosion, pH control, Norway spruce, mannan, galactoglucomannan, acetylation, hemicellulose, hydrothermal extraction.

Abstract:

Background: Acetylated galactoglucomannan (AcGGM) is a complex hemicellulose found in softwoods such as Norway spruce (*Picea abies).* AcGGM has a large potential as a biorefinery feedstock and source of oligosaccharides for high value industrial applications. Steam explosion is an effective method for extraction of carbohydrates from plant biomass. Increasing the reaction pH reduces the combined severity (R'$_0$) of treatment, affecting yields and properties of extracted oligosaccharides. In this study, steam explosion was used to extract oligosaccharides from Norway spruce wood chips soaked with sodium citrate and potassium phosphate buffers with pH of 4.0-7.0. Yields, monosaccharide composition of released oligosaccharides and biomass residue, their acetate content and composition of their lignin fraction were examined to determine the impact of steam explosion buffering on the extraction of softwood hemicellulose.

Results: Reducing the severity of steam explosion resulted in lower yields, although the extracted oligosaccharides had a higher degree of polymerization. Higher buffering pH also resulted in a higher fraction of xylan in the extracted oligos. Oligosaccharides extracted in buffers of pH >5.0 were deacetylated. Buffering lead to a removal of acetylations from both the extracted oligosaccharides and the hemicellulose in the residual biomass. Treatment of the residual biomass with a GH5 family mannanase from *Aspergillus nidulans* was not able to improve the AcGGM yields. No hydroxymethylfurfural formation, a decomposition product from hexoses, was observed in samples soaked with buffers at pH higher than 4.0.

Conclusions: Buffering the steam explosion reactions proved to be an effective way to reduce the combined severity (R'$_0$) and produce a wide range of products from the same feedstock at the same physical conditions. The results highlight the impact of chemical autohydrolysis of hemicellulose by acetic acid released from the biomass in hydrothermal pretreatments. Lower combined severity results in products with a lower degree of acetylation of both the extracted oligosaccharides and residual biomass. Decrease in severity appears not to be the result of reduced acetate release, but

rather a result of inhibited autohydrolysis by the released acetate. Based on the results presented,

the optimal soaking pH for fine tuning properties of extracted AcGGM is below 5.0.

Background:

Steam explosion (SE) is an effective and scalable method for solubilizing hemicellulose from plant biomass, applicable to a wide range of biorefinery feedstocks. SE extraction was successfully used as pretreatment for production of biogas from hay (1), sugarcane bagasse (2) and corn stover (3), birchwood (4) as well as the production of ethanol from spruce bark (5) and many other platform chemicals from a wide range of lignocellulose feedstocks (6).

Steam explosion combines hydrothermal treatment of biomass with defibration by a rapid release of pressure at the end of the process. These two processes are independent of each other, and results comparable with SE have been obtained by hydrothermal treatment with a mechanical refining step, as long as the treatment severity was the same (7). In the course of the hydrothermal pretreatment, a major part of the hemicellulose and lignin present in the secondary cell wall lamellae is separated from the adjacent cellulose microfibrils, and becomes water soluble (8). At the same time, some of the acetate naturally linked to the xylan and mannan in the lignocellulose is released and contributes to the autohydrolyis of biomass. Release of acetic acid is the reason for the low pH usually seen in the SE product slurry. Properties of SE treated material depend on a range of factors, the most important being the residence time and temperature in the vessel. Impact of temperature on the material is described by the severity factor $R_0 = e^{(T_{exp} - 100)/14.75}$ (9). A combined severity factor $R'_0 = (10^{-pH}) * (t * e^{(T_{exp} - 100)/14.75})$ (10) was developed to include the contribution of H$^+$ to the hydrolysis process. This combined severity factor was previously used to predict and compare the severities of treatments where pH, rather than temperature or residence time, was the variable (11, 12). Mitigating the severity of pretreatment by controlling pH is a potential means of fine-tuning the products.

A number of factors besides temperature and residence time also play a role, such as the biomass particle size and the rate of steam and liquid diffusion through the particle, the ratio of solids to liquid loaded into the SE vessel and the chemicals brought in from upstream processing

stages. During SE treatment, acetylated hemicellulose releases acetic acid, which decreases the pH and facilitates chemical hydrolysis of polysaccharides. Acetate mediated autohydrolysis depends on the diffusion of liquid through the biomass particles (13). Diffusion rate depends on the particle size and the surface to volume ratio. The final pH of the product slurry after hydrothermal pretreatment depends on the composition of the liquid fraction, its amount and buffering capacity. The intricacies of hemicellulose breakdown in hydrothermal pretreatment, and difficulties in the analysis of the process are brilliantly explained by Rissanen et al. (13).

For inclusion in microbial fermentation, conditions are usually selected with the aim of highest possible breakdown of biomass, while keeping the formation of chemicals inhibitory to enzymatic hydrolysis or fermentation to a minimum (14, 15). In literature pertaining SE and pre-treatments fermentability and end-product yields are often selected as the main evaluation criteria, favoring high severity conditions often using acids or sulphates as additives (6, 16). These high severity conditions yield oligosaccharides with low degree of polymerization (DP), low degree of acetylation (DA) and fewer branchings, which require fewer enzymes for hydrolysis to monosaccharides. For GGM, this means a partial or complete deacetylation and removal of galactose sidechains. In contemporary biorefining focused on production of higher value chemicals such as food and feed ingredients, nutraceuticals (17) or hydrocolloids (18), controlled extraction conditions yielding high molecular mass and high complexity can be a more attractive pretreatment option. With the right enzyme toolbox, further tailoring and breakdown into constituent monomers is easy to achieve, while synthesis of highly branched and decorated polysaccharides in large amounts is almost impossible. Obtaining more complex hemicelluloses is of interest for several reasons: more complex products with novel physicochemical properties open doors to new applications, higher complexity may improve selectivity in microbial degradation (19), and increase the biodiversity of gut microbiomes when used as prebiotics. More complex oligosaccharides that more closely resemble *in vivo* hemicellulose would also make attractive substrates for studying activity of carbohydrate active enzymes.

Galactoglucomannan (GGM) is the main hemicellulose in Norway spruce (*Picea abies*). It is a complex hemicellulose consisting of a backbone of β-(1→4)-D-Man*p* and β-(1→4)-D-Glc*p* residues with α-(1→6)-D-Gal*p* branches, prevalently attached to the Man*p*, and to a lesser extent on Glc*p* (19). An estimated 30% of the D-Man*p* residues of spruce GGM are *O*-acetylated at carbons 2, 3 and 6, as well as 4 in the non-reducing ends of oligosaccharides (19)Acetylation of spruce mannan is a particularly important feature, since it affects the accessibility of mannans to microbes, and the physicochemical properties of mannans in solution. At the same time, release of acetylations from hemicellulose and hydrolysis of polysaccharides by the released acetate is a crucial process for the solubilization of hemicellulose (8).

In this study, SE extraction was carried out with pH control resulting in a mitigation of treatment severity. Six experimental conditions at five pH levels as well as a control sample using water only were used for SE to yield significantly different oligosaccharides in the extract. The relationship between the combined severity factor and the product composition was evaluated by assessing the yields, apparent DP, oligosaccharide acetylation, monosaccharide composition of products and biomass residue, MALDI-ToF MS analysis of extracted oligosaccharides, NMR analysis of lignin released, and analysis of susceptibility of biomass residue to treatment with a GH5 mannanase.

Results and discussion:

Figure 1. Flowchart of sample treatment and analyses carried out. The steam exploded wood chips were transferred from the collection vessel to plastic buckets and allowed to cool, pH measurements were taken once the slurry reached room temperature. Water was then added to aid extraction. Samples were mixed and transferred to funnels laid with Whatman B1 filters. Aliquots of this filtrate were used for quantification of acetate content, total carbohydrate content and reducing sugars. Samples of the filtrate were freeze dried and used for monosaccharide composition analysis, and analysis of lignin by NMR. SE wood retained by the filteres was dried at 100°C for 36-48 hours, until steady weight was reached. Samples of dried extracted wood were used for monosaccharide composition and enzymatic hydrolysis.

A detailed description of sample handling and analysis pipeline is illustrated in the flowchart above (figure 1). Citrate and phosphate based buffers were selected due to their respective buffer ranges and temperature stability. In all samples except the citrate pH 4.0, the pH has dropped after SE due to release of acetate from the wood (table 1). Higher buffer concentrations would be necessary to keep the post-SE pH exactly as the soaking buffers, however this would cause more interference with downstream analysis. The range of buffers resulted in combined severities ranging from 0.004 to 0.519 in the buffer controlled samples. Non-buffered controls had the highest R'_0 at 1.68-1.75. The wide range of calculated R'_0 is entirely attributable to the buffered conditions, since other conditions in the reaction were the same. The large difference in R'_0 between the buffered samples illustrates the room for adjustment and possibility for fine-tuning granted by pH controlled extractions.

Table 1. Sample treatments, slurry pH after steam explosion and the combined severity factors calculated as in (11) which determine severities based on the pH after the treatment. In all samples buffering the SE reaction has resulted in final pH

higher (pH 4.22- 6.32) than that of the control samples (average pH 3.70). 0.5M citrate and 1M phosphate at pH 6.0

resulted in different final pH, highlighting the difference in the buffering capacity between citrate and phosphate.

Buffer:	Average pH:	St. dev.	Average Combined Severity R'_0:	St. dev.	Man:Glc:Gal ratio:	Bound acetate µmole/mg carbohydrate.
MilliQ H_2O Control	3.703	0.009	1.707	0.037	1.88: 1: 0.28	0.303
0.5M Citrate pH 4.0	4.227	0.009	0.511	0.011	2.71: 1: 0.39	0.306
0.5M Citrate pH 5.0	4.973	0.041	0.092	0.009	1.64: 1: 0.51	0.112
0.5M Citrate pH 6.0	5.553	0.012	0.024	0.001	0.67: 1: 0.53	n.d.
1M Phosphate pH 6.0	5.317	0.045	0.042	0.004	1.39: 1: 0.23	n.d.
1M Phosphate pH 6.5	5.917	0.017	0.010	0.000	0.19: 1: 0.11	n.d.
1M Phosphate pH 7.0	6.303	0.031	0.004	0.000	0.23: 1: 0.16	n.d.
						-

Yields and composition of extracted hemicellulose:

Higher severity treatment yielded higher amounts of solubilized carbohydrates, with the highest yield of 17.4 % average based on dry wood weight for the non-buffered samples (figure 2A). Yields dropped for the buffered samples, with only the citrate pH 4.0 among the buffered samples (average R'_0 = 0.511) being close to the non-buffered sample (13.1 % average yields). The total yield of soluble carbohydrates dropped rapidly with the decreasing R'_0 although the yields remained over 4 % (4.4 % for the potassium phosphate pH 7.0 buffered samples, R'_0=0.0045). Yields from the three least severe treatments (sodium citrate pH 6.0, average R'_0 = 0.0241; and potassium phosphate pH 6.5 and 7.0, R'_0 = 0.0104 and R'_0 = 0.0045, respectively) shift very slightly (6.1 % for citrate pH 6.0, 5.2 % and 4.4 % for phosphate pH 6.5 and 7.0, respectively) despite a considerable drop in the R'_0. This decrease in efficiency with increasing pH was attributed to reaction pH being higher than the pK_a of acetic acid (4.76). Under these conditions, the reactivity of acetic acid and its contribution to autohydrolysis of hemicellulose are markedly decreased. Characteristics of products from these low

severity treatments illustrate a baseline for extraction in a SE reaction with a minor contribution of autohydrolysis. The extracts approximate the products of an extraction with steam and temperature only.

In order to assess yields as well as the degree of hemicellulose breakdown occurring during extraction, total carbohydrate content of each sample was determined using the phenol-sulphuric acid method of Dubois (20). Concentrations of reducing sugars were estimated by Miller's dinitrosalycilic acid assay (21). For comparison of severity effects on the estimated length of oligosaccharides in the soluble fraction, the ratio of total carbohydrates to reducing sugars was used as an approximation for the DP of the solubilized oligosaccharides (Figure 2A). Comparison of yields and DP of extracted oligosaccharides shows the increase of average DP (from 2.52 at $R'_0 = 1.707$ to 5.22 at $R'_0 = 0.004$), accompanied by a reduction in yields (decrease from 17.4 % of dry wood weight at $R'_0 = 1.707$ to 4.4 % at $R'_0 = 0.004$). An overview of oligosaccharide length and sample composition is presented in MALDI-ToF MS spectra (figure S2). Multiple oligosaccharides with m/z over 1000 are present in all samples, despite the comparison of total to reducing sugars indicating the average DP range to be between 2.52 (control) to 6.99 (potassium phosphate pH 6.5). This apparent discrepancy is due to the fact that MALDI-ToF was not able to detect monosaccharides and cleary visualize the oligosaccharides <750 m/z due to high background from the salts and other contaminants in the samples.

Figure 2. A: Percentage yields of total carbohydrates (blue bars) from dry wood mass, and the average DP of extracted oligosaccharides (red bars), error bars show standard deviation between technical replicates. B: Bar chart of acetate in filtrate (blue bars), and acetate released from the oligosaccharides in solution (red bars) after KOH treatment. Error bars indicate the standard deviation between technical replicates. C: Scatterplot of acetate content of filtered samples at the various severities. D: Scatterplot of acetate content of dried biomass residue, dry wood raw material in red.

Composition of extracted hemicellulose:

Beside the yields and apparent DP, buffering the SE reaction had an impact on the composition of extracted oligosaccharides. A comparison of the monosaccharide composition of all samples and the extracted wood is summarized in figure 3, and supplementary tables S2 and S3. At lower severity, more xylo-oligosaccharides were released, with only the citrate buffered and control samples yielding GGM as the predominant hemicellulose. No rhamnose was detected in the dried solids biomass residue after any treatment. Loss of arabinose in the high severity samples can be attributed to hydrolysis observed previously in low pH extractions (22). In samples buffered with pH 6.0, 6.5 and 7.0 phosphate, the relative content of mannose in the solubilized carbohydrate fraction was several times lower than that of xylose (figure 3, supplementary table s2). Galactose content and the apparent Gal:Man ratio have increased with decreasing severity, although we were unable to ascertain if the galactose was bound to GGM oligosaccharides, or was present as monosaccharides resulting from debranching of GGM in the cell wall. The decrease in efficiency of extraction over the wide range of severities is apparent in figure 3, the content of hemicellulose left in dried biomass residue increases with the decrease in combined severity.

The gradual shift from extraction of AcGGM towards xylan and glucuronoxylan is illustrated in figure 4. In order to clear the MALDI-ToF spectrum and avoid ambiguity of m/z assignment (such as in the case of peak 1097 m/z, which appears in the hexose and pentose series), aliquots of the extracts were deacetylated by adding 100mM NaOH. The control sample and sodium citrate pH 4.0 samples spectra contain predominantly hexose peaks, while xylooligosaccharide peaks are dominant in the spectra of citrate pH 5.0 and 6.0 samples.

Extraction buffered with sodium citrate at pH 4.0 produced the highest relative content of GGM in the filtrate (figure 3) and with the highest degree of acetylation of extracts (figure 2B and 5). The apparent increase in relative mannan content in soluble fraction of citrate pH 4.0 buffered samples ($R'_0 = 0.511$) comes at a reduction of yield from 17.3% to 13.1% compared to the control

sample (figure 2A). The corresponding dried biomass residue samples have a very similar

monosaccharide distribution: 37.56% mannose and 6.01 % galactose for the control sample residue,

39.51% mannose and 6.92 % galactose for citrate pH 4.0 (table s2). SE with citrate pH 4.0 buffering

appears more selective towards mannan, while the unbuffered control had a higher overall

efficiency.

The Man:Glc:Gal ratio (table 1) is an indication of complexity of yielded

mannooligosaccharides. In high severity hydrothermal extraction, the α-(1→6)-D-Gal*p* branchings of

GGM are cleaved off (23). For the Norwegian Spruce (*Picea abies*) the Man:Glc:Gal ratios reported in

literature is 4:1:0.1 3.8:1:0.4 (19, 24). The ratio varies based on the wood and extraction methods.

When the GGM constituent ratios are considered, buffering with citrate at pH 5.0 has yielded the

best results, nearly doubling the galactose content of the extracted oligos from control samples

(table 1). The ratios were 1.88: 1: 0.28 Man:Glc:Gal in the control samples and 1.64:1:0.51 in the

citrate pH 5.0. At the same time, citrate at pH 5.0 increased the apparent DP of the oligosaccharides

from 2.52 to 3.34 (figure 2A). The improvement in Man:Glc:Gal ratio was accompanied with a

pronounced decrease in yield (7.93% for citrate pH 5.0), and the mannose content of the extract

(32.55% for citrate pH 5.0 vs 46.41% for control). Citrate pH 5.0 extracts contained 28.09% xylose,

nearly twice as much as the control (15.94% for xylose) (table s2, figure), and had nearly three times

lower degree of acetylation (figure 2B).

Figure 3. Top: Relative monosaccharide composition of carbohydrates in the dried, washed solids. Bottom: Relative

monosaccharide composition of carbohydrates in aqueous extracts of steam exploded wood. The composition of untreated

spruce chips raw material (wood) is provided for comparison.

Figure 4. MALDI-ToF MS Spectra of extract samples deacetylated with NaOH. In the control and sodium citrate pH 4.0

samples, GGM peaks are the main components, with small xylooligosaccharide peaks alongside GGM in the sodium citrate

Figure 5 MALDI-TOF MS spectra of extracted oligosaccharides from the buffer control (black), sodium citrate pH 4.0 (blue), sodium citrate pH 5.0 (red), sodium citrate pH 6.0 (green). Peak labelled 1097.42* is either a double acetylated mannohexose or non-acetylated octapentose. Xyl – xylose, H-hexose, MeGlcUA – methylglucuronic acid, Ac-acetylation.

Acetate content of soluble fractions:

Acetate content in the filtrate decreased quickly with increasing severity (figure 2C). The same trend was apparent in analysis of acetate content in biomass residue. Biomass from buffered samples contained between 0.064-0.040 µmole of acetate per mg of biomass (figure 2D), while the control samples contained 0.142 µmole of acetate per mg. Dried biomass from control samples retained 65.8% of the acetate measured in wood raw material (0.142 µmole vs 0.218 µmole of acetate per mg). Since it is difficult to estimate the factual DP of oligosaccharide products, acetylation values were calculated as µmole of acetate per mg of solubilized carbohydrates.

In the severity range between the control samples and the samples buffered with sodium citrate pH 6.0, hemicellulose peaks seen in MALDI-ToF MS gradually became deacetylated (figure 5). The relative intensities of peaks corresponding to acetylated mannooligosaccharides indicate that the highest content of acetylated mannooligos was extracted in the control sample. Acetylated mannooligos are the majority of peaks in the control and sodium citrate pH 4.0 samples, and disappear in sodium citrate pH 6.0 samples.

Aliquots of the aqueous extracts were treated with KOH to deacetylate the oligosaccharides in solution. KOH treatment removed the acetylations on oligos in solution, and allowed for

comparison between the free acetate and bound acetate. Only the Citrate pH 4.0, 5.0, and the control samples contained appreciable amounts of acetate bound to carbohydrates (figure 2B, table 1). Despite the fact that high pH and low severity conditions yield more acetate per mg of released hemicellulose, the acetate was present free in solution. Whether this occurred as a result of pH in the SE vessel or occurred during storage of the sample (since buffer solution is still present) is unclear. From previous, unpublished experimental results at the same scale, as well as pilot scale where over 700 kg of spruce was processed, we know that storage at the control sample pH (3.6 - 4.0) did not cause a deacetylation even at ambient temperatures, for two to four weeks.

Acetylation of extracted oligosaccharides is a characteristic crucial for their physicochemical properties. The DA affects water solubility, susceptibility to enzymatic hydrolysis and availability as a carbon source for microbes. Release of acetate during hydrothermal pretreatment is one of the mechanisms of cell wall breakdown, and a decrease in severity would be expected to correlate with a decrease in the acetate released and in the amounts of acetate bound to oligosaccharides. This was however, not the case as more acetate was released with higher buffer pH. This may be due to de-esterification which is accelerated at higher pHs (25).

Enzymatic treatment of solid residue.

Enzymatic hydrolysis was tested as a means to assist the release of hemicellulose from wood treated with SE in conditions of inhibited autohydrolysis. Samples of dried residual biomass were treated with a GH5 family endomannanase from *Aspergillus nidulans* (26) to find out if severity of SE had an effect on the availability of hemicellulose in the steam exploded wood to hydrolytic enzymes. Even at low combined severity, the hemicellulose matrix is exposed to extreme conditions and undergoes defibration in the pressure release. These conditions were hypothesized to open the secondary cell wall matrix and render the hemicellulose more accessible to mannanases. GH5 family mannanases have been shown to be more efficient on less acetylated substrates (27), and since a

13

large part of the acetate was removed in the steam explosion, it was hypothesized that a hydrolytic enzyme could to a larger extent access the residual mannan and thus improve the yields of manno-oligosaccharides. However, mannanase treatment of dried residual biomass from SE did not release appreciable amounts of manno-oligosaccharides, indicating that mannan in the biomass residue remains largely inaccessible to hydrolytic enzymes, regardless of the material being acetylated (high severity) or non-acetylated (low severity). While there was an apparent effect of the mannanase when the relative content of carbohydrates in enzyme treatment solution was analyzed (figure 5), the only observable effect was a slight increase in the combined galactose and mannose fraction of the released oligosaccharides as compared to the control sample incubated at the same conditions in buffer without the enzyme. Enzymatic treatment with this enzyme was not a viable means of improving the yields of low severity SE.

Figure 6. Content of galactose and mannose as a fraction of total carbohydrates extracted with GH5 mannanase treatment. Red bars represent the Gal+Man fraction in mannanase treated samples; blue bars represent control samples with no enzyme.

NMR analysis of lignin content in the solubilized fraction:

Figure 7. HSQC 2D NMR Spectra of lignin content in biomass residues: (A) sodium citrate pH 4.0 buffered sample, (B) no buffer control, (C) sodium citrate pH 6.0 and (D) potassium phosphate pH 7.0. 5-hydroxymethylfurfural (5-HMF) and Guaicyl are depicted in the lower right of panel A, signals are colored and numbered according to the structures they relate to.

The HSQC 2D-NMR experiments taken of the solvable fraction of the samples shows the proton-carbon corresponding peaks. The spectra mainly contain carbohydrate signals, however there are detectable amounts of aromatic signals in all the samples (figure 6). The C_5/H_5-signal for guaiacyl unit (G5) at 114.9/6.7 ppm has the highest intensity in the sample citrate buffer pH 4 (figure

6A) and in the control (figure 6B), and only the control sample shows the C_6/H_6-signal for guaiacyl

unit (G6) at 118.6/6.7. Control sample (figure 6A) had a pH of 3.7 after steam explosion. Both the

control (figure 8A) and citrate pH 4.0 (figure 6B) samples were steam exploded at a lower pH (3-4)

and the degradation of lignocellulose is more intense for both in comparison to the higher pH steam

exploded samples, citrate pH 6 (figure 6C) and phosphate pH 7 (figure 6D). During SE the lignin

undergoes hydrolysis and degrades into smaller units of lignin (28). These units should be detectable

in the solvable fraction if they are small enough. With a lower pH, as in sample A and B the

hydrolysis is more extensive and lignin was detected in the solvable fraction (figure 6). In addition to

the signals from degraded lignin, there were some signals from dehydrated carbohydrates in the

form of 5-hydroxymethylfurfural (5-HMF, (29)), these were again only visible in citrate buffered

sample pH 4 (A) and in the control (B) (table 2). The pH is therefore important for control of both

lignin and carbohydrate degradation.

Table 2. Determination of the $^{13}C/^1H$ correlation signals acquired in 2D-NMR HSQC of the samples and semi quantitative analysis of lignin. Based on the summarized integrated areas of 5-HMF and guaiacyl relative to co-extracted mannose, signals is calculated per 100 mannose C1/H1 signal (%).

Label	δ_C/δ_H (ppm)	Assignment	A (Citrate pH 4)	B (control)
G5	114.9/6.7	C_5/H_5 in a Guaiacyl unit	66 %	22 %
G6	118.6/6.7	C_6/H_6 in a Guaiacyl unit	—	12 %
F3	124.1/7.5	C_3/H_3 in a 5-HMF unit	28 %	8 %
F4	109.4/6.6	C_4/H_4 in a 5-HMF unit	41 %	9 %
F6	55.4/4.5	C_6/H_6 in a 5-HMF unit	-42 %	-9 %

The signals for 5-HMF (F) and guaiacyl (G) unit were integrated in NMR with the C_1/H_1 signal

of mannose as an internal reference signal (30). In the citrate buffer pH 4 sample the G5-signals was

66% (calculated per 100 mannose C_1/H_1, table 2) in comparison to control which had only 22%. This

means that the relative amount of lignin is higher in the citrate buffer than in the control, even though the final pH in control sample was lower, as is expected based on existing research (31). As the initial pH in the control was not 3.7 before SE, the degree of hydrolysis seems to be more severe with continuously low pH. The same effect of more severe degradation is also detected with the carbohydrate fraction, as there is more 5-HMF, a common decomposition product of hexoses (32), in citric buffer (A) than control (B) (table 2). Besides the effect on properties of extracted oligosaccharides, inhibition of polysaccharide autohydrolysis in samples soaked with buffers >5.0 prevented the formation of HMF.

Optimal pH range for the production of acetylated galactoglucomannan.

From the wide range of combined severities tested in this study, between $R'_0=1.707$ and $R'_0=0.092$ (controls, citrate pH 4.0 and 5.0 buffered samples) appears to be the best range for production of acetylated galactoglucomannan. Extracts within this range contained acetylated oligosaccharides with varying DP, DA and Man:Glc:Gal ratios. At the same time, only the control and citrate pH 4.0 samples contained detectable levels of HMF. In the range between unbuffered and pH 5.0, buffering can mitigate the deacetylation, autohydrolysis and formation of HMF, at the cost of yield. As seen in the comparison between the control sample and citrate pH 4.0 the apparent loss in yield is partly due to increased specificity towards mannan extraction. Some general trends are apparent in the data presented here: increased combined severity results in higher yields and higher degree of acetylation of extracted oligosaccharides, while at the same time reducing the degree of polymerization. Further experiments into steam explosion production of tailored oligosaccharides from Norway spruce should be focused on this severity range.

Conclusions:

Introducing buffers to a steam explosion reaction has shown to be an efficient approach for mitigating the severity of the treatment, and production of a wide range of oligosaccharides from the same feedstock at the same temperature and pressure. Vast differences in monosaccharide composition, oligosaccharide size and degree of acetylation of the solubilized carbohydrate fraction were caused by the difference in pH. Notably, higher pH resulted in more pronounced deacetylation of residual biomass and extracted oligosaccharides.

Altering the pH did not reduce the severity by preventing the acetate release from the biomass, but by limiting acid hydrolysis of hemicellulose. Buffering mitigates the reactivity of acetate once it is released. The results show that the role of temperature and pressure is mainly to create conditions where autohydrolysis can occur. When the autohydrolysis was inhibited by buffering, the yields dropped and the breakdown of oligosaccharides was reduced. This study clearly shows that pH largely affects product composition and yields. It has been argued that pH has more impact on SE (12) reactions than temperature or pressure, and the results presented here support this claim.

Materials and Methods:

Buffers:

1M sodium citrate and 2M potassium phosphate buffers were prepared by mixing 1M solutions of sodium citrate (Sigma-Aldrich, Germany) and citric acid (Sigma-Aldrich, Germany), and 2M solutions of di- and mono-basic potassium phosphate (Sigma-Aldrich, Germany) were mixed to reach the desired pH. Citrate buffers produced were pH 4.0, 5.0, and 6.0, phosphate pH was 6.0, 6.5 and 7.0. The higher concentration of phosphate buffers was used to counteract the poor pH retention after SE in the phosphate buffered samples observed in initial trial experiments (unpublished).

Wood:

Dry Norway spruce (*Picea abies*) wood was milled using a hammer mill with a 2 mm sieve. 500 gram samples of spruce chips were soaked with buffers and MilliQ water in a 1: 1: 1 (g: mL: mL) ratio prior to SE. Water was added to ensure the buffers were thoroughly mixed into the wood, resulting in final buffer concentrations of 0.5 M for sodium citrate and 1 M for potassium phosphate. The wood chips were stirred until the sample was thoroughly soaked and transferred into the SE reactor.

Steam Explosion and extraction of water-soluble material:

Soaked spruce chips were hydrothermally treated in a steam explosion unit (Cambi, Asker, Norway) consisting of a 20 L pressure vessel and a flash tank with collection bucket. Steam was generated in a 25 kW electric boiler (Parat, Flekkefjord, Norway). The steam explosion unit is described in detail in (33). Treatment conditions were 200° C, 14.5 bar, biomass residence time was 10 minutes.

Handling of extracts and residuals:

After SE, water was added, the slurry was stirred for extraction and filtered through a whatman B1 filter paper (Sigma Aldritch, Norway). The residual water-insoluble material was squeezed to release the remaining soluble oligosaccharides, which were combined with the extract. Aliquots were frozen to determine extract yield and to supply samples for carbohydrate, lignin and acetyl analysis. 200 mL of each sample was freeze dried for the analysis of constituent neutral monosaccharides (GC) and uronic acid (colorimetry) of the released oligosaccharides. Insoluble materials were dried in an oven at 100°C for 36-48 hours, to constant weight, then milled on a cutter mill (Retsch, Haan, Germany) with a 0.5 mm sieve.

Poly- and oligosaccharide constituent sugars, carbohydrate content and reducing sugar in extract and non-soluble residuals:

Concentration of carbohydrates in solution were quantified according to the Dubois method (20), and reducing sugars content according to the Miller method (21). Calibration curves for both colorimetric methods were based on glucose. Constituent monosaccharide of residuals and extracts were quantified by GC via alditol acetates after acid hydrolysis (34) and uronic acids in the hydrolysates were determined by a colorimetric assay (35).

MALDI-ToF analysis:

MALDI-ToF analysis of hydrolysis product was conducted on an UltraFlextreme MALDI-ToF instrument (Bruker Daltonics GmbH, Germany) equipped with a nitrogen 337 nm laser beam. Samples were prepared by applying 2 µL of a 9mg/mL solution of 2,5-dihydroxybenzoic acid (Sigma-Aldrich, Germany) in 30% acetonitrile (VWR) to an MTP 384 ground steel target plate (Bruker Daltonics GmbH, Germany), adding 1 µL of sample (0.1-1 mg/mL) and mixing the drop with the pipette. Sample drops were then dried under a stream of warm air.

Acetate content analysis:

For the analysis of free acetate content in solution, the filtered liquid fraction washed from the biomass was diluted 1:2 with MilliQ water (to measure acetate in solution) or 100 mM KOH (to release the acetate bound to the oligosaccharides). 50 µL samples of the liquid phase were collected and analyzed by HPLC. All values were corrected for the concentration of oligosaccharides in solution and exact weight of biomass in the sample.

For the analysis of acetate content in the biomass residue, 100 mg ±10 % samples of the dried, milled residue were soaked overnight with 500 µL of 0.1 M KOH, left in a thermomixer

(Eppendorf, Oslo, Norway) overnight at 1000 rpm, 40 °C. After 18 hours, 500 μL of MilliQ water was added to the samples, which were then mixed by vortexing and spun down at x10000 g, for 5 minutes, and analyzed by HPLC. All values were corrected for the concentration of oligosaccharides in solution and exact weight of biomass in the sample.

HPLC:

Acetate content was analysed by HPLC using a REZEX ROA-Organic Acid H+ (Phenomenex, Torrance, California, USA) 300x7.8mm ion exclusion column, isocratic elution with 0.6 mL/min 4mM H_2SO_4 at 65 °C and UV detection at 210 nm.

Enzymatic treatment:

Milled, dry samples were washed with water to remove remaining soluble carbohydrates and buffer salts from the SE slurry, dried and resuspended in 25 mL of 50 mM sodium acetate buffer at pH 5.5. A GH5 family mannanase from *Aspergillus nidulans* (26) was applied to the sample with loadings of 0.01 mg : 1mg (1%), 0.1 mg : 1mg (10%) and 0.3mg : 1mg (30%) of enzyme : mannan in samples, based on an estimate of 20 % of the substrate being mannan. Samples were left in a shaking incubator overnight at 50° C, which is the optimum temperature for enzymatic activity.

NMR of lignin fraction:

The NMR spectra were recorded on a Bruker Ascend 400 spectrometer (400 MHz) at 320 K using a 5 mm PABBO probe. The samples (45 mg) were dissolved in DMSO-d_6 (1 mL), sonicated for 30 min and filtered through glass wool to remove any undissolved particles directly into the NMR-tube. Two of the samples did not fully dissolve. The Heteronuclear Single Quantum Coherence (HSQC)

spectroscopy recorded with a spectral width of 0 – 12 ppm and 0 – 250 ppm in ^{1}H and ^{13}C, respectively. The number of scans for both were 512 at 27°C. For the ^{1}H-^{13}C parameters the relaxation time was 1.5 s and the free induction decay dimensions was 2048 and 256, while the number of scans were 120 at 27°C. Integrations were done with MestReNova (version 9.1.0), where the C1 of mannose were used as an internal reference.

Supplementary:

A sample of Norwegian spruce extracted by milled wood lignin (36) (MWL) was run as a reference standard for HSQC NMR.

Figure S1. 2D-NMR HSQC of Norwegian spruce lignin (Milled Wood Lignin extracted (MWL)), focused on ^{1}H: 2.7 – 7.7 and ^{13}C: 50.0 – 135.4 ppm.

Figure S2. MALDI-ToF spectra of extracted oligosaccharides samples from all treatment. Relative intensities show the most prevalent oligosaccharide sizes to be in the 1000-1500m/z range (DP6-DP9 for hexoses) and highly acetylated in the control

and citrate pH 4.0 samples. In further treatments the hexose peaks are gradually replaced with xylooligosaccharide peaks at much higher intensities and with no acetylations. The peak at 723 m/z is a persistent contamination.

Table S1. Determination of the $^{13}C/^{1}H$ correlation signals acquired in the 2D-NMR HSQC spectrum of MWL spruce.ß-O-4 reflect the ß-aryl ether as sketched in figure S1, G2, -5 and -6-reflects the aromatic signals and MeO reflects the methoxyl-group in the guaiacyl units sketched in figure S1.

Label	δ_C/δ_H (ppm)	Assignment
MeO	55.7/3.7	C/H is methoxyl- in C_3 position on a guaiacyl unit
ß–O–4α	71.9/4.8	C_α/H_α from β–O–4 lignin bonding pattern
ß–O–4ß	86.1/4.1	C_β/H_β from β–O–4 lignin bonding pattern
ß–O–4γ	59.7/3.5	C_γ/H_γ from β–O–4 lignin bonding pattern
G2	111.0/7.0	C_2/H_2 in a Guaiacyl unit
G5	114.9/6.8	C_5/H_5 in a Guaiacyl unit
G6	118.9/6.8	C_6/H_6 in a Guaiacyl unit

Table S2. Monosaccharide composition of carbohydrates in freeze dried aliquots of filtered, water soluble fractions.

Sample:	Combined severity R'_0:	Rha	Fuc	Ara	Xyl	Man	Gal	Glc
Control	1.707	0.90	n.d.	4.95	15.94	46.41	7.10	24.68
Citrate pH 4.0	0.511	0.95	n.d.	2.97	14.30	54.02	7.87	19.89
Citrate pH 5.0	0.092	1.60	n.d.	7.82	28.09	32.55	10.17	19.78
Phosphate 6.0	0.042	0.75	n.d.	5.29	17.27	40.59	6.95	29.14
Citrate pH 6.0	0.024	2.22	n.d.	12.72	41.35	13.40	10.52	19.79
Phosphate pH 6.5	0.010	0.63	n.d.	6.99	23.38	10.10	6.11	52.79
Phosphate 7.0	0.004	1.08	n.d.	8.06	27.49	10.47	7.16	45.75

Table S3. Monosaccharide composition of dried residual biomass.

Sample:	Combined severity R'$_0$:	Rha	Fuc	Ara	Xyl	Man	Gal	Glc
Control	1.707	n.d.	n.d.	n.d.	22.62	37.56	6.01	30.20
Citrate pH 4.0	0.511	n.d.	n.d.	0.94	22.09	39.51	6.92	27.60
Citrate pH 5.0	0.092	n.d.	n.d.	2.49	18.51	48.33	8.14	19.37
Phosphate pH 6.0	0.042	n.d.	n.d.	3.28	17.63	46.15	7.42	22.16
Citrate pH 6.0	0.024	n.d.	n.d.	3.58	18.91	47.62	7.57	18.84
Phosphate pH 6.5	0.010	n.d.	n.d.	4.70	20.56	43.42	7.07	20.11
Phosphate pH 7.0	0.004	n.d.	n.d.	5.39	22.36	41.22	6.90	19.48
Wood	N/A	3.90	0.00	1.95	8.72	19.89	2.68	66.77

Table S4 Acetate present in filtered slurry and released from solubilized carbohydrates in KOH treatment. Data from Figure 2B,C and D.

Combined severity R'$_0$:	Acetate in solution in µmole/mg carbohydrate.	Alkali released acetate in µmole/mg carbohydrate.	Acetate in biomass residue in µmole/mg biomass.
1.707	0.083	0.303	0.143
0.511	0.406	0.306	0.063

0.092	1.128	0.112	0.064
0.042	1.712	n.d.	0.061
0.024	2.201	n.d.	0.068
0.010	2.333	n.d.	0.048
0.004	2.639	n.d.	0.081
Wood	-	-	0.218

Declarations:

Ethics approval and consent to participate: Not applicable

Competing interests: None of the authors have any competing interests in the content of this manuscript.

Consent for publication: All authors consent to publication.

Availability of data and material: All raw data and material samples available upon reasonable request.

Authors' contributions: Experimental design (L.M., S.H.K. and B.W.) and conducting the experiments (L.M. S.H.K. and I.A.). All authors contributed in writing the manuscript.

References:

1.   Bauer A, Lizasoain J, Theuretzbacher F, Agger JW, Rincon M, Menardo S, et al. Steam explosion pretreatment for enhancing biogas production of late harvested hay. Bioresource Technology. 2014;166:403-10.

2.   Vivekanand V, Olsen EF, Eijsink VGH, Horn SJ. Methane Potential and Enzymatic Saccharification of Steam-exploded Bagasse. Bioresources. 2014;9(1):1311-24.

3.   Lizasoain J, Trulea A, Gittinger J, Kral I, Piringer G, Schedl A, et al. Corn stover for biogas production: Effect of steam explosion pretreatment on the gas yields and on the biodegradation kinetics of the primary structural compounds. Bioresource Technology. 2017;244:949-56.

4.   Biely P, Cziszarova M, Uhliarikova I, Agger JW, Li XL, Eijsink VGH, et al. Mode of action of acetylxylan esterases on acetyl glucuronoxylan and acetylated oligosaccharides generated by a GH10 endoxylanase. Biochimica et Biophysica Acta General Subjects. 2013;1830(11):5075-86.

5.   Kemppainen K, Inkinen J, Uusitalo J, Nakari-Setala T, Siika-aho M. Hot water extraction and steam explosion as pretreatments for ethanol production from spruce bark. Bioresource Technology. 2012;117:131-9.

6.   Sun Y, Cheng JY. Hydrolysis of lignocellulosic materials for ethanol production: a review. Bioresource Technology. 2002;83(1):1-11.

7.   Schutt F, Westereng B, Horn SJ, Puls J, Saake B. Steam refining as an alternative to steam explosion. Bioresource Technology. 2012;111:476-81.

8.   Ramos LP. The chemistry involved in the steam treatment of lignocellulosic materials. Quimica Nova. 2003;26(6):863-71.

9.   R. P. Overend EC. Fractionation of lignocellulosics by steam-aqueous pretreatments. Philosophical Transactions of the Royal Society of London Series A, Mathematical and Physical Sciences. 1987;321(1561):523-36.

10.   Chum HL, Johnson DK, Black SK, Overend RP. Pretreatment-Catalyst effects and the combined severity parameter. Applied Biochemistry and Biotechnology. 1990;24(1):1.

11.   Kabel MA, Bos G, Zeevalking J, Voragen AGJ, Schols HA. Effect of pretreatment severity on xylan solubility and enzymatic breakdown of the remaining cellulose from wheat straw. Bioresource Technology. 2007;98(10):2034-42.

12.   Pedersen M, Meyer AS. Lignocellulose pretreatment severity - relating pH to biomatrix opening. New Biotechnology. 2010;27(6):739-50.

13.   Rissanen JV, Grenman H, Xu CL, Krogell J, Willfor S, Murzin DY, et al. Challenges in understanding the simultaneous aqueous extraction and hydrolysis of spruce hemicelluloses. Cellulose Chemistry and Technology. 2015;49(5-6):449-53.

14.   Chandra RP, Bura R, Mabee WE, Berlin A, Pan X, Saddler JN. Substrate pretreatment: The key to effective enzymatic hydrolysis of lignocellulosics? In: Olsson L, editor. Biofuels. Advances in Biochemical Engineering-Biotechnology. 1082007. p. 67-93.

15.   Jönsson LJ, Martín C. Pretreatment of lignocellulose: Formation of inhibitory by-products and strategies for minimizing their effects. Bioresource Technology. 2016;199:103-12.

16.   Singh J, Suhag M, Dhaka A. Augmented digestion of lignocellulose by steam explosion, acid and alkaline pretreatment methods: A review. Carbohydrate Polymers. 2015;117:624-31.

17.   Tester RF, Al-Ghazzewi FH. Mannans and health, with a special focus on glucomannans. Food Research International. 2013;50(1):384-91.

18.   Willför S, Sundberg K, Tenkanen M, Holmbom B. Spruce-derived mannans – A potential raw material for hydrocolloids and novel advanced natural materials. Carbohydrate Polymers. 2008;72(2):197-210.

19.   Lundqvist J, Teleman A, Junel L, Zacchi G, Dahlman O, Tjerneld F, et al. Isolation and characterization of galactoglucomannan from spruce (Picea abies). Carbohydrate Polymers. 2002;48(1):29-39.

20.   Dubois M, Gilles KA, Hamilton JK, Rebers PA, Smith F. Colorimetric method for determination of sugars and related substances. Analytical Chemistry. 1956;28:350-6.

21.   Miller GL. Use of dinitrosalicylic acid reagent for determination of reducing sugar. Analytical Chemistry. 1959;31(3):426-8.

22.   Westereng B, Michaelsen TE, Samuelsen AB, Knutsen SH. Effects of extraction conditions on the chemical structure and biological activity of white cabbage pectin. Carbohydrate Polymers. 2008;72(1):32-42.

23.   Lundqvist J, Jacobs A, Palm M, Zacchi G, Dahlman O, Stålbrand H. Characterization of galactoglucomannan extracted from spruce (Picea abies) by heat-fractionation at different conditions. Carbohydrate Polymers. 2003;51(2):203-11.

24.   Willför S, Sjöholm R, Laine C, Roslund M, Hemming J, Holmbom B. Characterisation of water-soluble galactoglucomannans from Norway spruce wood and thermomechanical pulp. Carbohydrate Polymers. 2003;52(2):175-87.

25.   Kravtchenko TP, Arnould I, Voragen AGJ, Pilnik W. Improvement of the Selective Depolymerization of Pectic Substances by Chemical Beta-Elimination in Aqueous-Solution. Carbohydrate Polymers. 1992;19(4):237-42.

26.   Dilokpimol A, Nakai H, Gotfredsen CH, Baumann MJ, Nakai N, Abou Hachem M, et al. Recombinant production and characterisation of two related GH5 endo-beta-1,4-mannanases from Aspergillus nidulans FGSC A4 showing distinctly different transglycosylation capacity. Biochimica Et Biophysica Acta-Proteins and Proteomics. 2011;1814(12):1720-9.

27.   Arnling Bååth J, Martínez-Abad A, Berglund J, Larsbrink J, Vilaplana F, Olsson L. Mannanase hydrolysis of spruce galactoglucomannan focusing on the influence of acetylation on enzymatic mannan degradation. Biotechnology for Biofuels. 2018;11(1):114.

28.   Heikkinen H, Elder T, Maaheimo H, Rovio S, Rahikainen J, Kruus K, et al. Impact of Steam Explosion on the Wheat Straw Lignin Structure Studied by Solution-State Nuclear Magnetic Resonance and Density Functional Methods. J Agric Food Chem. 2014;62(43):10437-44.

29.   Li J, Henriksson G, Gellerstedt G. Carbohydrate reactions during high-temperature steam treatment of aspen wood. Appl Biochem Biotechnol. 2005;125(3):175.

30.   Sette M, Wechselberger R, Crestini C. Elucidation of lignin structure by quantitative 2D NMR. Chemistry (Weinheim an der Bergstrasse, Germany). 2011;17(34):9529-35.

31.   Li Y, Liu W, Hou Q, Han S, Wang Y, Zhou D. Release of Acetic Acid and Its Effect on the Dissolution of Carbohydrates in the Autohydrolysis Pretreatment of Poplar Prior to Chemi-Thermomechanical Pulping. Industrial & Engineering Chemistry Research. 2014;53(20):8366-71.

32.   García-Aparicio MP, Ballesteros I, González A, Oliva JM, Ballesteros M, Negro MJ. Effect of inhibitors released during steam-explosion pretreatment of barley straw on enzymatic hydrolysis. Applied Biochemistry and Biotechnology. 2006;129(1):278-88.

33.   Horn SJ, Nguyen QD, Westereng B, Nilsen PJ, Eijsink VGH. Screening of steam explosion conditions for glucose production from non-impregnated wheat straw. Biomass Bioenerg. 2011;35(12):4879-86.

34.   Vestby LK, Møretrø T, Ballance S, Langsrud S, Nesse LL. Survival potential of wild type cellulose deficient Salmonella from the feed industry. BMC Veterinary Research. 2009;5(1):43.

35.   Englyst HN, Quigley ME, Hudson GJ. Determination of dietary fibre as non-starch polysaccharides with gas-liquid chromatographic, high-performance liquid chromatographic or spectrophotometric measurement of constituent sugars. The Analyst. 1994;119(7):1497-509.

36.   Crestini C, Melone F, Sette M, Saladino R. Milled Wood Lignin: A Linear Oligomer. Biomacromolecules. 2011;12(11):3928-35.

```
┌─────────────────┐
│ Steam explosion at│
│ 14.5 bar, 200° C, 10│
│ minutes residence│
│ time.           │
└─────────────────┘
         │
         ▼
┌─────────────────┐        ┌─────────────────┐
│ Cooling to room │───────▶│ Aliquots of filtrate│
│ temperature,    │        │ collected.      │
│ filtration.     │        └─────────────────┘
└─────────────────┘                 │
         │                          ▼
         ▼                 ┌─────────────────┐
┌─────────────────┐        │ Free and bound  │
│ Retained wood oven│      │ acetate content,│
│ dried at 100° C. │       │ total carbohydrate│
└─────────────────┘        │ content and     │
         │                 │ reducing sugars │
         ▼                 │ analysis.       │
┌─────────────────┐        └─────────────────┘
│ Monosaccharide  │                 │
│ composition     │                 ▼
│ analysis.       │        ┌─────────────────┐
└─────────────────┘        │ Samples of filtrate│
         │                 │ freeze dried.   │
         ▼                 └─────────────────┘
┌─────────────────┐                 │
│ 500 mg samples of│                ▼
│ wood washed with│        ┌─────────────────┐
│ MilliQ water, treated│   │ Monosaccharide  │
│ with GH5        │        │ composition     │
│ Mannanase.      │        │ analysis, NMR of│
└─────────────────┘        │ lignin fraction.│
                           └─────────────────┘
```
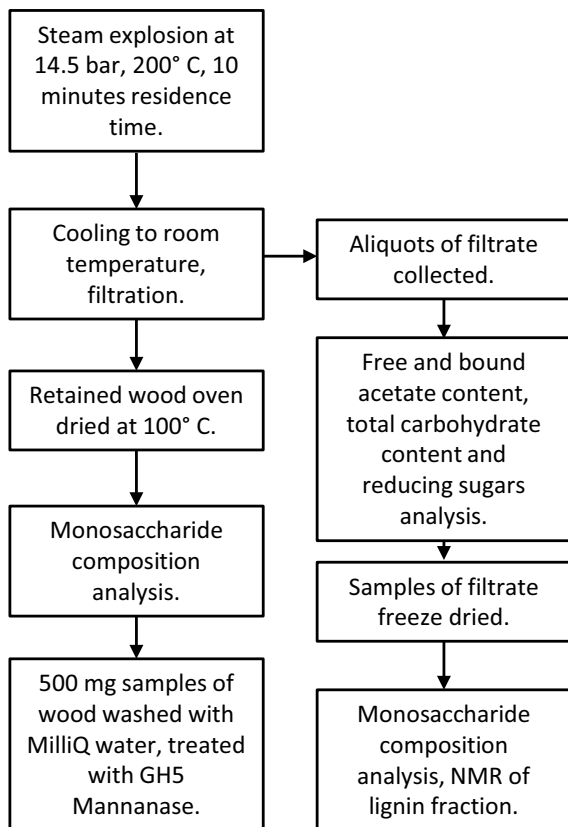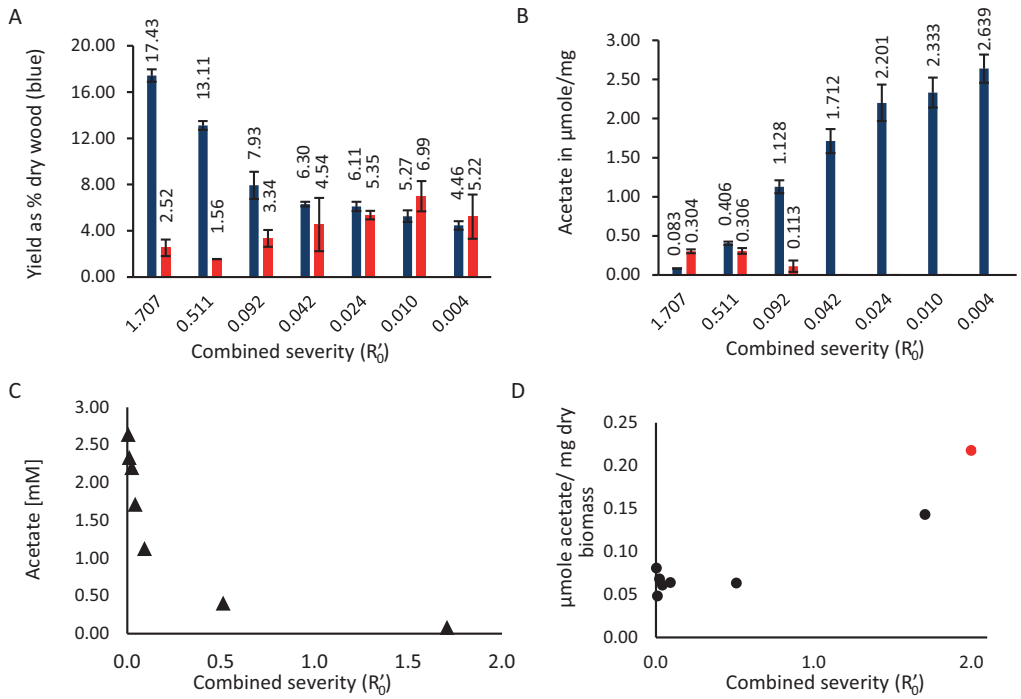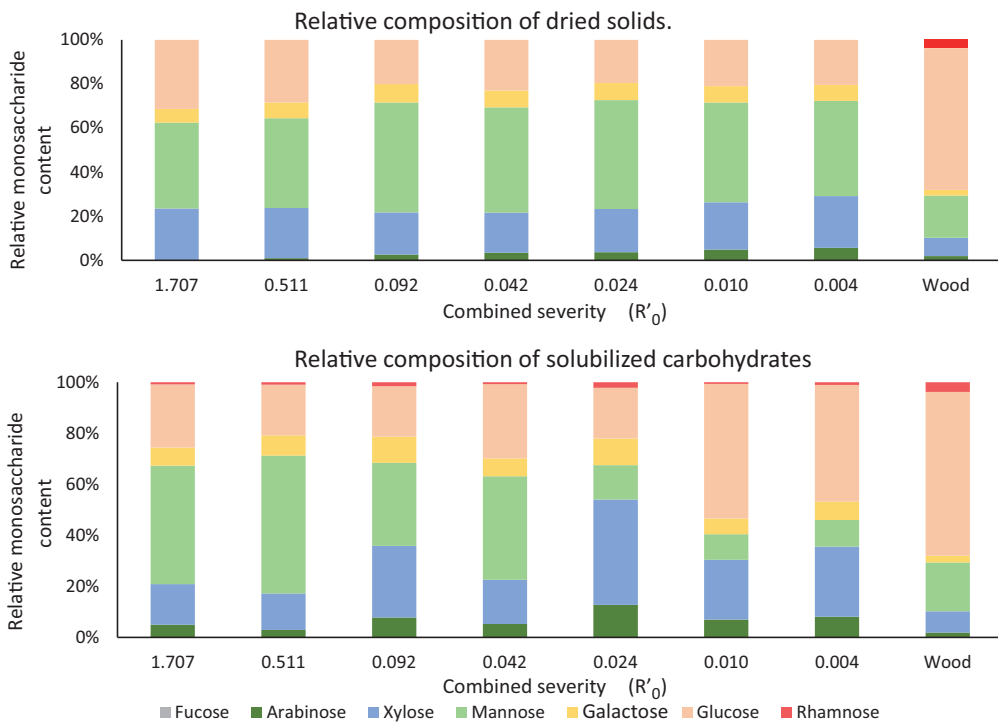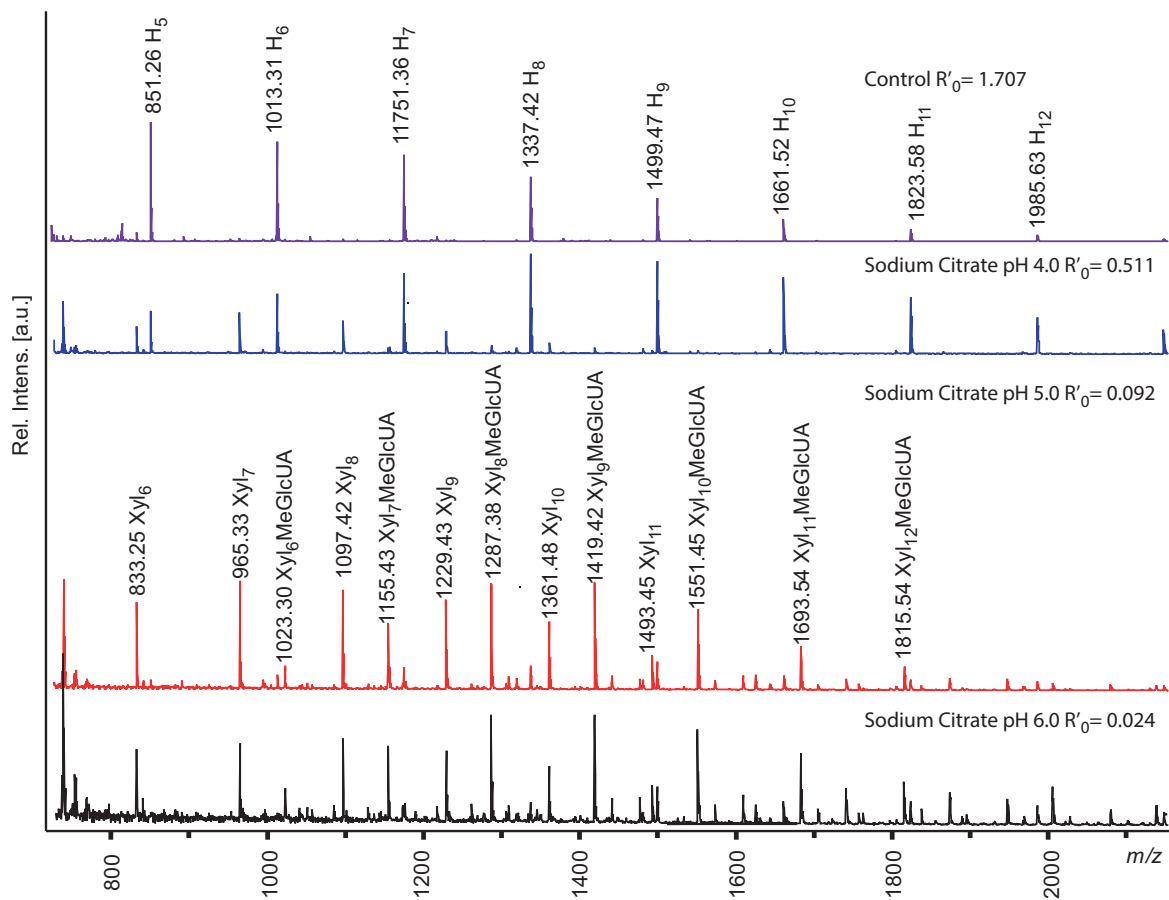
Figure 1

Figure 2

Figure 3

Figure 4
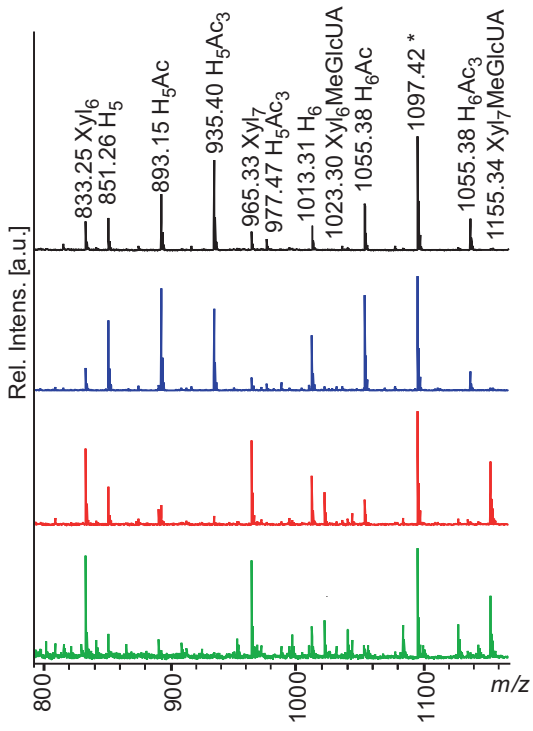
Figure 5
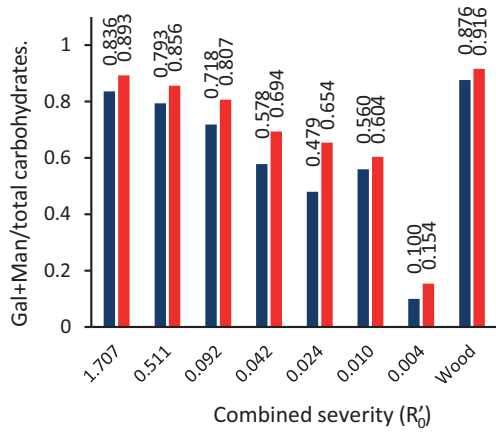
Figure 6

Figure 7

Figure S1